

https://dspace.org/

Nongeographic variation in the striped mouse Rhabdomys dilectus chakae (Rodentia: Muridae)

Neves, Candice Nikita

2018

https://hdl.handle.net/10539/26294

Neves, Candice Nikita, (2018) Non-geographic variation in the striped mouse, Rhabdomys dilectus chakae (Rodentia: Muridae), University of the Witwatersrand, Johannesburg, https://hdl.handle.net/10539/26294.

Downloaded from a DSpace repository. https://dspace.org/

Nongeographic variation in the striped mouse *Rhabdomys dilectus chakae* (Rodentia: Muridae)

Candice Nikita Neves

A dissertation submitted to the Faculty of Science, University of the Witwatersrand, Johannesburg in fulfilment of the requirements for the degree of Master of Science.

Johannesburg, 2018

Declaration

I declare that this dissertation is my own unaided work. It is being submitted for the degree of Master of Science in the University of the Witwatersrand, Johannesburg. It has not been submitted before for any degree or examination in any other university.



Candice Nikita Neves

23/05/2018

Abstract

The morphological variation between populations is shaped by adaptive responses to prevailing environmental conditions and/or not adaptive stochastic effects. Within-population variation is mainly related to age and sexual dimorphism, as well as temporal and spatial variation in environmental conditions. The aim of this study was to investigate patterns of variation in the skull, mandibles, and dentition in a population of the African four-striped mouse *Rhabdomys dilectus chakae*. Geometric morphometrics was used to assess the variation related to allometry and age, sexual dimorphism, and the inter-annual variation between specimens collected in different years (1975, and 1994-1997). A review of the literature on the application of geometric morphometrics to rodent morphological variation was conducted and landmark morphometrics were concluded to be the most appropriate methods for the skull and the mandible analyses, with a separate analysis using landmarks and semi-landmarks to analyse the variation of mandibular curves, and outline morphometrics with an Elliptic Fourier analysis of the upper molars. Images of the skull (ventral and lateral view at 5x magnification), mandible (at 6.8x magnification), and the three left upper molars (at 10.5x magnification) were captured using a stereoscopic microscope. Landmarks were digitized on the skull and mandible images, with semi-landmarks digitized on mandible images, and outlines were digitized on molars. Multivariate analysis of variance was used to analyse shape and size variation due to age, sex, and year of sampling and a multivariate regression was used to analyse allometry. A PCA was used to visualize shape variation, and boxplots of log-centroid size to visualize size variation between age classes, sexes, and years of sampling. Shape variation was significantly predicted by age and year of sampling, while size was significantly predicted by age, sex, and year of sampling. Size significantly contributed to shape variation, although size alone did not appear to explain much of the variation present. Most age-related variation in shape was due to differences between the first three age classes and age class IV, while size increased with increased age (i.e. growth). Males were larger than females although no sexual shape dimorphism was evident between sexes. Typical of species with male-male competition, *Rhabdomys dilectus chakae* demonstrated sexual size dimorphism; larger males have greater mating opportunities. Specimens from 1994 and 1997 had more variable shapes and were consistently smaller than those collected in 1975, 1995 and 1996, except for dentition where these latter specimens were smaller than those collected in 1994 and 1997. Annual variation in morphology may be a plastic response to prevailing local climatic conditions (i.e. rainfall and temperature),

resulting in annual variation in diet, affecting the skull and dentition. Further studies should consider more populations in the species to assess the generalizability of the findings, particularly annual variation, and to consider spatial variation across the distribution of a population.

Acknowledgements

I would like to thank the National Research Foundation and the University of the Witwatersrand for funding my research. Special thanks also to the National Museum of Bloemfontein for the use of their Willem Pretorius specimens and to the South African Weather Service for the use of their climate data. I am eternally grateful to my supervisors, Prof Neville Pillay and Dr Teresa Kearney for reading many, many drafts and providing valuable feedback. I would also like to thank the Behaviour lab for the coffee breaks and distractions from stress, the commiserations about statistical and writing difficulties, and for all the encouragement that got me to the end. To all my friends that helped to provide excuses for procrastination, and to Lauren who kept me focused at the end and provided a sounding board that helped me finish. And last, but most certainly not least, I am profoundly grateful to my mom, Tracy-lee, and my dad, Carlos, who helped with reading drafts, and never once hesitated in offering support.

Table of Contents

Declaration ii
Abstract iii
Acknowledgements v
List of Figures viii
List of Tables xii
List of Appendices xiii
Chapter 1 1
Introduction 1
Rationale 1
1.1. Sources of Geographic Morphological Variation 2
1.1.1. Environmental gradients and diet 2
1.1.2. Phylogenetic variation 3
1.1.3. Stochastic variation 4
1.2. Sources of Non-Geographic Variation 4
1.2.1 Sexual dimorphism 4
1.2.2. Ontogenetic variation 6
1.3. Four-striped Mouse *Rhabdomys* 6
1.4. Aims and objectives 9
Chapter 2 10
A review of Geometric morphometrics methods 10
Landmark morphometrics 10
Semi-landmark morphometrics 23
Outline morphometrics 24
Conclusion 25
Chapter 3 27
Methods and Materials 27
Specimens 27
Aging 28
Image capturing and digitization 29
Analysis of semi-landmarks for the Mandible 32
Analysis of Molar Outlines 33
Descriptive comparisons in annual climatic data and form change 34
Chapter 4 35
Results 35
4.1 Ventral skull landmark analysis 35
Analysis of ventral cranial shape and size 35
Allometry of the ventral skull 37
Shape comparisons of the ventral skull with PCA 39
4.2. Lateral skull landmark analysis 42
Analysis of lateral cranial shape and size 42
Allometry of the lateral skull 47
Shape comparisons of the lateral skull with PCA 49
4.3. Mandible landmark analysis 53
Analysis of mandibular shape and size 53
Allometry of the mandible 55

Shape comparisons of the mandible with PCA 58
4.4. Mandible landmark and semi-landmark curve analyses 60
Analysis of mandibular curve shape and size 60
Allometry of mandibular curves 62
Shape comparisons of the mandibular curves with PCA 65
4.5. Outline analysis of Molars 68
Analysis of shape and size of the first upper molar 68
Allometry of the first upper molar 70
Shape comparisons of the first upper molar with PCA 73
Analysis of shape and size of the second upper molar 76
Shape comparisons of the second upper molar with PCA 82
Analysis of shape and size of the third upper molar 85
Allometry of the third upper molar 87
Shape comparisons of the third upper molar with PCA 91
4.5. Descriptive comparison of climate data and form across years 94
4.6. Summary 97

Chapter 5 101

Discussion 101
Allometry and age-related variation 101
Sexual dimorphism 103
Year of sampling 105
Comparisons with southern African rodents 108
Conclusions 109

References 111

Appendices 131

List of Figures

Figure 1.1. Distribution map of the *Rhabdomys* genus in South Africa, created using only sampled localities that have been genotyped ……8
Figure 3.1. Adult age classes (by Henschel *et al.* 1982) based on the degree of tooth wear of the molar cusps of the cranial molar row ……28
Figure 3.2. Landmark placement for: a) the ventral view of the skull (31 landmarks); b) the lateral view of the skull (15 landmarks); and c) the lateral view of the mandible (13 landmarks) ……...30
Figure 3.3. Landmarks and semi-landmarks used in the semi-landmark analysis of the lateral view of the mandible……32
Figure 3.4. Outlines of the left upper molars with 64 equidistant points (red dots) digitized on a) the first upper molar, b) the second upper molar, and c) the third upper molar…….….33
Figure 4.1. Variation in log-centroid size of the ventral skull between the sexes (top-left), age classes (top-right), and years of sampling (bottom)……..……...36
Figure 4.2. Multivariate regression of shape (using the regression score) on size (log-centroid size) of the ventral skull……...37
Figure 4.3. Allometric relationship between log-centroid size and ventral skull shape in the four age classes…….38
Figure 4.4. Allometric relationship between log-centroid size and ventral skull shape among years of specimen collection……38
Figure 4.5. Allometric relationship between log-centroid size and ventral skull shape between the sexes……...39
Figure 4.6. Allometry-adjusted Principal Component Analysis of the first two principal components indicating the spread of the four age classes in the ventral skull…….40
Figure 4.7. Allometry-adjusted Principal Component Analysis of the first two principal components indicating the spread across year of specimen collection in the ventral skull….41
Figure 4.8. Allometry-adjusted Principal Component Analysis of the first two principal components indicating the spread for the sexes in the ventral skull……42
Figure 4.9. Variation in log-centroid size of the ventral skull between the sexes (top-left), age class (top-right), and year of sampling (bottom)……..44
Figure 4.10. Variation in log-centroid size of the lateral skull for the sex:year of sampling interaction……46

Figure 4.11. Variation in log-centroid size of the lateral skull for the age:year of sampling interaction…….46
Figure 4.12. Multivariate regression of shape (using the regression score) on size (log-centroid size) of the lateral skull……..47
Figure 4.13. Allometric relationship between age classes for the lateral skull……48
Figure 4.14. Allometric relationship between log-centroid size and the shape of the lateral skull between years of specimen collection…….48
Figure 4.15**.** Allometric relationship between log-centroid size and lateral skull shape between the sexes…….49
Figure 4.16. Allometry-adjusted Principal Component Analysis of the first two principal components indicating the spread of the four age classes for the lateral skull……50
Figure 4.17. Allometry-adjusted Principal Component Analysis of the first two principal components indicating the spread across year of specimen collection for the lateral skull….52
Figure 4.18. Allometry-adjusted Principal Component Analysis of the first two principal components indicating the spread for the sexes for the lateral skull……53
Figure 4.19. Variation in log-centroid size of the left mandible between the sexes (top-left), age classes (top-right), and years of sampling (bottom)……..55
Figure 4.20. Multivariate regression of shape (using the regression score) on size (log-centroid size) of the mandible……..56
Figure 4.21. Allometric relationship between log-centroid size and the shape of the mandible for age classes……...56
Figure 4.22. Allometric relationship between log-centroid size and the shape of the mandible for years of specimen collection……...57
Figure 4.23. Allometric relationship between log-centroid size and the shape of the mandible for the sexes……..57
Figure 4.24. Allometry-adjusted Principal Component Analysis of the first two principal components indicating the spread of the four age classes for the mandible……58
Figure 4.25. Allometry-adjusted Principal Component Analysis of the first two principal components indicating the spread across year of specimen collection for the mandible…….59
Figure 4.26. Allometry-adjusted Principal Component Analysis of the first two principal components indicating the spread for the sexes for the mandible……60
Figure 4.27. Variation in log-centroid size of the left mandible sampled using landmarks and semi-landmarks between sex (top-left), age class (top-right), and year of sampling (bottom)……62

Figure 4.28. Multivariate regression of shape (using the regression score) on size (log-centroid size) of the mandibular curves……...63
Figure 4.29. Allometric relationships of age classes for the mandible, sampled using semi-landmarks…….63
Figure 4.30. Allometric relationships between log-centroid size and the shape of the mandible, sampled using semi-landmarks for years of specimen collection……...64
Figure 4.31. Relationship of allometry between log-centroid size and the shape of the mandible, sampled using semi-landmarks for the sexes……..64
Figure 4.32. Allometry-adjusted Principal Component Analysis of the first two principal components indicating the spread of the four age classes for the mandibular curves…….66
Figure 4.33. Allometry-adjusted Principal Component Analysis of the first two principal components indicating the spread for year of specimen collection for the mandibular curves……...67
Figure 4.34. Allometry-adjusted Principal Component Analysis of the first two principal components indicating the spread for the sexes for the mandibular curves…….68
Figure 4.35. Variation in log-centroid size of the first upper molar between age classes (top-left), sex (top-right), and year of sampling (bottom)……70
Figure 4.36. Multivariate regression of shape (using the regression score) on size (log-centroid size) of the first upper molar……..71
Figure 4.37. Allometric relationship between log-centroid size and first upper molar shape in the four age classes……...71
Figure 4.38. Allometric relationship between log-centroid size and first upper molar shape among years of specimen collection……....72
Figure 4.39. Allometric relationship between log-centroid size and first upper molar shape between the sexes……72
Figure 4.40. Allometry-adjusted Principal Component Analysis of the first two principal components indicating the spread of the four age classes for the first upper molar……74
Figure 4.41. Allometry-adjusted Principal Component Analysis of the first two principal components indicating the spread across year of specimen collection for the first upper molar ……..75
Figure 4.42. Allometry-adjusted Principal Component Analysis of the first two principal components indicating the spread for the sexes for the first upper molar……76
Figure 4.43. Variation in log-centroid size of the second upper molar between age classes (top-left), year of sampling (top-right), and sex (bottom)……78

Figure 4.44. Multivariate regression of shape (using the regression score) on size (log-centroid size) of the second upper molar…….79
Figure 4.45. Allometric relationship between log-centroid size and second upper molar shape in the four age classes……..80
Figure 4.46. Allometric relationship between log-centroid size and second upper molar shape among years of specimen collection……81
Figure 4.47. Allometric relationship between log-centroid size and second upper molar shape between the sexes…….82
Figure 4.48. Allometry-adjusted Principal Component Analysis of the first two principal components indicating the spread of the four age classes for the second upper molar……83
Figure 4.49. Allometry-adjusted Principal Component Analysis of the first two principal components indicating the spread across year of specimen collection for the second upper molar…….84
Figure 4.50. Allometry-adjusted Principal Component Analysis of the first two principal components indicating the spread for the sexes for the second upper molar……...85
Figure 4.51. Variation in log-centroid size of the third upper molar between years of sampling (top-left), sex (top-right), and age class (bottom)…….87
Figure 4.52. Multivariate regression of shape (using the regression score) on size (log-centroid size) of the third upper molar…….88
Figure 4.53. Allometric relationship between log-centroid size and third upper molar shape in the four age classes……...89
Figure 4.54. Allometric relationship between log-centroid size and third upper molar shape among years of specimen collection……90
Figure 4.55. Allometric relationship between log-centroid size and third upper molar shape between the sexes…….91
Figure 4.56. Allometry-adjusted Principal Component Analysis of the first two principal components indicating the spread of the four age classes for the third upper molar……...92
Figure 4.57. Allometry-adjusted Principal Component Analysis of the first two principal components indicating the spread across year of specimen collection for the third upper molar…….93
Figure 4.58. Allometry-adjusted Principal Component Analysis of the first two principal components indicating the spread for the sexes for the third upper molar……..94

List of Tables

Table 2.1. Rodent geometric morphometric studies used in the literature review……...12
Table 3.1. Definitions of age classes defined by degree of tooth wear by Henschel *et al.* (1982) ...……...28
Table 4.1. MANOVA results of the shape and size components of the symmetric variation in the ventral skull……35
Table 4.2. MANOVA results of the shape and size components of the symmetric variation in the lateral skull ……43
Table 4.3. MANOVA results of the shape and size components of the symmetric variation in the mandible ……54
Table 4.4. MANOVA results of the shape and size components of the symmetric variation in the mandible using semi-landmark analysis ……61
Table 4.5. MANOVA results of the shape and size components of the symmetric variation in the first upper molar ……69
Table 4.6. MANOVA results of the shape and size components of the symmetric variation in the second upper molar ……...77
Table 4.7. MANOVA results of the shape and size components of the symmetric variation in the third upper molar……86
Table 4.8. Weather data in different years of specimen sampling obtained from the South African Weather Service (2018) and associated relative form change in each of the traits ……95
Table 4.9. Summary of main experimental results……...97

List of Appendices

Appendix 1a. Landmark definitions adapted from Maestri *et al.* (2017) & Jojić *et al.* (2011), for the 31 landmarks used on the ventral skull……...131
Appendix 1b. Definitions for the 15 landmarks used on the lateral view of the skull definitions adapted from Maestri *et al.* (2017) & dos Reis *et al.* (2002a).……132
Appendix 1c. Landmark definitions for the 13 landmarks used for the mandible adapted from Shintaku *et al.* 2016), Samuels (2009), and Cardini & Tongiorgi (2003)……...133
Appendix 2. Table of ANOVA results of measurement error for 30 specimens, with two sets of images digitized twice for the ventral skull, lateral skull, and mandible each……..133
Appendix 3. ANOVA results of the variation in asymmetry in the ventral skull, lateral skull, and mandible (using landmark analysis, and landmarks combined with semi-landmarks)...134
Appendix 4. Figures indicating the cumulative harmonic Fourier power of the upper molars and the information each harmonic cumulatively explained…….135
Appendix 5. Accumulative proportion of variance explained by PC Axes……...138

Chapter 1

Introduction

Rationale

Environmental change frequently results in the extinction of many species that are incapable of adapting or dispersing, especially when environmental conditions change rapidly (Holmes *et al.* 2016*;* Cahill *et al.* 2012). It is, however, possible for some species to adapt and diversify in the face of these changing environmental conditions, particularly in the highly adaptable rodent clade (Auffray et al. 2009). Rodents display remarkable plasticity in reproductive (Vessey & Vessey 2007; Schradin & Pillay 2006), physiological (Kronfeld-Schor & Dayan 2008), and morphological traits (Anderson *et al*. 2014) that allow them to adapt to rapidly changing environments.

When abiotic environmental conditions change, the vegetation characteristics of the environment may change in response (Renaud *et al.* 2005). As a result of changing vegetation, animals may need to utilise new or previously uncommon resources for food and shelter (Auffray *et al.* 2009). Species may become adapted to utilise the new resources, often through morphological changes to aid in more efficient feeding (Holmes *et al.* 2016; Ledevin *et al.* 2010a; Renaud 2005). For example, in populations of deer mice *Peromyscus maniculatus* occurring along an altitudinal gradient, each population is morphologically distinct, linked to local climatic conditions, which affect morphology mainly through diet and physiological adaptation for more efficient thermoregulation (Holmes *et al.* 2016). Individuals in different populations may therefore utilise different foods across geographical ranges depending on the resources available to them and thus be morphologically adapted to those diets (Renaud *et al.* 1996).

The genetics of the genus *Rhabdomys* (Thomas, 1916) have recently received increasing interest. Studies (Castiglia *et al.* 2012; du Toit *et al.* 2012; Rambau *et al.* 2003) have proposed that a revision of the taxonomy is necessary from a single species (*Rhabdomys pumilio* (Sparrman, 1784) to two species (*R. pumilio* and *R. dilectus* (De Winton, 1897)), each with their own subspecies (see Castiglia *et al.* 2012), as well as two additional species *R. intermedius* and *R. bechuanae* (du Toit *et al.* 2012). Since the molecular study by Rambau *et al.* (2003), numerous behavioural studies have also provided support for this taxonomic distinction between the two species of *Rhabdomys,* but no published work has investigated the morphological variation that may exist within or between these two species.

In a previous study of a population of *R. dilectus chakae*, I found that intraspecific mandibular size and shape variation was not sexually dimorphic or influenced by age but that there was an effect of the interaction between size and sex on shape variation of the mandible (Neves 2015). Just the previously mentioned study on mandibular size and shape variation has been performed on any species in the genus *Rhabdomys*. In the current study, I build upon my earlier research to consider size and shape variation of the crania, mandibles and dentition in a population of the sub-species, *R. dilectus chakae* (Wroughton, 1905), in South Africa.

1.1. Sources of Geographic Morphological Variation

Adaptation can be a rapid response by an individual to environmental stress and arises as a result of phenotypic variation already present in a population (Hoffman & Sgrò 2011). The phenotypic variation provides an opportunity for selection to act and genetic variation enables selection to effect change within the population (Zelditch *et al.* 2004). If the phenotypic response to that stress has adaptive value and confers a benefit to the individual that increases their reproductive success, the adaptive response is far more likely to be passed on to offspring (Ellis *et al.* 2006). Selection should then act in favour of the adaptation, eventually leading to divergence in the trait from other populations (Holt & Gaines 1992). Over evolutionary time, given a high adaptive capacity, and sufficient rapid environmental stress to induce further adaptation, speciation may occur as populations are driven further apart phylogenetically (Ghalambor *et al.* 2007).

1.1.1. Environmental gradients and diet

Spatial clines may develop rapidly when environmental changes occur over gradients and result in variations in the expressed phenotypes of organisms (Auffray *et al.* 2009). These variable phenotypic traits usually occur as a result of changes in the patterns of rainfall, which then affect the composition of the vegetation in the environment, thus resulting in variation in food availability (Renaud *et al.* 2005). In a phenotypically variable population, the phenotypic characters of the mandible and skull best suited to the new diet would be selected for (Auffray *et al.* 2009). The combination of the pre-existing variation within the population and the new niche that becomes available as a result of changes to the vegetation composition would thus act as a selection pressure driving the morphology of individuals in a population (Schluter 2001).

Cranial morphology is affected by the diet of animals in a variety of ways. Molar shape is related to greater grinding efficiency (van Dam 1997; Renaud *et al.* 2005), and cranial and mandibular morphology may vary as a result of increased surface attachment at the points of insertion of muscles, such as the masseter muscle, which leads to increased bite force and thus results in improved feeding efficiency (Michaux *et al.* 2007a; Anderson *et al.* 2014; Astùa *et al.* 2015). For example, when environmental conditions change, causing the food types available to become harder than they were previously, laboratory mice develop longer and deeper mandible shapes to increase the mechanical advantage for food consumption (Anderson *et al.* 2014). Diet influences molar, mandibular and skull shape in many species of rodents, with convergent morphological shapes appearing in different species (Samuels 2009). For example, insectivorous rodents have reduced dentition, thin zygomatic arches and elongated rostra since mastication is largely absent in these species, while herbivorous rodents have larger molars, larger zygomatic arches and a wider rostrum which aid in intense mastication (Samuels 2009).

When resources are spread along gradients, individuals in each population along that gradient usually develops variations in morphology best suited to its particular environment. The edible dormouse *Glis glis* shows variation along the coast of the Black Sea, where the molar shape varies longitudinally, with larger, more diamond-shaped molars at the western point of the cline and smaller more square molars at the eastern end due to differences in ecology and vegetation (Helvaci *et al.* 2012). The *Arvicanthis* genus of Africa also shows evidence of a latitudinal trend with larger crania in the north and smaller crania in the south due to adaptation to micro-niches, although the authors do not explain how (Fadda & Corti 2001).

1.1.2. Phylogenetic variation

Variation may not only result from adaptation to the environment but may occur as a result of diverging phylogenetic signals amongst increasingly more distantly related taxa (Freckleton & Jetz 2009). Consequently, it is expected that more closely related taxa will show similarities in their phenotypes given their shared common evolutionary history (Freckleton & Jetz 2009). In marmots *Marmota* spp., for example, mandible morphology is more similar between more closely related taxa (Cardini 2003). It has also been found that divergence in morphological structures in the genus *Marmota* tend to become more frequent over longer evolutionary periods (Caumal & Polly 2005).

1.1.3. Stochastic variation

Stochastic variation is variation as a result of unpredictable changes. Such changes may be variation in local climatic conditions over time which alter the local environments enough that the animals in those environments may need to respond to these new conditions. This can be seen in the current larger body size of the California ground squirrel *Spermophilus beecheyi* compared to specimens that lived during the last glacial maximum (21 000 years ago); the difference has been linked to increased winter precipitation which changes the abundance of food in winter currently (Blois *et al.* 2008).

Such rapid changes in the environment may lead to rapid morphological changes, particularly in short-lived species which must respond quickly in order to survive (Stump *et al.* 2018). In deer mice *Peromyscus maniculatus*, for instance, three populations with specimens collected 100 years apart in the Sierra Nevada Mountains in the United States of America, have become differently adapted to the local environmental conditions, (Holmes *et al*. 2016). Similarly, both the southern African vlei rat *Otomys irroratus* and the Angoni vlei rat *Otomys angoniensis* have smaller cranial sizes, with a correlated decrease in body size over a period of 100 years, possibly linked to increased annual precipitation over time although the mechanism was not explained (Nengovhela *et al.* 2015).

1.2. Sources of Non-Geographic Variation

1.2.1 Sexual dimorphism

Sexual dimorphism occurs in many groups of animals with internal fertilization (Fairbairn 2007) and is driven largely by the differences in the reproductive roles of each sex (Stillwell *et al.* 2010). This is often related to sex-specific roles in reproduction, in which females invest more in larger gametes and offspring care (Andersson 1994). In contrast, males produce large quantities of energy inexpensive sperm and invest in reproduction by attempting to mate with many females (Trivers 1972).

In polygynous mammals, males can be larger in size than females (Lindenfors *et al.* 2007) due to the competition between male conspecifics for mates (Schulte-Hostedde *et al.* 2001), with larger males able to defend their claim on a mate more easily (Eisenberg 1981) or indicating their superior quality (e.g. the handicap hypothesis; Hamilton and Zuk 1982). Size may vary between the sexes for other reasons. In some species, males have developed combative structures which are used in battles (Preston *et al.* 2003). This is clearly evident in males of many species of ungulates where large-horned males ward off conspecific male

competitors using their horns, whereas females of these species tend to have reduced horns or no horns at all (Packer 1983). Sexual shape dimorphism in the grass mice species *Akodon cursor* and *Akodon montensis* is likely driven by competition among males, resulting in males having larger attachment points for the masseter and temporalis muscles which increases bite strength for mate defence (Astùa *et al.* 2015). Similarly, variation in the shape of the carapace occurs in males of the Greek tortoise *Testudo graeca graeca*, in which males with wider shell openings having better mobility which allows them to successfully compete against males with more narrow openings (Kaddour *et al* 2008).

When sexual dimorphism is female-biased, the dimorphism may be due to fecundity selection (Stillwell *et al.* 2010) where larger females, by virtue of their greater size, have greater reproductive output. For example, sex-reversed (X*Y chromosomal configuration) female African pygmy mouse *Mus minutoides* tend to be larger, with a greater bite force (Ginot *et al.* 2017) and have larger litter sizes and probabilities of breeding than traditional XX females (Saunders *et al.* 2014). Small male sizes may also hold advantages, particularly when food is limiting because smaller sizes do not require as much energy for metabolic maintenance, allowing small males to spend more time on mate acquisition rather than foraging (Blanckenhorn *et al.* 1995). Larger female sizes in the Crested newt *Triturus cristatus* are associated with larger trunk volumes capable of holding more eggs (Malmgren & Thollesson 1999). Similarly, female tortoises *Testudo horsfieldii* with larger abdominal volumes are capable of carrying more eggs (Bonnet *et al.* 2001).

Where fecundity selection is not the driving force in sexual dimorphism, females may be larger than males because of intraspecific niche divergence, where the sexes of a species utilise different parts of their habitat or consume different prey items (Butler & Losos 2002; Greenberg & Olsen 2010). In the Arufura filesnake *Acrochordus arafurae*, females are significantly larger in both body and head size, have relatively larger jaws (Camilleri & Shine 1990), and consume larger prey than the males (Houston & Shine 1993). Dimorphism between the sexes as a result of intraspecific niche divergence occurs in cottonmouth snakes *Agkistrodon piscivorus* where males eat larger prey and consequently have longer quadrate bones and a larger quadrate surface area than females to accommodate larger prey sizes (Vincent *et al.* 2004).

Sexual dimorphism is not always present in skull morphology when selection does not favour variation in cranial traits (Schulte-Hostedde *et al.* 2001). Several species are sexually monomorphic in size and shape of both body and teeth, such as the bank vole *Myodes glareolus* in which no sexual variation was found in the molars (Ledevin *et al.*

2010a), the European woodmouse *Apodemus sylvaticus* which lacked sexual variation in mandibular and molar size and shape (Renaud 2005), and all African species of unstriped grass mice *Arvicanthis* which lack both size and shape dimorphism in cranial structure (Fadda & Corti 2001). Sexual monomorphism may occur as a result of similarity in diets leading to similar shapes and sizes of cranial structures (Lewis *et al.* 2002). Alternatively, a similarity in response to competitors (whether for food or mates) may result in both sexes developing similar morphological adaptations to aid in combat (such as larger masseter insertion points to increase bite force; Stockley & Bro-Jørgensen 2011).

1.2.2. Ontogenetic variation

Growth results in changes in most morphological features as animals age. In addition, phenotypic characters may be subject to different selection pressures at different stages of an individual's life (Zelditch *et al.* 1992). For example, in the unstriped grass mice genus *Arvicanthis*, younger individuals have larger neurocrania with shorter rostra compared to older individuals (Fadda & Corti 2001). It has been suggested that variation between young and old individuals is largely due to variation in the environmental conditions during the early developmental period of the animal's growth, which heavily influence its' form (Leirs *et al.* 1994). As a result, animals of the same population but of different cohorts, having experienced different environmental conditions may develop differences in the size and/or shape of different morphological features (Le Gailliard *et al.* 2010).

Variation in the size and shape of molars in the European woodmouse *Apodemus sylvaticus* molars are the result of progressive wear from grinding action, such that older mice have smaller occlusal surfaces and more rounded molar outlines with a flat posterior region, whereas young mice have larger occlusal surfaces and narrower molars with sharp back cusps due to the reduced or absence of molar wear (Renaud 2005). Mandibular shape also varies through aging through bone growth and epigenetic bone re-modelling. For example, older wood mice have a somewhat higher articular condyle, a more curved alveolar region and a reduced coronoid process than the younger wood mice (Renaud 2005).

1.3. Four-striped Mouse *Rhabdomys*

The Four-Striped Mouse (until recently described as a single species, *Rhabdomys pumilio* (Sparrman, 1784)), is a diurnal murid rodent, weighing approximately 30-40g as adults (Kingdon 1974), with a widespread distribution across southern Africa and a limited

distribution into East Africa (Skinner & Chimimba 2005; Monadjem *et al.* 2015). Molecular and karyotypic results have provided evidence for the presence of at least four species within *Rhabdomys* indicating that a thorough taxonomic revision is necessary as suggested by Rambau *et al.* (2003) and du Toit *et al.* (2012). Mitochondrial and nuclear DNA suggest the presence of two distinct lineages, the xeric-adapted *Rhabdomys pumilio* (2n=48) and the mesic-adapted *Rhabdomys dilectus*, with two subspecies separated by cytotypes and sequence differences (*R. d. dilectus*, 2n=46 and *R. d. chakae*, 2n=48; Taylor 2000; Rambau *et al.* 2003). *Rhabdomys pumilio* consists of three distinct, geographically separated lineages: the Coastal subclade (separated into Coastal A and Coastal B, *R. pumilio*); the Central subclade (called *R. intermedius*); and the Northern subclade (called *R. bechuanae*; du Toit *et al.* 2012; Figure 1). Divergence within the *Rhabdomys* genus has been linked to historical environmental change and subsequent vegetation shifts in various regions in southern Africa, particularly across biomes (Le Grange *et al.* 2015; Ganem *et al.* 2012; Meynard *et al.* 2012).

In some localities, multiple species and subspecies can be found living in sympatry and can only be differentiated through molecular testing of nuclear and mitochondrial DNA and karyotyping. This is evident in Fort Beaufort (du Toit *e al.* 2012) where the *R. pumilio* Coastal B clade co-occurs with *R. intermedius* (Wroughton, 1905) and *R. d. chakae* (Figure 1). Similarly, populations of *R. d. dilectus* and *R. bechuanae* (Thomas, 1892) in the Free State also occur in a contact zone (Figure 1; Ganem *et al.* 2012), while in Gauteng contact zones exist between the two *R. dilectus* subspecies (Le Grange *et al.* 2015).

Despite the separation into several species, the genus *Rhabdomys* is a generalist omnivore that consumes seeds, plants and insects (Happold 2013; Monadjem *et al.* 2015). Its diet varies according to habitat, with mesic, grassland species consuming mainly seeds, berries, and herbs and with more protein-rich foods (such as grass seeds and insects) being consumed during the spring and summer months (Schradin 2005). *Rhabdomys pumilio* in the xeric Succulent Karoo consumes plant material from shrubs and succulents year round, but have an abundance of protein-rich foods such as wildflowers, newly emerged plant material and insects during the spring months (Schradin 2005).

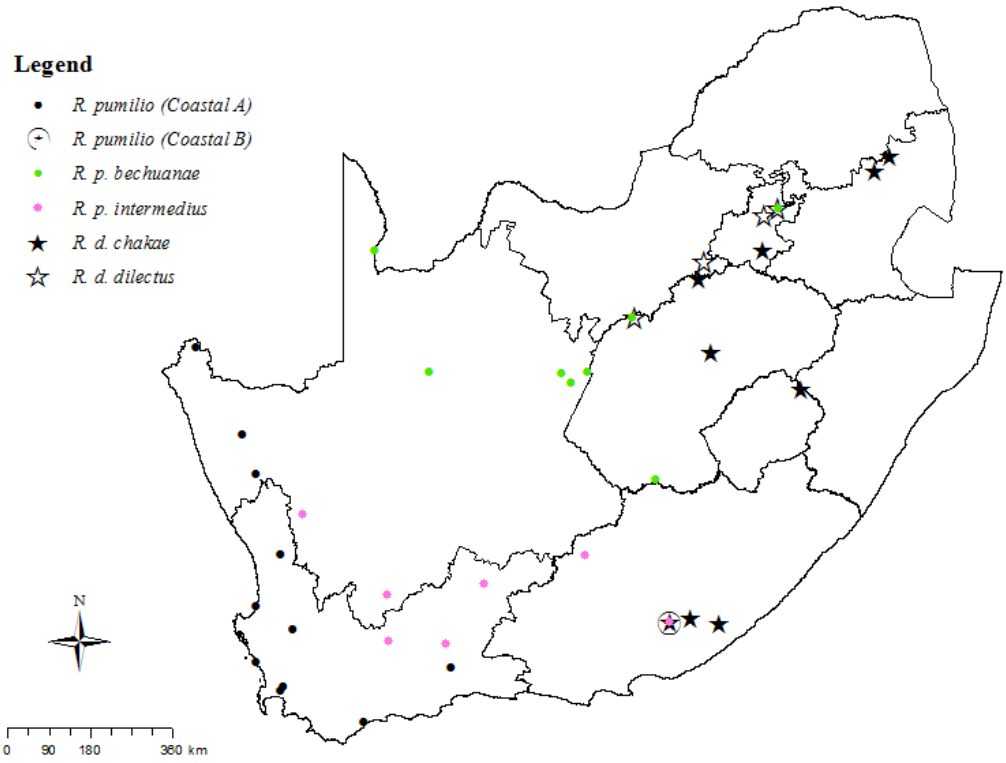


Figure 1.1. Distribution map of the *Rhabdomys* genus in South Africa created using only sampled localities that have been genotyped. The Coastal B clade (indicated with a large circle) is a mitochondrial lineage that is unique to Fort Beaufort; while the Coastal A, Central (*R. p. intermedius*) and Northern (*R. p. bechuanae*) clades are more widely distributed (indicated with small circles). The distributions of the *R. pumilio* clade are approximations based on populations in South Africa that have been genetically identified.

The species also vary behaviourally. For example, in the arid Succulent Karoo, *R. pumilio* is facultatively group-living; groups hold territories comprising of multiple breeding females, a single polygynously breeding male and their progeny of different ages (Schradin & Pillay 2005a). Such colonies are a consequence of high population density leading to habitat saturation because of limited nesting sites (Schradin & Pillay 2004). Groups can disband, resulting in solitary living when population density is low (Schradin et al. 2012). In the mesic grasslands of the Drakensberg foothills, however, the *R. dilectus* occurring here is always solitary and territorial, with male territories overlapping with those of several females and reduced within-sex territorial overlap between females but not males, resulting in a promiscuous mating system (i.e. both females and males mate with several partners; Schradin & Pillay 2005b). Here, the sexes associate only during mating (Schradin & Pillay 2005b).

Home ranges in the arid environment are smaller than in the grasslands but change in size when resource abundance changes (Schradin & Pillay 2005a; Schradin & Pillay 2006).

A cross-breeding study between the two species (above) found reduced interfertility and heightened aggression between males and females of different species (Pillay 2000). In behavioural studies, female *R. d. chakae* (a mesic-adapted species) preferred males of their own species, while *R. pumilio* females preferred males of their own species or males of *R. d. chakae* than males from *R. d. dilectus* (Pillay *et al.* 2006). These studies indicate partial behavioural divergence acting as a pre-mating reproductive barrier.

1.4. Aims and objectives

The aim of my study was to establish the patterns of intraspecific (within population) variation in the cranial morphology of *Rhabdomys dilectus chakae* from Willem Pretorius Nature Reserve in the Free State Province, South Africa. I analysed variation in the skulls, mandibles and dentition using geometric morphometrics. My objectives were to investigate patterns in variation related to 1) allometry, 2) age class, 3) sexual dimorphism, and 4) inter-annual variation (i.e. variation between years sampled). In order to establish the geometric morphometric methods most appropriate for my study, I first conducted a literature review of rodent studies so as to develop an understanding of the application of geometric morphometrics in small rodent systematics.

I predicted that dentition would vary among age classes as the molars became worn through mastication (Renaud 2005). I also predicted shape variation attributable to age in the skulls and mandibles as a result of differences in food hardness of diet with more robust skulls and mandibles in older specimens and more gracile skulls and mandibles younger specimens (Anderson *et al.* 2014). I predicted sexual size dimorphism in skulls with females smaller and more robust than males, as is commonly found in rodents (Astùa *et al.* 2015), although I did not expect to find sexual shape dimorphism in the mandibles, or dentition as rodents, including *Rhabdomys dilectus chakae* from another population (Neves 2015), tend not to show variation in shape (Fadda & Corti 2001). Given the link that has been demonstrated between variable climatic conditions, such as rainfall and temperature, and morphology (Fadda & Corti 2001). I asked whether shape and size would vary inter-annually in the skulls, mandibles and dentition because of inter-annual variation in weather patterns (Nengovhela *et al.* 2015; Renaud 2005).

Chapter 2

A review of Geometric morphometrics methods

The field of morphometrics has undergone a change in techniques from what has been termed "traditional morphometric" approaches to a geometric approach, termed "geometric morphometrics" (Sheets *et al.* 2006). Traditional morphometrics utilises measures of linear morphological characters, such as distances and ratios to analyse variation but can only provide information on the size variation of a structure for any given population. Geometric morphometrics provides a useful method for the analysis of shape (in the anatomy of both plants and animals) through the application of Cartesian coordinates to anatomical loci or to the curves of structures defined on morphological features (Adam *et al.* 2013). Traditional morphometrics cannot provide the spatial, or shape, variation that may be of importance in understanding variation between and among taxa and that are easily obtained through geometric morphometrics (Zelditch *et al*. 2004). Additionally, traditional linear morphometrics are not as sensitive to variability as geometric morphometrics and so linear methods may fail to identify variation when it is present, particularly in rodents where variation may be subtler (Claude 2013). For this reason, I restricted my review to methods of geometric morphometrics, and which is applicable to my research.

In this short review, I assessed the use of geometric morphometrics (hereafter GM) in studies of rodents in order to understand the application of GM methods in rodent systematics and to then apply them to my own research. To do this, I conducted a literature search using appropriate search words ("rodents", "morphological analysis", "geometric morphometrics", "shape analysis", "landmarks", "outline analysis" and "semi-landmark analysis"), and used three public search engines (BioOne, Science Direct, and Web of Science) to find published studies on rodent morphometric studies.

Landmark morphometrics

Landmarks are sets of homologous anatomical points expressed as *xy*-coordinates (when using two-dimensional data) or as *xyz*-coordinates (when using three-dimensional data) that are used to quantify variation in size and shape of different biological structures (Claude 2013). Through the use of the Procrustes superimposition, these coordinates are translated, rotated, and scaled to a uniform centroid size and transformed so as to minimize the Procrustes distance between the landmark configuration of each specimen and the consensus

configuration (Rohlf & Slice 1990). Landmarks are the most commonly used method of form analysis (i.e. analysis of both shape and size) as 62 of the 90 studies that I considered used landmark morphometrics (Table 2.1; studies 1-62). Landmarks were most frequently used in studies that considered variation in crania (studies 1-51) but were also the method most frequently used when studying mandibular form variation as 19 of 29 studies (Table 2.1; studies 38-58) that investigated form change in the mandible used landmark morphometrics. Landmark morphometrics are also the earliest methods used in form analysis and while this might explain the large number of studies that used landmarks to some degree, the first outline study in my review was published only three years later in 2001 (Table 2.1; study 88).

Three types of landmarks are recognized in landmark morphometrics. Type I landmarks are points placed at the intersection of tissues, and most frequently occur at sutures where different bones intersect. Type II landmarks are points of maximum curvature and concavity, and type III landmarks are the anterior-most and posterior-most points of a structure (Bookstein 1991). Type I landmarks are the most easily located, and are thus the most preferred landmarks used, whereas type III landmarks are the least preferred, due to their propensity for bias in the digitization process (Bookstein 1991). The propensity for bias exists due to the inexact anatomical definitions which make the location of Type III landmarks more subjective. Nonetheless, in all the studies that I considered (Table 2.1) which used landmarks (and did not incorporate semi-landmarks in any way; see below) to investigate form change, a combination of all three landmark types was always used for sampling. This is likely because landmark analysis detects variation at the landmark points and not between them (Richtsmeier *et al.* 2005), and therefore any variation occurring at anatomical extrema would not be sampled if the more ambiguous landmarks were excluded.

To obtain any meaningful results, images must be accurately captured, and landmarks must be reliably digitized across specimens, otherwise any information obtained in the analysis will be biased and uninformative (Webster & Sheets 2010). If landmarks are adequately sampled across the structure of interest, there is a high degree of accuracy in the shape analysis (Richtsmeier *et al.* 2005). However, if regions are not sufficiently sampled, any variation, or lack thereof, cannot be assumed to be a realistic explanation of variation (Zelditch *et al.* 2004) which is particularly disadvantageous.

Landmarks must also be homologous and comparable across specimens (Zelditch *et al.* 2004), which can sometimes pose a problem in studies concerning fossils where

Table 2.1. Rodent geometric morphometric studies used in the literature review.

Study No.	Taxon	Analytical method	Skeletal structure	Fossil/Modern	Citation
1	*Neotoma cinerea*	Landmarks	Skull	Modern	Cordero & Eppes 2012
2	*Arvicanthis* sp.	Landmarks	Skull	Modern	Corti & Fadda 1996
3	*Proechimys* spp	Landmarks	Skull	Modern	Corti *et al.* 1998
4	*Arvicanthis* sp.	Landmarks	Skull	Modern	Fadda & Corti 1998
5	*Ctenomys* spp	Landmarks	Skull	Modern	Fernandes *et al.* 2009
6	*Otomys saundersiae*	Landmarks	Skull	Modern	Taylor *et al.* 2005
7	*Urotrichus talpoides*	Landmarks	Skull	Modern	Wilson 2013
8	*Mastomys natalensis*	Landmarks	Skull	Modern	Breno *et al.* 2011
9	*Calomys* spp.	Landmarks	Skull	Modern	Cordeiro-Estrela *et al.* 2016
10	*Thrichomys apereoides*	Landmarks	Skull	Modern	dos Reis *et al.* 2002a
11	*Apodemus flavicollis*	Landmarks	Skull	Modern	Jojiç *et al.* 2011
12	*Thrichomys apereoides*	Landmarks	Skull	Modern	dos Reis *et al.* 2002b
13	*Calomys callosus, Eliurus majori, Mus musculus praetextus, Praomys delectorum, Rattus tanezumi, Rhabdomys pumilio*	Landmarks	Skull	Modern	Jamniczky & Hallgrimsson 2009
14	*Ctenomys* spp.	Landmarks	Skull	Modern	de Freitas *et al*. 2012
15	*Crocidura goliath subspp.*	Landmarks	Skull	Modern	Jacquet *et al.* 2013
16	*Dinaromys bogdanovi*	Landmarks	Skull	Modern	Kryštufek *et al.* 2012
17	*Marmota* spp.	Landmarks	Skull	Modern	Cardini *et al.* 2006
18	*Dasymys* spp.	Landmarks	Skull	Modern	Mullins *et al.* 2004
19	*Aethomys ineptus, Arvicanthis niloticus*	Landmarks	Skull	Modern	Abdel-Rahman *et al*. 2009
20	*Otomys* spp.	Landmarks	Skull	Modern	Taylor *et al.* 2011
21	*Meriones* spp.	Landmarks	Skull	Modern	Yazdi *et al.* 2013
22	*Apodemus speciosus*	Landmarks	Skull	Modern	Shintaku *et al*. 2010
23	*Praomys delectorum*	Landmarks	Skull	Modern	Bryja *et al.* 2013
24	*Gerbilliscus* spp.	Landmarks	Skull	Modern	Abiadh *et al.* 2010
25	*Gerbilliscus* spp.	Landmarks	Skull	Modern	Colangelo *et al.* 2010

Table 2.1. continued…

Study No.	Taxon	Analytical method	Skeletal structure	Fossil/Modern	Citation
26	*Mastomys* spp.	Landmarks	Skull	Modern	Lalis *et al.* 2009
27	*Graomys* spp.	Landmarks	Skull	Modern	Martinez & Di Cola 2011
28	*Apodemus flavicollis*	Landmarks	Skull	Modern	Oleksyk 2004
29	*Ctenomys rionegrensis*	Landmarks	Skull	Modern	D'Antro & Lessa 2006
30	*Tachyoryctes macrocephalus, Sphiggurus mexicanus, Spermophilus* spp.*, Spalax* spp.*, Spalacopus cyanus, Sigmodon* spp.*, Sciurus aberti, Cavia aperea, Rhynchomys soricoides, Rhizomys pruinosus, Rhinosciurus laticaudatus, Rattus* spp.*, Phloeomys cumingi, Petromus typicus, Geomys bursarius,Ondatra zibethicus, Petaurista petaurista, Neofiber allen, Peromyscus maniculatus, Pedetes capensis, Pappogeomys tylorhinus, Oxymycterus dasytrichus, Oryzomys* spp.*, Orthogeomys grandis, Castor* spp.*, Onychomys leucogaster, Oecomys bicolor, Neotoma* spp.*, Nectomys squamipes, Tamias palmeri, Nannospalax leucodon, Myospalax myospalax, Myocastor coypus, Hyomys goliath, Microtus californicus, Melanomys caliginosus, Marmota flaviventris, Mallomys rothschildi, Lemmus trimucronatus, Ichthyomys tweedii, Hydromys chrysogaster, Hydrochoerus*	Landmarks	Skull	Both	Samuels & Van Valkenburgh 2009

Table 2.1. continued…

Study No.	Taxon	Analytical method	Skeletal structure	Fossil/Modern	Citation
	hydrochaeris, Heterocephalus glaber, Heliophobius argenteocinereus, Glaucomys sabrinus, Gerbillurus paeba, Geoxus valdivianus, Georychus capensis, Erethizon dorsatum, Dipus aegypticus, Desmodillus auricularis, Cynomys gunnisoni, Ctenomys conoveri, Cryptomys hottentotes,, Crateromys schadenbergi, Colomys goslingi, Clethrionomys californicus, Chelemys macronyx, Cannomys badius, Bathyergus suillus, Arvicola terrestris, Archboldomys luzonensis, Aplodontia rufa, Anomalurus derbianus, Ammospermophilus leucurus, Aconaemys fuscus, Tachyoryctes splendens, Tamiasciurus hudsonicus, Thomomys talpoides, Uromys caudimaculatus, Coendou prehensilis				
31	*Tachyoryctes*	Landmarks	Skull	Modern	Boelchini & Corti 2004
32	*Malacomys* spp.	Landmarks	Skull	Modern	Bohoussou *et al.* 2015
33	*Mastomys natalensis*	Landmarks	Skull	Modern	Lalis *et al.* 2015
34	*Graomys*	Landmarks	Skull	Modern	Martinez & Gardenal 2016
35	*Scaptermys tumidus*	Landmarks	Skull	Modern	Quintela *et al.* 2016
36	*Meriones* spp.	Landmarks	Skull	Modern	Yazdi *et al.* 2015
37	*Thrichomys asperoides*	Landmarks	Skull	Modern	Costa *et al.* 2004
38	*Cavia aperea, Galea leucoblephara, Microcavia australis, Dolichotis patagonum, Pediolagus salinicola,*	Landmarks	Skull Mandible	Modern	Alvarez *et al.* 2015

Table 2.1. continued…

Study No.	Taxon	Analytical method	Skeletal structure	Fossil/Modern	Citation
	Hydrochoerus hydrochaeris, Kerodon rupestris, Dasyprocta sp.*, Cuniculus paca, Chinchilla* sp.*, Lagidium viscacia, Proechimys guyannensis, Octodon* spp.*, Myocastor coypus, Thrichomys* sp.*, Aconaemys* spp.*, Abrocoma cinerea complex, Lagostomus maximus, Spalacopus cyanus, Pipanacoctomys aureus, Octomys mimax, Octodontomys gliroides, Tympanoctomys barrerae, Ctenomys* spp.				
39	*Apodemus* spp.	Landmarks	Skull Mandible	Modern	Jojic *et al.* 2012
40	*Galea leucoblephara, Microcavia australis, Dolichotis patagonum, Pediolagus salinicola, Hydrochoerus hydrochaeris, Cavia aperea, Kerodon rupestris, Cuniculus paca, Chinchilla* sp.*, Lagidium viscacia, Proechimys guyannensis, Octodon* spp.*, Myocastor coypus, Thrichomys* sp.*, Aconaemys* spp.*, Abrocoma cinerea, Lagostomus maximus, Spalacopus cyanus, Pipanacoctomys aureus, Octomys mimax, Octodontomys gliroides, Tympanoctomys barrerae, Ctenomys* spp.	Landmarks	Skull Mandible	Modern	Alvarez & Perez 2013
41	*Ctenodactylus* spp.*, Felovia vae, Massoutiera mzabi, Laonastes*	Landmark	Skulls Mandible	Modern	Hautier *et al.* 2012

Table 2.1. continued…

Study No.	Taxon	Analytical method	Skeletal structure	Fossil/Modern	Citation
	aenigmamus, Abrocoma spp*., Capromys* spp*., Geocapromys brownie, Hydrochaerus hydrochaeris, Kerodon rupestris, Dolichotis patagonum, Galea spixii, Cavia* spp*., Microcavia australis, Lagostomus* spp*., Chinchilla lanigera, Logidium* spp*., Ctenomys* spp*., Myoprocta* spp*., Dasyprocta* spp*., Dinomys branicki, Chaetomys subpinosus, Echimys chrysurus, Mesomys hispidus, Myocaster coypus, Proechimys* spp*., Trichomys aperoides, Coendou* spp*., Erethizon dorsatum, Shiggurus mexicanus, Atherurus* spp*., Hystrix* spp*., Thecurus spp., Spalacopus* spp*., Trichys lipura, Octodon* sp*., Octodontomys gliroides, Petromus typicus, Thryonomys swinderianus*				
42	*Apodemus speciosus*	Landmarks	Skull Mandible	Modern	Shintaku & Motokawa 2016
43	*Peromyscus spp.*	Landmarks	Skull Mandible	Modern	McPhee 2003
44	*Spermophilus spp.*	Landmarks	Skull Mandible	Modern	Gunduz *et al.* 2007
45	*Calomyscus spp.*	Landmarks	Skull Mandible	Modern	Akbarirad *et al.*2016
46	*Hydrochoerus spp.*	Landmarks	Skull Mandible	Modern	Aeschbach *et al.* 2016

Table 2.1. continued…

Study No.	Taxon	Analytical method	Skeletal structure	Fossil/Modern	Citation
47	*Octodon spp., Echimys* spp*., Abrocoma* spp*., Ctenomys spp., Octomys* spp*., Prospaniomys* spp*., Euryzygomatomys* spp*., Kannabateomys* spp*., Myocastor* spp*., Proechimys* spp*., Thrichomys* spp*., Aconaemys spp., Clyomys* spp*., Octodontomys* spp*., Spalacopus* spp*., Tympanoctomys* spp.	Landmarks	Skull Mandible	Both	Alvarez & Arnal 2015
48	*Marmota* spp.	Landmarks Landmarks Outline (Eigenshape)	Skull Mandible Molars	Modern	Caumal *et al.* 2005
49	*Mus cypriacus*	Landmarks Outline (EFT) Outline (EFT)	Skull Mandible Molars	Modern	Cucchi *et al.* 2006
50	*Rattus* spp.	Landmarks Outlines (EFT)	Skull Molar	Modern	Claude 2013
51	*Mus musculus domesticus*	Landmarks Outlines (EFT)	Skull Molars	Modern	Kamilari *et al.* 2013
52	*Sylvaemus uralensis, Myodes glareolus*	Landmarks	Mandible	Modern	Bol'shakov *et al.* 2015
53	*Euryzygomatomys spinosis, Trinomys* spp*., Thrichomys aperoides, Isothrix bistriata, Lonchothrix emiliae, Phyllomys brasiliensis, Makalata armata, Trinomys* spp.	Landmarks	Mandible	Modern	Monteiro *et al.* 2005
54	*Cavia* spp*., Galea spp., Tympanoctomys* spp*., Kerodon* spp*., Dolichotis* spp*., Pediolagus* spp*., Hydrochoerus* spp*., Dasyprocta* spp*., Cuniculus spp.,*	Landmarks	Mandible	Modern	Alvarez & Perez 2013

Table 2.1. continued…

Study No.	Taxon	Analytical method	Skeletal structure	Fossil/Modern	Citation
	Chinchilla spp., Lagidium spp., *Lagostomus* spp., *Abrocoma* spp., *Myocastor spp., Microcavia spp., Proechimys* spp., *Thrichomys* spp., *Aconaemys* spp., *Ctenomys* spp., *Octodon spp., Octomys* spp., *Pipanacoctomys* spp., *Spalacopus* spp.				
55	*Sciurus Niger*	Landmarks	Mandible	Modern	Swiderski 2003
56	*Mus domesticus*	Landmarks	Mandible	Modern	Leamy *et al.* 2001
57	*Mus musculus*	Landmarks	Mandible	Modern	Klingenberg & McIntyre 1998
58	*Myosorex* spp.	Landmarks	Mandible	Both	Matthews & Stynder 2011a
59	*Microtus californicus*	Landmarks	Molars	Modern	McGuire 2010
60	*Microtus* spp.	Landmarks	Molars	Both	Wallace 2006
61	*Microtus* spp.	Landmarks	Molars	Both	McGuire *et al.* 2011
62	*Aethomys* spp.	Landmarks	Molars	Both	Matthews & Stynder 2011b
63	*Mus* spp.	Landmarks & Semi-landmarks	Skull	Modern	Macholan *et al.* 2008
64	*Belomys pearsonii, Petaurista spp., Pteromys volans, Hylopetes alboniger, Sciurus vulgaris, Callosciurus erythraeus, Tamiops* spp., *Dremomys* spp., *Spermophilus* spp., *Tamias sibiricus, Marmota* spp., *Trogopeterus xanthipes, Ratufa bicolor, Callosciurus pygerythrus, Menetes berdmorei, Sciurotamias davidianus, Aeretes melanopterus, Aplodontia rufa, Graphiurus murinus, Glis glis, Glirulus*	Landmarks & Semi-landmarks	Skulls	Modern	Lu *et al.* 2014

Table 2.1. continued…

Study No.	Taxon	Analytical method	Skeletal structure	Fossil/Modern	Citation
	japonicas, Eliomys quercinus, Dryomys nitedula, Muscardinus avellanarius				
65	*Crocidura* spp.	Landmarks & Semi-landmarks	Mandible	Both	Cornette *et al.* 2015
66	*Mus*	Landmarks & Semi-landmarks	Mandible	Modern	Renaud *et al.* 2015
67	*Ogmodontomys* spp.	Landmarks & Semi-landmarks	Molars	Fossil	Marcolini *et al.* 2009
70	*Karnimata sp., Progonomys* sp.	Landmarks & Semi-landmarks	Molars	Fossils	Kimura *et al.* 2013
71	*Mus musculus*	Landmarks & Semi-landmarks Outlines (Unspecified)	Molars Molars	Modern	Ledevin *et al.* 2016
72	*Arvicola terrestris, Microtus* spp.	Semi-landmarks Outlines (Eigenshape)	Molars	Modern	Polly *et al.* 2011
73	*Marmota* spp.	Outlines (Eigenshape)	Molars	Fossils	Polly 2003
74	*Arvicola cantiana*	Outlines (CDFT)	Molars	Both	Escude *et al.* 2008
75	*Arvicola* spp., *Microtus* spp.	Outlines (CDFT)	Molars	Modern	Escude *et al.* 2013
76	*Gliridae, Ctenodactylidae, Dipodidae, Anomaluridae, Cricetidae, Nesomyidae, Muridae, Pedetidae*	Outlines (EFT)	Mandible	Modern	Hautier *et al.* 2008
77	*Hypnomys, Eliomys*	Outlines (EFT)	Mandible	Both	Hautier *et al.* 2009
78	*Apodemus sylvaticus*	Outlines (EFT)	Mandible	Modern	Renaud & Michaux 2007
79	*Rattus rattus*	Outlines (EFT)	Mandible	Modern	Bover *et al.* 2010
80	*Progonomys clauzoni*	Outlines (EFT)	Molars	Fossil	Lazzari *et al.* 2010
81	*Anthracomys, Castillomys, Castomys, Huerzelerimys, Occitanomys, Paaraethomys, Progonomys, ,*	Outlines (EFT)	Molars	Both	Cano *et al.* 2013

Table 2.1. continued…

Study No.	Taxon	Analytical method	Skeletal structure	Fossil/Modern	Citation
	Rhagapodemus, Stephanomys Abditomys, Chropodymus, Golunda, Hadromys, Haeromys, Hapalomys, Hyomys, Kadarsanomys, Leporillus, Mallomys, Mastacomys, Melomys, Millardia, Papagonomys, Pelomys, Phloemys, Pogonomys, Solomys,Spelaeomys, Uromys, Vandeluria, Aethomys, Anisomys, Apodemus, Apomys, Arvicanthis, Bandicota, Bunomys, Coccymys, Crateromys, Dasymys, Eropeplus, Grammomys, Hybomys, Hylomyscus, Leggadina, Lemniscomys, Lenomys, Leopoldomys, Lorentzimys, Malacomys, Margaretamys, Mastomys, Maxomys, Micromys, Mus, Niviventer, Notomys, Oenomys, Potecheir, Praomys, Pseudohydromys, Pseudomys, Rattus, Rhabdomys, Stochomys, Sundamys, Thallomys, Thammomys, Tokudaia, Zelotomys, Zyzomys, Archboldomys, Colomys, Crossomys, Crunomys, Chrotomys, Echiothirx, Hydromys, Leptomys, Melasmothrix, Parahydromys, Paulamys, Rhynchomys, Sommeromys, Tateomys, Anthracomys, Castillomys, Castromys, Huerzelerimys, Occitanomys, Paraethomys, Progonomys,				

Table 2.1. continued…

Study No.	Taxon	Analytical method	Skeletal structure	Fossil/Modern	Citation
	Rhagapodemus, Stephanomys				
82	*Mus* spp.	Outlines (EFT)	Molars	Both	Michaux *et al.* 2007a
83	*Mus*	Outlines (EFT)	Molars	Both	Stoetzel *et al.* 2013
84	*Myodes glareolus*	Outlines (EFT)	Molars	Modern	Guerecheau *et al.* 2010
85	*Aethomys* spp., *Apodemus* spp., *Arvicanthis spp., Bandicota bengalensis, Berylmys bowersii, Chiromyscus chiropus, Dasymys* spp., *Chiropodomys gliroides, Colomys goslingi, Crateromys heaneyi, Dephomys eburnea, Golunda ellioti, Hapalomys longicaudatus, Hydromys chrysogaster, Hylomyscus stella, Lamottemys okuensis, Lemniscomys barbarus, Lenothrix canus, Leopoldamys edwardsi, Malacomys* spp., *Mastomys* spp., *Micromys minutus, Millardia meltada, Muriculus imberbis, Mus* spp., *Nesokia indica, Notomys alexis, Oenomys hypoxanthus, Otomys* spp., *Pelomys fallax, Phloemys cumingi, Pitecheir melanurus, Praomys* spp., *Rattus* spp., *Rhabdomys pumilio, Rhynchomys* sp., *Stenocephalemys* spp., *Sundamys muelleri, Thallomys paedulcus, Thamnomys rutilans, Tokudaia osimensis, Vandeleuria oleracea, Zelotomys hildegardeae, Acomys cahirinus, Deomys ferrugineus, Lophuromys flavopunctatus, Uranomys*	Outlines (EFT/RFT)	Mandible	Modern	Michaux *et al.* 2007b

Table 2.1. continued…

Study No.	Taxon	Analytical method	Skeletal structure	Fossil/Modern	Citation
	ruddi, Gerbillus pyramidum, Meriones shawi, Tatera guineae, Dendromus sp.*,Dendroprionomys rousseloti, Steatomys* sp.*, Clethrionomys, Microtus spp., Ondatra zibethicus, Nectomys squamipes, Nesoryzomys* sp.*, Neusticomys oyacpocki, Rhizomys pruinosus*				
86	*Apodemus sylvaticus, Stephanomys*	Outlines (EFT/RFT)	Molars	Both	Renaud *et al*. 2006
87	*Mus musculus domesticus*	Outlines (RFT)	Mandible	Modern	Renaud & Auffray 2009
88	*Apodemus* spp.	Outlines (RFT)	Mandible	Modern	Renaud & Millien 2001
89	*Stephanomys ramblensis, Occitanomys* spp.	Outlines (RFT)	Molars	Fossil	Renaud & Van Dam 2002
90	*Apodemus sylvaticus*	Outlines (RFT)	Mandible Molars	Modern	Renaud 2005

specimens may not necessarily be intact (Arbour & Brown 2014). In such cases, it may then be beneficial to include semi-landmarks or use outline methods instead. Studies that investigated form variation in fossils used either semi-landmark methods or outline methods, with two exceptions. The two studies that used landmark analysis were, however, conducted on the molars of species of fossil *Microtus* which provide more easily defined positions for landmarks due to the complexity in cusps (consisting of lingual triangles; Ledevin *et al.* 2010b) than the molars of other rodent species.

Semi-landmark morphometrics

Sometimes the use of type III landmarks is unavoidable because specimens may have limited type I and type II landmark points available (Mitteroecker & Gunz 2009). Incorporating type III landmarks can lead to a loss of shape information due to the digitizing inaccuracies that result from observer error (Escude *et al.* 2013). One way to overcome the deficiencies of incorporating type III landmarks is to use semi-landmarks (Zelditch *et al.* 2004). Ten studies used semi-landmarks in their analyses, with studies 63-71 (Table 2.1) using a combination of landmarks and semi-landmarks in conjunction with one another, while study 72 used semi-landmarks alone. Two of the nine studies (63 and 64) that used a combination of landmarks and semi-landmarks analysed skulls, a further two (studies 65 and 66) analysed mandibles and the remaining five analysed molars (studies 67-71). The single study (study 72) that used semi-landmarks alone analysed molars (Table 2.1).

Semi-landmark points are not fixed in the same way that landmark points are, but are, instead, slid along the curve (if using two-dimensional data) or surface (if using three-dimensional data) in relation to one another during analysis (Adams *et al.* 2013). Semi-landmarks are slid along curves and surfaces with the aim of minimising the Procrustes distance (Rohlf & Slice 1990) or the bending energy (Bookstein 1989) between the consensus configuration and the specimen's shape configuration.

Semi-landmarks also differ from landmarks in that while the curves that are used for semi-landmarks must be homologous between specimens, the points do not have to be homologous themselves (Bookstein *et al.* 2002). This is especially helpful in paleontological studies where specimens may not always be completely intact or contain the same clear homologous landmark points (Cornette *et al.* 2015). By including semi-landmarks in landmark analyses, we are able to gain more information about the shape of curves (Zelditch *et al*. 2004) and overall more shape information than we might have obtained with only a few

landmark points (Sheets *et al* 2004). While the use of semi-landmarks provides the advantage of sampling curves that might not have been sampled through the use of landmarks alone, an important drawback is that semi-landmarks do not provide the same amount of information as landmarks (Zelditch *et al.* 2004). They thus have to be down-weighted when used in conjunction with landmarks or they may introduce error into the data (Zelditch *et al.* 2004).

Outline morphometrics

When there are too few anatomical points for landmark-based analysis, outlines can be used to study variation in curved structures instead (Escude *et al.* 2013). Like with closed curves, outlines are valuable only when the internal components of a structure (i.e. those not part of the outline) are not of interest (Zelditch *et al.* 2004). Outline methods thus tend not to be used in studies of skulls because morphological structures within the outline such as the incisive foramen, molar rows, and tympanic bullae are usually of interest. Instead, outlines seem to be most frequently utilised when analysing molars (Table 2.1, studies 48-51 and 71-90). The occlusal surface of molars tends to be heavily impacted by wear and, as such, homologous points become difficult to place (Renaud 2005). Outline methods are less sensitive to artefacts of wear than landmark methods and are therefore preferred when analysing molar shape variation (Renaud *et al.* 1996).

The Elliptical Fourier Transform (EFT) method is the most frequently used statistical method for outline analysis with 12 of the 24 (Table 2.1, studies 49-51 and 76-84) outline-based studies using this method of analysis. Four studies used the Radial Fourier Transform (RFT) method (studies 87-90), although two studies used a combination of EFT and RFT methods (studies 85 and 86). Three studies used Eigenshape analysis (studies 48, 72, and 73), two studies used the Complex Discrete Fourier Transform (CDFT) method (studies 74 and 75) and one study did not indicate the method that was used for analysis (study 71).

The EFT method of Fourier Analysis is based on the separate decomposition of the incremental changes of the coordinates as a function of the cumulative outline length through the use of ellipses (Kuhl & Giardina 1982). Anatomical points do not have to be homologous or comparable across specimens, like as with landmark-based analysis, because variation in the curves are of interest (Zelditch *et al.* 2004). Points along the outline do not necessarily have to be equally spaced (Rohlf & Archie 1984), and the final coefficients used in the analysis can be normalized for size (Bonhomme *et al.* 2014). The EFT method also allows for highly accurate reconstructions of molar shapes from the Fourier coefficients, using the

inverse Fourier transform method for visualization purposes (Rohlf & Archie 1984). This method is however sensitive to noise due to error that may be present in the outline (Haines & Crampton 2000) and because it uses a series of ellipses to estimate shape, it deals poorly with pointed shapes (Zelditch *et al.* 2004). However, despite the clear disadvantages of the EFT method, the frequency of the use of the EFT method (Table 2.1, studies 76-79) was almost equal to that of the Radial Fourier Transform (RFT) method in my review of the literature of shape variation in mandibles.

The RFT method is based on the decomposition of the radii calculated as the distance between the centroid and the points on the outline (Zahn & Roskies 1972). It is able to analyse more complex curves from pointed shapes, although it is not as useful for shapes that have many concave curves as there is no single centroid point (Rohlf & Archie 1984). This may explain why the RFT (Table 2.1, studies 87, 88, and 90) and EFT (studies 76-79) methods appear to be used almost equally as frequently in mandibular outline analysis since both have clear disadvantages. The RFT also allows for a moderately accurate reconstruction of outlines using the inverse Fourier transform (Renaud & Michaux 2003), although these reconstructions are not as accurate as those reconstructed using the Fourier coefficients from the EFT analysis (Michaux *et al.* 2007a). Only four studies used the RFT method, studies 87, 88, and 90 analysed variation in mandibles, and studies 89 and 90 used this method in molars.

Two additional methods were found in the literature, which were used far less frequently for unknown reasons. Studies 48, 72, and 73 (Table 2.1) used Eigenshape analysis which derives orthogonal shape functions through the use of a principal components analysis and uses these functions to test for variation among specimens (Lohmann 1983). Studies 74 and 75 used the Complex Discrete Fourier Transform method, which allows complex curves to be treated as they would be using the EFT method, by representing the outline as a complex number (Table 2.1).

Conclusion

Each geometric morphometric method has its own advantages and disadvantages which influences the type of analysis conducted. Based on my appraisal of the literature, I chose to use landmarks to analyse the skulls (in both ventral and lateral view) and the mandibles for shape variation in my study. Because semi-landmarks provide a better understanding of curves, I used semi-landmark analysis to analyse shape variation in the curves of the mandibles. Murid rodents have molars that are fairly simple, with very few anatomical loci

for landmark placement, and have occlusal surfaces that are heavily altered through wear (Renaud *et al.* 1996), and I thus used outline analysis to analyse the molars.

Chapter 3

Methods and Materials

Specimens

One hundred and seventy adult specimens (specimens with fully erupted third cranial molars) of *Rhabdomys dilectus chakae* were loaned from the National Museum in Bloemfontein. These specimens were collected from the Willem Pretorius Nature Reserve (27˚13'56.38"E; 28˚18'26.14"S) in the Free State Province between February 1994 and March 1997, with two additional specimens collected in August 1975.

The *Rhabdomys* population at Willem Pretorius Nature Reserve was genotyped by du Toit *et al.* (2012) and determined to be a single population of *Rhabdomys dilectus chakae,* which makes it particularly suitable for this analysis because there was no uncertainty over species assignment. At least two contact zones and syntopy between *Rhabdomys* species have been located at other locations in the Free State Province (Ganem *et al.* 2012). By using a population that could confidently be assigned to one species, I was able to control for any variation that may have resulted due to incorrect species identification and interspecific variation. Using specimens from a single population also controlled for any geographic variation, i.e. variation which results from differences in geographically separated populations that may experience different environmental pressures, and which might impact the variation in the shape of the crania, mandibles, and dentition.

Specimens with crania, mandibles, and dentition that were damaged, and therefore missing homologous anatomical landmark or curve points, were excluded from the analyses. As such, the number of specimens eventually used in my study varied as follows: 159 specimens in the ventral skull data set, 159 specimens in the lateral skull data set, 116 specimens in the mandible data set, and 169 specimens for the molar row data set. As a result of the damage present in some specimens, the mandibles from the two specimens from 1975 were not included in my analyses. As such year of sampling for the mandible consists only of specimens from 1994 to 1997.

The National Museum of Bloemfontein also provided sex and year of capture information for each of the loaned specimens and this information along with age class were the variables I tested for variation in relation to/association with size and shape.

Aging

Henschel *et al.* (1982) described five age classes for *Rhabdomys pumilio* based on patterns of molar wear, comprising of one juvenile and four adult age classes. The juvenile age class that these authors described referred to individuals without fully erupted third molars. Since my study was concerned with adult specimens, the first age class was excluded, leaving the four adult classes. Specimens were aged by the degree of wear on the left cranial molar row (Table 3.1), and age classes used ranged from little to no wear on the cusps to molars with very little to no evidence of cusps left (Figure 3.1).

Table 3.1. Definitions of age classes defined by degree of tooth wear by Henschel *et al.* (1982). Only adult specimens with fully erupted third molars were considered in my study. The first to third molars have been abbreviated M_1, M_2, and M_3 respectively

Age	Definition
Class I	Little to no wear evident on the molar cusps, cusps on all three molars are defined with little dentine visible
Class II	Moderate wear on cusps, to the degree that the middle cusps of M_1 and M_2 have merged wear surfaces
Class III	Considerable wear on molar cusps, only slight presence of merged cusps visible on M_1 and M_2; M_3 only have small remnants of cusps visible
Class IV	Cusps completely worn on M_2 and M_3, only small remnants of cusps visible; M_1 has only slight evidence of cusps with most of the occlusal surface worn

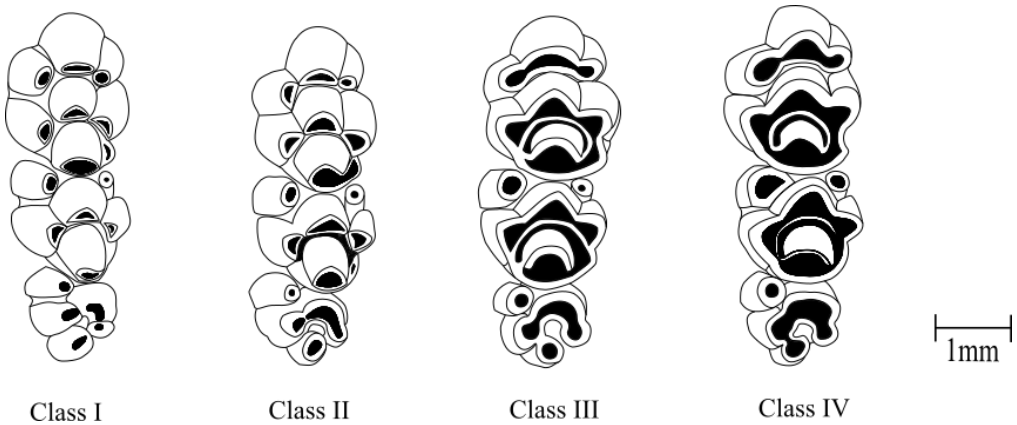


Figure 3.1. Adult age classes (by Henschel *et al.* 1982) based on the degree of tooth wear of the molar cusps of the cranial molar row.

Image capturing and digitization

Images were captured for the ventral skull, left and right sides of the lateral skull (at 5x magnification), the right and left lateral aspect of the mandible (at 6.8x magnification), and the occlusal surface of the left cranial molar rows (at 10.5x magnification), using a Discovery V12 Stereoscopic microscope (Zeiss, Germany) and were saved as .TIFF files. A scale bar was captured for each image to provide a reference for the size of each morphological structure. Specimens were then re-photographed, which allowed me to calculate any measurement error associated with the reorientation of the specimens by comparing image-capturing accuracy between and digitization error within the two sets of images. To ensure uniform orientation of the skulls and mandibles, each structure was placed on a bed of small black beads (0.8mm in diameter) in a ceramic crucible (7.6 cm in diameter), which allowed for easy manoeuvrability of the specimen and provided a 'mould' for the placement from one specimen to another.

I created .TPS files for each of the data sets using *tpsUtil 1.70* (Rohlf 2015a) and then used *tpsDig2* (Rohlf 2015) to digitize two-dimensional landmarks for the skull in ventral view (Figure 2a; see Appendix 1a for landmark definitions), the skull in lateral view (Figure 2b; see Appendix 1b for landmark definitions), and the mandible in lateral view (Figure 2c; see Appendix 1c for landmark definitions). Semi-landmarks for the mandible data set and outlines for the occlusal surface of the molars were also digitized using *tpsDig2* (Rohlf 2015b).

Links files were created for each dataset in *tpsUtil 1.70* (Rohlf 2015a), connecting landmarks that follow on from one another. A paired landmarks file was also created in *tpsUtil 1.70* (Rohlf 2015a) for the ventral skull data set. Because the ventral skull has object symmetry, instead of the matching symmetry found in the lateral skull and mandible, it was necessary to indicate which landmarks were left-right pairs to allow the effect of asymmetry to be calculated (Klingenberg *et al.* 2002).

Landmark analyses for the Ventral Skull, Lateral Skull, and Mandible

Landmarks were chosen to ensure adequate coverage of the skulls and mandibles and were selected based on those most commonly found in the literature (Shintaku & Motokawa 2016; Anderson *et al.* 2014; Jojić *et al.* 2012; Jojić *et al.* 2011; Lalis *et al.* 2009; Samuels 2009; Cardini & Tongiorgi 2003) and a sample of 30 specimens for each dataset was digitized and analysed for imaging and digitization measurement error (ME). Each of the two images that were taken were digitized twice for each specimen in the sample and the four repeats were

then analysed using a Procrustes ANOVA (Klingenberg & McIntyre 1998). The Procrustes ANOVA separated the variance into within- and among-individual components (i.e. variance between images and digitizations of individual specimens, and variance among specimens themselves) as described by Bailey & Byrnes (1990).

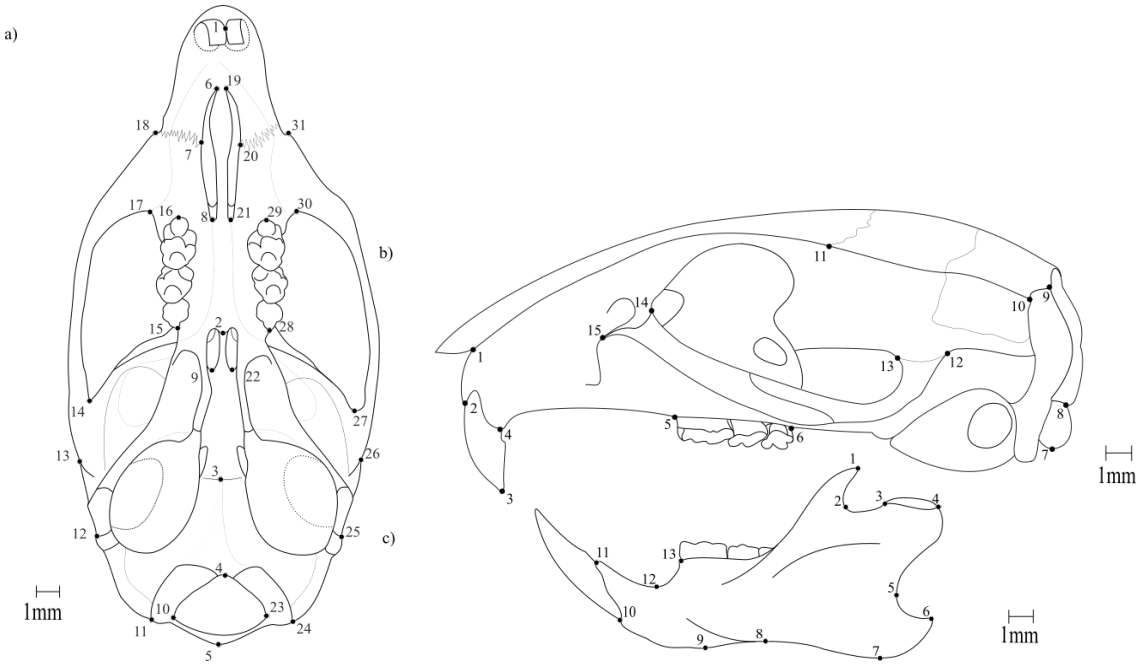


Figure 3.2. Landmark placement for: a) the ventral view of the skull (31 landmarks); b) the lateral view of the skull (15 landmarks); and c) the lateral view of the mandible (13 landmarks).

The percentage ME was then calculated by dividing the within-mean square (MS) by the sum of the within- and among-mean square multiplied by 100. Measurement error for the ventral skull, lateral skull, and mandible was found to be below the suggested 15% or murid rodents (Abdel-Rahman *et al.* 2009; Polly 2001; Bailey & Byrnes 1990; see Appendix 2 for ME results) and so each set of images for each structure was digitized only once.

Because the ventral aspect of the skull has object symmetry instead of the matching symmetry of the mandible and lateral aspect of the skull (Klingenberg *et al.* 2002), both left and right sides of the skull were digitized on the same image for two images per individual. The matching symmetry of the lateral aspect of the skull and mandible therefore resulted in four images per specimen, two for each side. These specimens were therefore digitized once per image, with two images of each side (i.e. left and right) for the lateral aspect of the skull and mandible (providing two replicates of either side for each individual).

After digitization was completed for both image replicates for the ventral, and lateral skull, and the mandible, I read the .TPS files into *RStudio* (R Core Team 2014) and used the Generalized least-squares Procrustes Analysis (GPA) method (Rohlf & Slice 1990) for bilateral symmetry to eliminate non-shape related variation in the landmark configurations in the *Geomorph* package (Adams *et al.* 2017) in *RStudio*. The GPA does this by rotating, transforming and scaling all configurations to a common centroid size (Zelditch *et al.* 2004), using the first specimen in the data set as a reference configuration. After all specimens had been configured, the average shape was calculated, and all specimens were then reconfigured using the new centroid size as the template (Adams *et al.* 2004). Variation was then separated into asymmetric and symmetric variation present in the data set. Within the asymmetric component of variation, the asymmetry resulting from biologically significant, fluctuating asymmetry (variation between the interaction the individual*side factors) and directional asymmetry (between different sides of the specimens) were calculated using a Procrustes ANOVA in the *Geomorph* package (Adams *et al.* 2017). The Procrustes ANOVA found significant differences for the sides factor, as well as the individual:side interaction for at least one of the components for each morphological unit. Therefore, all further analyses were conducted on the left half of the skulls and mandibles (see Appendix 3 for asymmetry ANOVA results) to limit the effects of asymmetry.

After the asymmetric and symmetric components had been separated, I used a MANOVA (the *Geomorph* package) on the symmetric component data to analyse shape variation with sex, age, and year as explanatory variables. This was done for the ventral skull, lateral skull, and mandible independently. Where significant differences for the independent factors were found, I used a Procrustes ANOVA with pairwise comparison of homogeneity of slopes tests to determine where the differences in shape occurred.

Centroid sizes were extracted for all specimens in a data set and a MANOVA was used to test for variation in sex, age and year in relation to size, and, where significant factors were found, I used a Procrustes ANOVA with pairwise comparison of homogeneity of slopes to determine where the significant differences occurred. Box plots were created to display centroid size variation in the explanatory variables graphically. An allometric regression was used to test for associations between shape (as the regression scores of the Procrustes-aligned coordinates) and size (log-centroid size). From the multivariate regression, I obtained allometry-free residuals, and these were used to visualize the scatter of variation among specimens in shape space using a Principal Component Analysis (PCA; *Geomorph* package) for each data set. The cumulative proportion of variation explained by the PC axes for

approximately 95% of shape variation was 21 PCs for the ventral skull, 18 for the lateral skull, and 15 for the mandible (Appendix 5). Shape variation among specimens was visualized using relative warp plots as they show variation from the average shape (consensus configuration) as deformations on grids.

Analysis of semi-landmarks for the Mandible

Semi-landmark analyses were conducted for the mandibles for all specimens with intact mandibles. Since the semi-landmark protocol can sample curves, I tested the variation of curve shape in the mandibles (Gunz & Mitteroecker 2013), while still weighting those landmarks that were included. From the landmark analysis, type III landmarks, i.e. those points defined in relation to other points, which can be more ambiguous than other types of landmarks, were excluded from the sliding landmark analysis. The semi-landmarks were used to more effectively sample these curves, instead. I thus used seven landmarks and 38 sliding semi-landmarks along five curves on the mandibles (Figure 3.3) for my analysis.

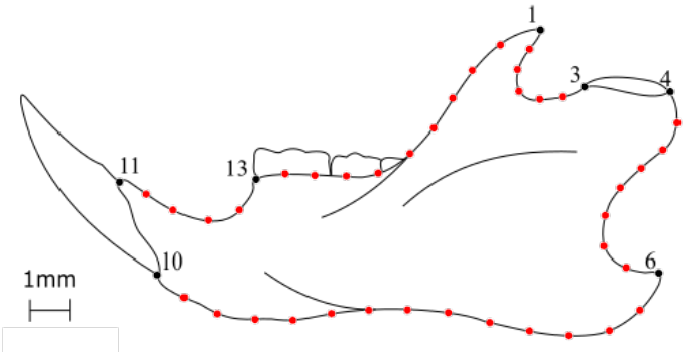


Figure 3.3. Landmarks and semi-landmarks used in the semi-landmark analysis of the lateral view of the mandible. Seven landmarks (indicated by black points) and 38 sliding semi-landmarks (indicated by red points) over five curves were used in this analysis.

Using *tpsUtil* (Rohlf 2015a), I created a slider file for each structure and *tpsDig2* (Rohlf 2015b) to digitize the semi-landmark points. This slider file was used to differentiate the semi-landmarks from the landmarks during the analysis in *Geomorph* (Adams *et al.* 2017). The average mandibular shape (which serves as the reference shape) was estimated from all semi-landmarks and landmarks by GPA (Sheet *et al.* 2004). In the GPA, semi-landmarks were slid along the outline of a structure between landmarks until they matched (as smoothly as they could) the semi-landmarks on the reference configuration (Adams *et al.* 2004). The aligned coordinates for the landmarks and semi-landmarks were then used in a MANOVA to analyse shape variation related to sex, age, and year and a pairwise comparison

of homogeneity of slopes test was used to determine where the differences in shape occurred. A MANOVA with centroid size as a dependent factor was used to analyse size variation related to sex, age, and year. A pairwise comparison of homogeneity of slopes was used to determine where differences in size occurred. Using a multivariate regression, the effects of allometry on shape was analysed with the symmetric component of variation regressed onto log-transformed centroid size. To visualize shape variation, I computed a PCA and TPS deformation grids of the extremes in shape variation among the specimens. A cumulative percentage of 95% of variation was found in the first 20 PC axes (Appendix 5).

Analysis of Molar Outlines

The scale was set for each image in *tpsDig2* (Rohlf 2015b) using the scale bar in the original .TIFF images and curves were digitized using the "draw curves" tool to digitize curve points in the closed outline around the molar. The starting point of the molar outline was the most anterior point of the first cusp of molar and points were digitized in a clockwise direction. Since the occlusal surface of molars are directly affected by wear, digitization was focused at the base of the crown of the molars (Renaud 2005). Outline points were overestimated in the digitization but were then resampled to 64 equidistant points for each outline for both sets of left molar images to calculate the measurement error associated with the digitization process (Figure 3.4). The number of points most commonly used in the literature (Lazzari *et al.* 2010; Guerecheau *et al.* 2010; Renaud *et al.* 2006) was 64, and after resampling, I found 64 points provided sufficient coverage of the outline.

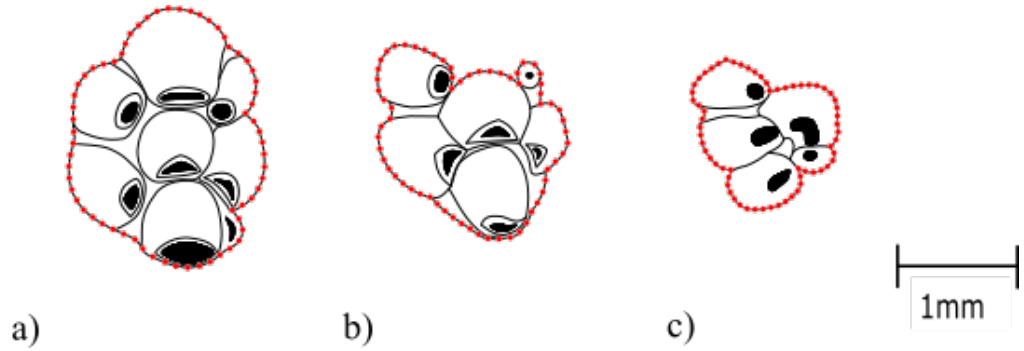


Figure 3.4. Outlines of the left upper molars with 64 equidistant points (red dots) digitized on a) the first upper molar, b) the second upper molar, and c) the third upper molar.

I analysed the outlines using the Elliptical Fourier Analysis (EFA) method in *Momocs*, by calculating harmonic coefficients from the imported .TPS file. To determine the number of harmonics to retain, I calculated the mean sums of squares for the coefficients of

each harmonic. I calculated the cumulative harmonic Fourier power and plotted this against the harmonic ranks using the functions from the '*Momocs'* package (Bonhomme *et al.* 2014) in *RStudio.* The cumulative harmonic Fourier power spectrum provided a measure of how much shape information was explained as harmonic rank increased (Appendix 4). I thus retained the second to seventh harmonics for the first upper molar, and the second to fifth harmonics for both the second and the third upper molars for further shape analysis, but excluded the first, which is the harmonic associated with size (Bonhomme *et al.* 2014).

The first 15 principal components, which represented ~95% cumulative variance, of extracted Fourier Coefficients were used to perform a MANOVA to test for shape variation with sex, age, and year as explanatory variables. Where significant differences were found, I used a pairwise MANOVA to analyse where differences were located within groups. Lastly, I performed multivariate regressions to test for an allometric effect between size and shape for each of the molars.

I ran a PCA on the elliptic Fourier coefficients of each of the molars and then plotted the ordination of individuals on the first two PC axes for each dental structure to visualize the scatter of variation in the samples. A cumulative percentage of 95% of variation was found in the first 15 PC axes for the first upper molar, and 13 PC axes for the second and third upper molars (Appendix 5). Deformation grids of the maximum and minimum extremes of both PC axes were plotted alongside the PCA to visualize the extent of shape change along the first two PC axes.

Descriptive comparisons in annual climatic data and form change

I obtained rainfall and temperature data for each year of sampling from the South African Weather Service (2018) for the nearest weather station to the Willem Pretorius Nature Reserve. The Welkom weather station (26˚40ˈ12.00" E; 27˚59ˈ24.00" S) is 60km from Willem Pretorius Nature Reserve. I used these data to descriptively interpret patterns of inter-annual variation in morphology in the specimens in my study. *Rhabdomys dilectus* breed at the beginning of the spring months and the breeding period can extend up until the onset of Autumn (Schradin 2005). For this reason, a given year was considered to start from the onset of the breeding season (September of the previous year) and end August of the year in question. I compared annual changes to the local climatic conditions (total rainfall, average maximum temperature, and average minimum temperature) to relative changes in size and shape for each anatomical structure to the conditions in the previous year.

Chapter 4

Results

4.1 Ventral skull landmark analysis

Analysis of ventral cranial shape and size

To avoid redundancy in information and to limit the effect of asymmetry, the left and right sides of the ventral skull were averaged, and all remaining statistical analyses were conducted on the averaged data. The shape MANOVA (Table 4.1) of the ventral skull showed that age class and year of sampling were significant predictors of shape variation (Table 4.1), while sex, and the interactions between sex, age and year were not significant predictors for the shape model (Table 4.1). The size MANOVA (Table 4.1) conducted on centroid size also showed age class and year of sampling to be significant predictors of size variation. Sex (Figure 4.1), and the interaction factors between sex, age, and year of sampling were not significant predictors for the ventral skull size model (Table 4.1).

Table 4.1. MANOVA results of the shape and size components of the symmetric variation in the ventral skull. Values in bold are statistically significant

Component	Effect	d.f.	MS	F	p-value
Shape	Sex	1, 131	0.00095839	1.30	0.218
	Age	**3, 131**	**0.00212632**	**2.88**	**<0.001**
	Year	**3, 131**	**0.00171316**	**2.32**	**0.002**
	Sex:Age	4, 131	0.00063669	0.86	0.578
	Sex:Year	3, 131	0.00046521	0.63	0.893
	Age:Year	8, 131	0.00073848	1.00	0.156
	Sex:Age:Year	4, 131	0.00059423	0.80	0.480
Size	Sex	1, 131	9.7088	3.19	0.083
	Age	**3, 131**	**9.3356**	**3.06**	**0.026**
	Year	**3, 131**	**11.6295**	**3.82**	**0.004**
	Sex:Age	4, 131	0.9253	0.30	0.769
	Sex:Year	3, 131	3.6771	1.21	0.237
	Age:Year	8, 131	1.4302	0.47	0.771
	Sex:Age:Year	4, 131	3.3409	1.10	0.247

A pairwise comparison of the homogeneity of slopes for significant shape factors detected significant differences only between age classes III and IV and between the years 1994 and 1996, and 1996 and 1997. Age classes I and II were not significantly different from each other or from age classes III and IV. Specimens from 1975 and 1995 were not significantly different from each other or from specimens from 1994, 1996, and 1997. Specimens from 1994 and 1997 were also not significantly different from one another.

Pairwise comparison of homogeneity of slopes for size factors showed significant differences between age classes I-II, I-III, I-IV, II-IV, and III-IV (Figure 4.1), although not between age classes II and III (Figure 4.1). A pairwise comparison of homogeneity of slopes for years of sampling showed that 1997 and 1994, and 1997 and 1996 (Figure 4.1) were significantly different from one another. However, 1975 and 1995 were not significantly different from any other years.

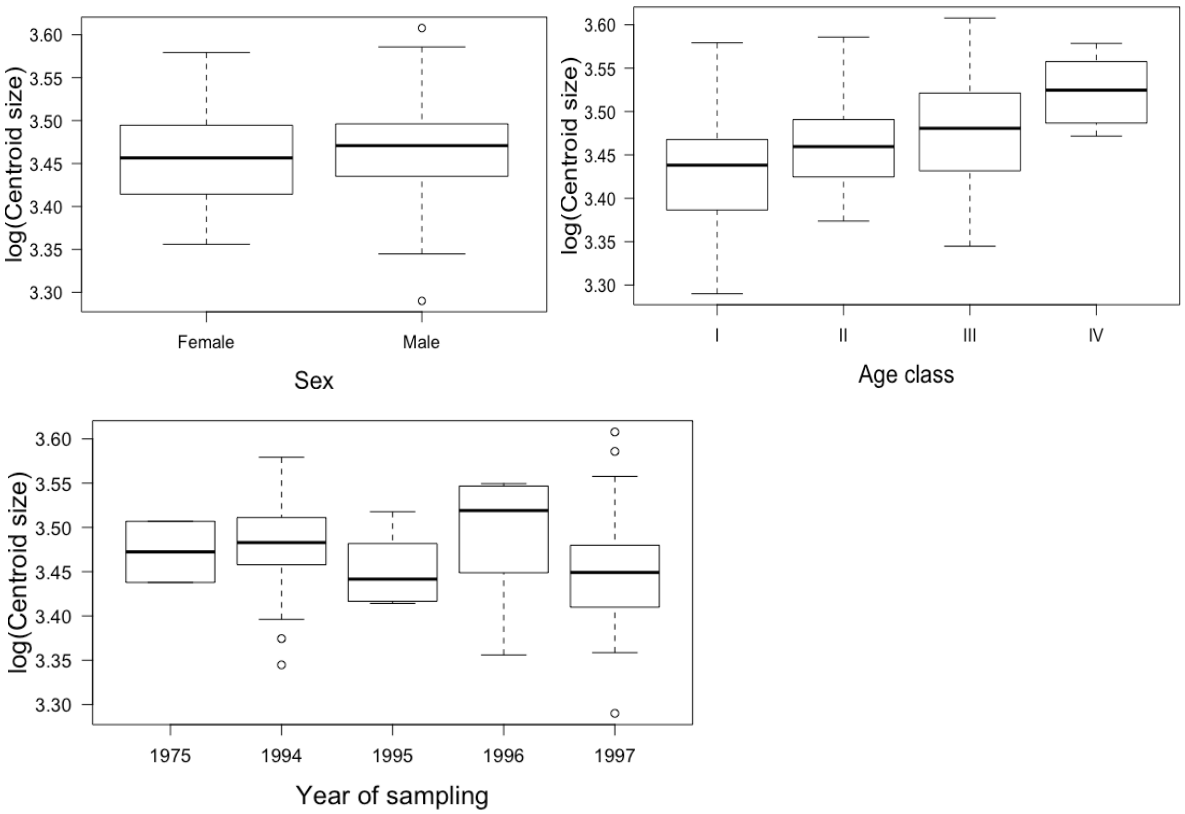


Figure 4.1. Variation in log-centroid size of the ventral skull between the sexes (top-left), age classes (top-right), and years of sampling (bottom). The box represents the interquartile range from the 1st quartile (bottom of box) to the 3rd quartile (top of box) with the median indicated as a black line within the box. The horizontal ends of the whiskers indicate the minimum (bottom) and maximum (top) values. Open circles indicate outliers.

Allometry of the ventral skull

A multivariate regression of shape on log- centroid size showed that size was a highly significant predictor of shape F=15.30; d.f.=1, 157; p<0.001) in the ventral skull (Figure 4.2), although the multivariate regression did not explain much of the variability (R^2=0.09). A multivariate regression of shape on log-centroid size showed that while both age (Figure 4.3) and year (Figure 4.4) were positively allometric, sex (Figure 4.5) was negatively allometric.

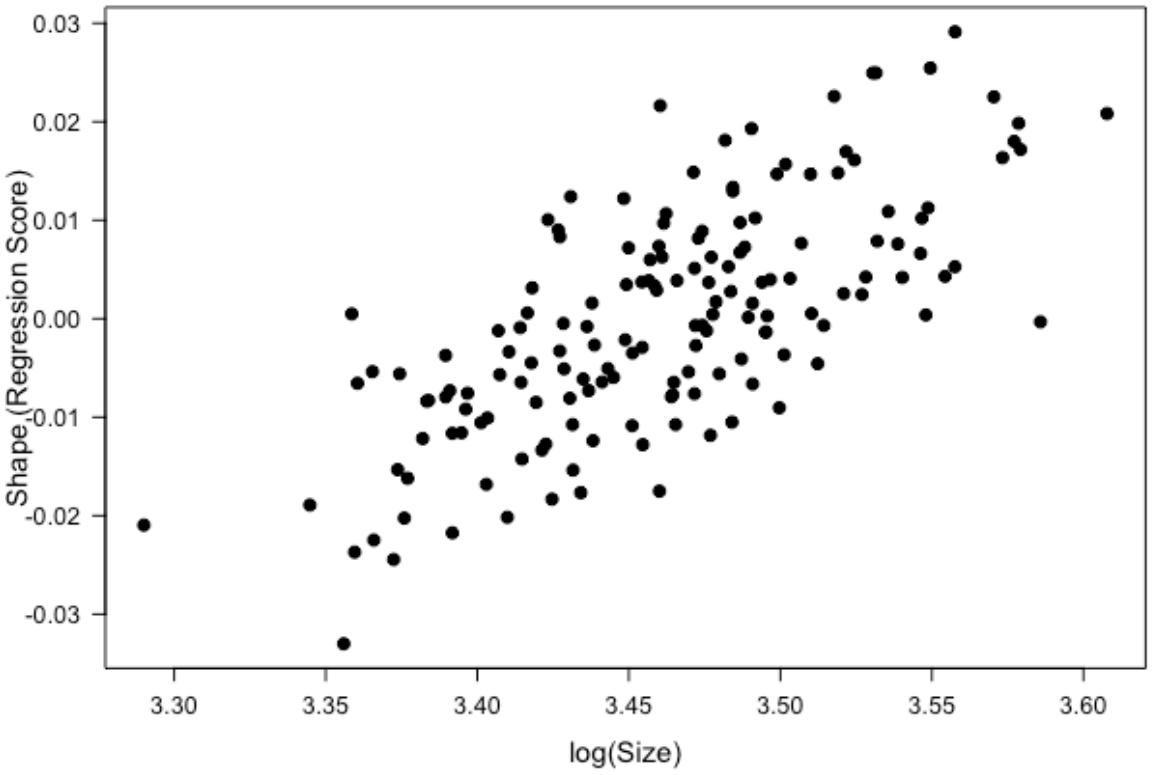


Figure 4.2. Multivariate regression of shape (using the regression score) on size (log-centroid size) of the ventral skull.

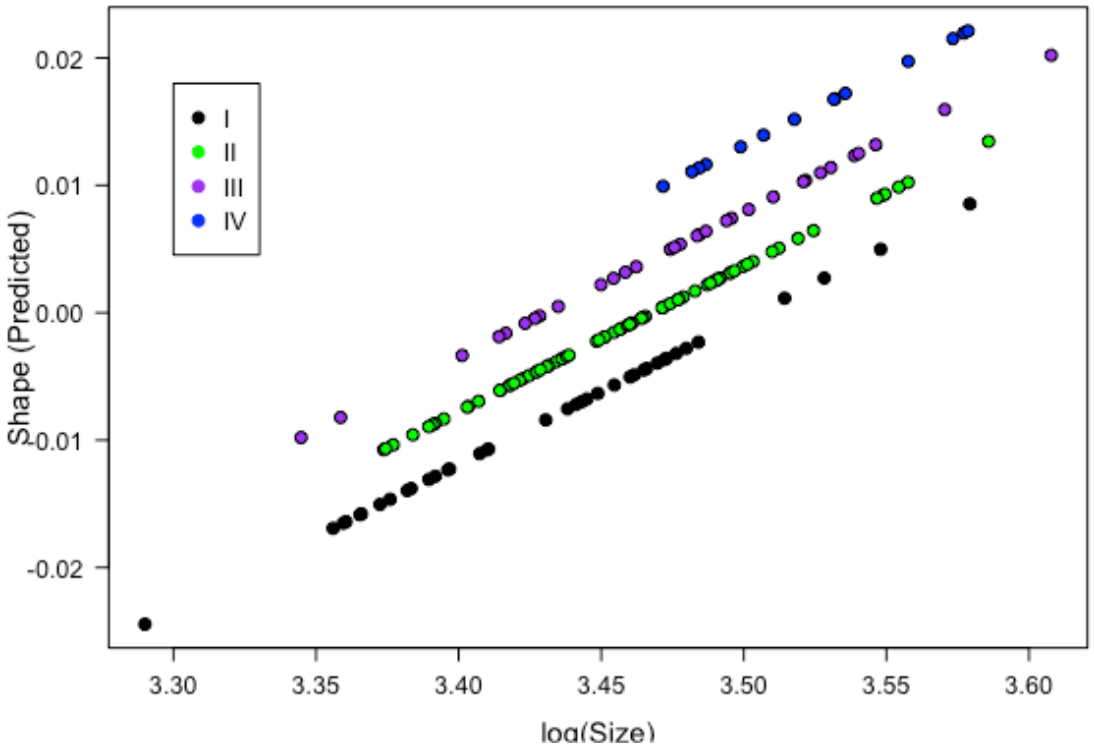


Figure 4.3. Allometric relationship between log-centroid size and ventral skull shape in the four age classes.

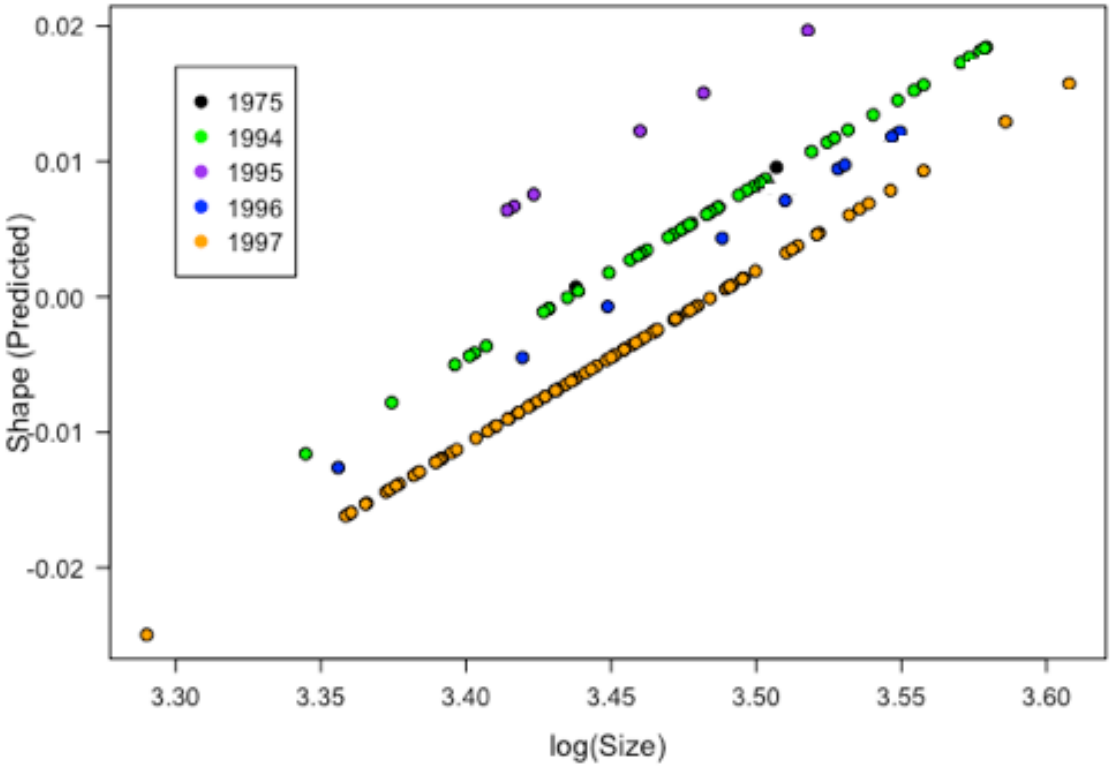


Figure 4.4. Allometric relationship between log-centroid size and ventral skull shape among years of specimen collection.

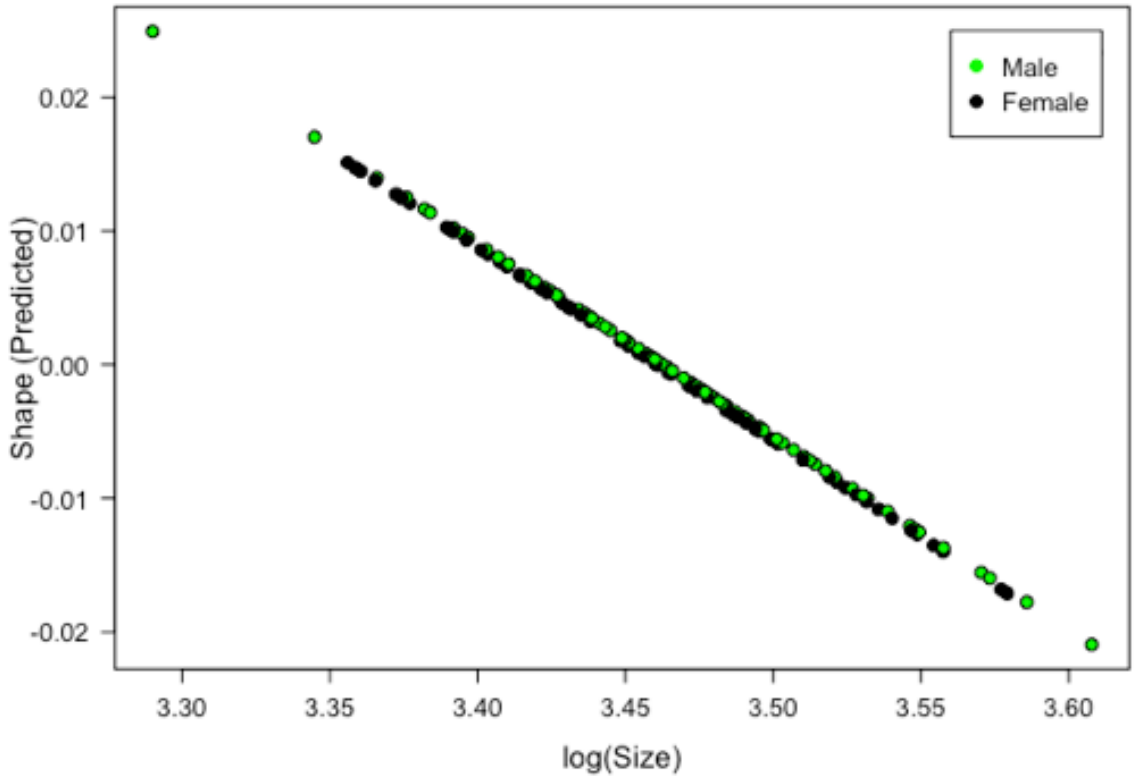


Figure 4.5. Allometric relationship between log-centroid size and ventral skull shape between the sexes.

Shape comparisons of the ventral skull with PCA

As a result of the large effect of centroid size on shape, I calculated allometry-free residuals using a multivariate linear regression and used these residuals in an allometry-free Principal Component Analysis (PCA). The size-corrected PCA was plotted with four Relative Warp plots to illustrate the extremes along PC 1 and PC 2 (Figures 4.6, 4.7, 4.8). Results from the shape MANOVA were not supported by the PCA as all four age classes clustered together. Age class I and age class II were, however, more spread out, with more variable shapes than age class III and age class IV. Age class I and age class II thus consisted of a range of shapes, including individuals with short, but broad neurocrania with smaller foramen magnum openings, at the upper end along PC1 (Figure 4. 6) and more elongated rostra and neurocrania, with larger foramen magnum openings at the lower end of PC1 (Figure 4.6). Age class IV clustered more tightly toward the negative half of PC 1 and the positive half of PC 2 with elongated neurocrania, and an elongated and narrower rostrum, and less protruding jugal regions (Figure 4.6). Age class III, like age class IV, clustered more along the negative region of PC 1, although unlike age class IV it was more spread along PC 2 with individuals with broader rostra and neurocrania and slightly more protruding jugal regions (Figure 4.6).

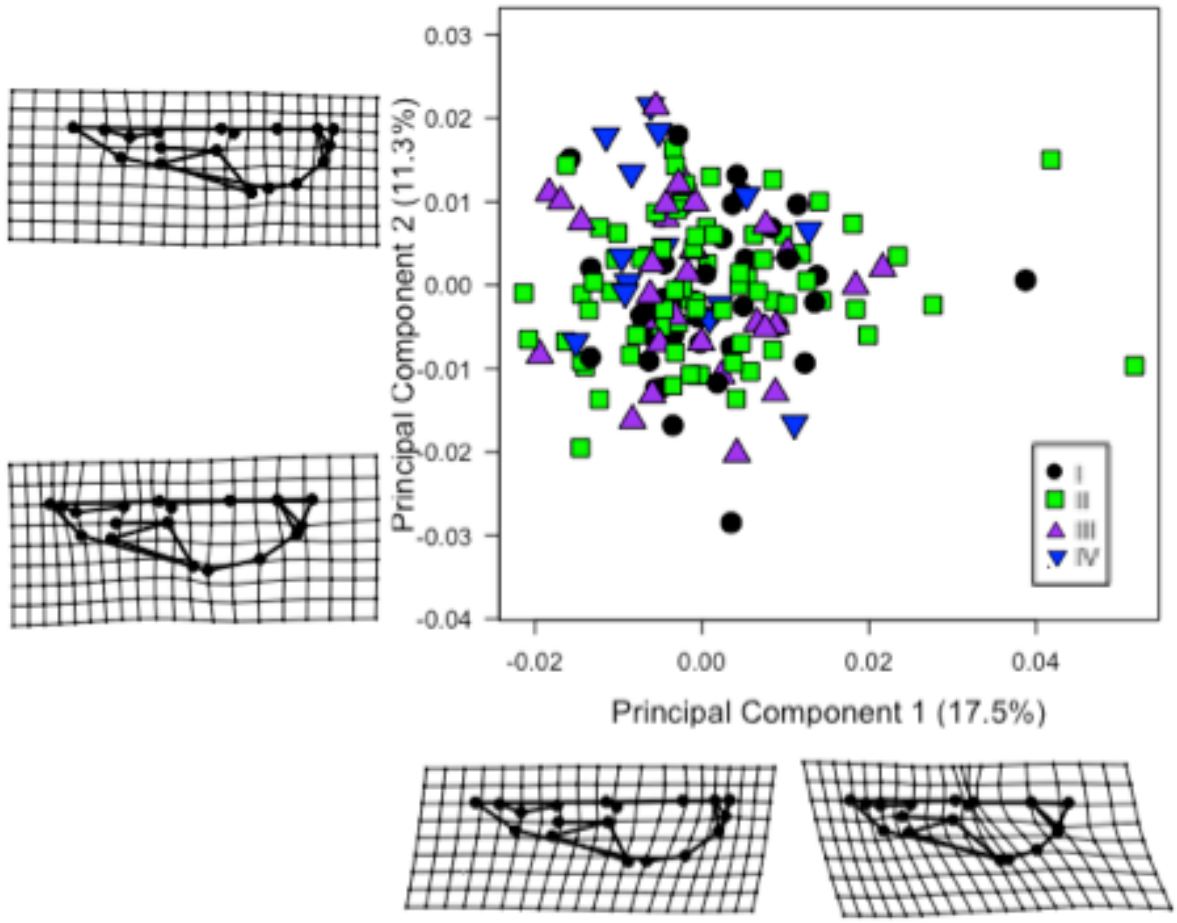


Figure 4.6. Allometry-adjusted Principal Component Analysis of the first two principal components indicating the spread of the four age classes in the ventral skull. Relative warp plots along the two axes indicate the minimum and maximum shape configurations along those axes. Relative warp plots have been magnified by a scale of three to more clearly illustrate variation.

There was a large amount of overlay between year of sampling, with specimens from 1997 most widely spread across the PCA and specimens from 1995 more clustered to the minimum extreme of PC1 and maximum extreme of PC 2 (Figure 4.7). While specimens from 1995 had longer, narrower neurocrania and rostra, those specimens collected in 1996 plotted at the minimum extreme of PC 1with an elongated, broader neurocrania but with a shorter, broader rostrum (Figure 4.7). Specimens collected in 1994, plotted more centrally along PC 2, but clustered more toward the minimum extreme of PC 1, with longer rostra and wider incisive foramina (Figure 4.7). Specimens from 1997 had a wider spread along both PCs, with specimens ranging from short and narrow neurocrania and rostra, to individuals with elongated but narrow rostra and neurocrania (Figure 4.7).

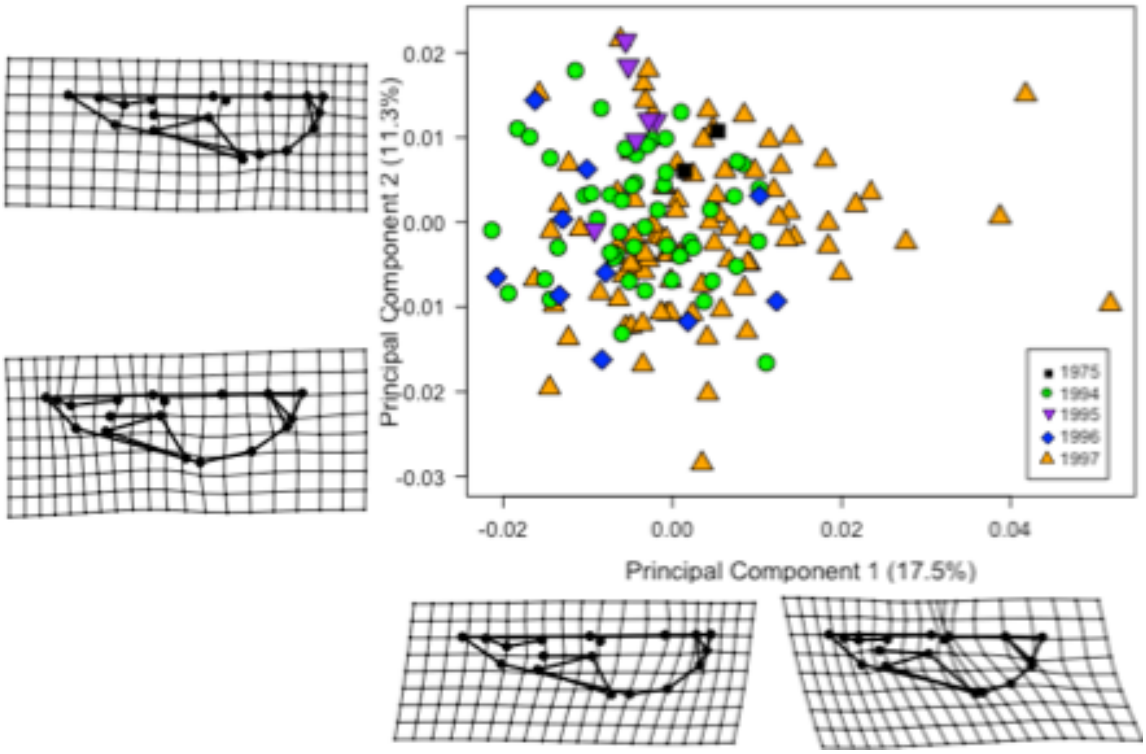


Figure 4.7. Allometry-adjusted Principal Component Analysis of the first two principal components indicating the spread across year of specimen collection in the ventral skull. The relative warp plots have been magnified by a factor of three to more clearly illustrate the differences between the two extremes of each axis.

The PCA also supported the statistical results (Table 4.1) indicating no significant difference in shape between the sexes (Figure 4.8). Males and females were fairly spread out, although the outliers in the data set were those of females and spread toward the positive extreme of PC 1 (with shortened neurocrania and larger foramen magna openings) and the negative extreme of PC 2 (with broader rostra and neurocrania; Figure 4.8).

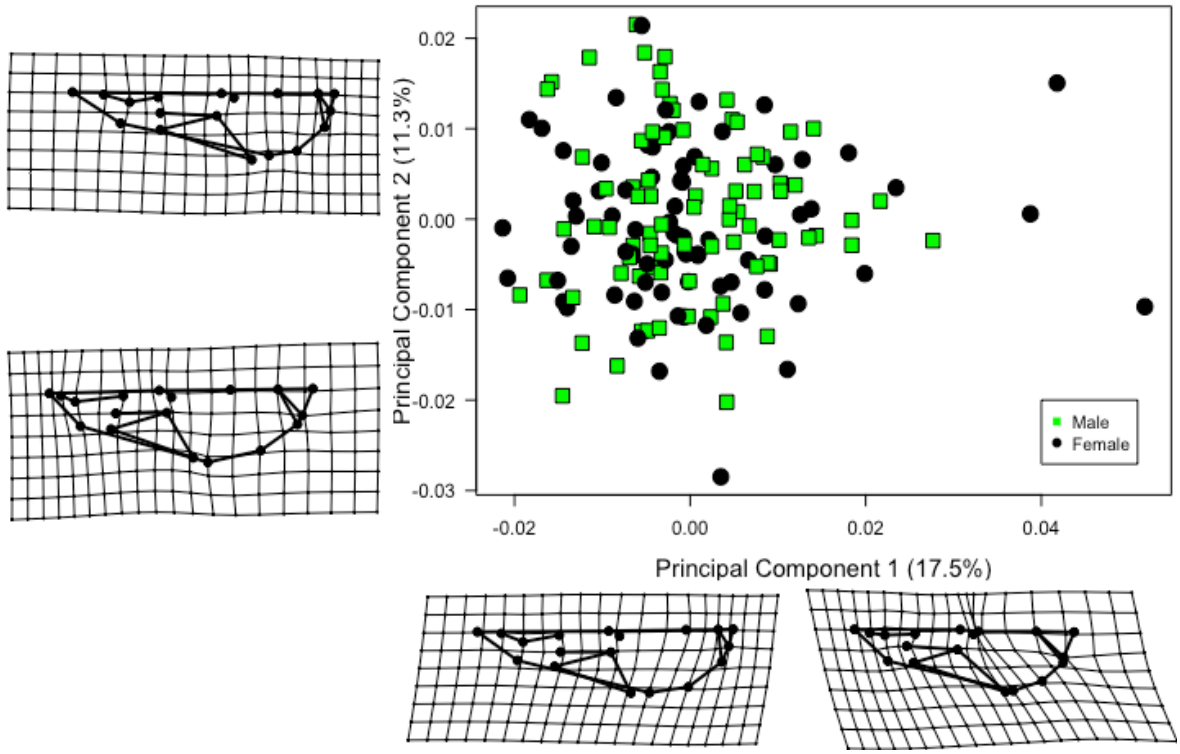


Figure 4.8. Allometry-adjusted Principal Component Analysis of the first two principal components indicating the spread for the sexes in the ventral skull. Relative Warp plots have been magnified by a scale of three to better illustrate shape differences between extrema.

4.2. Lateral skull landmark analysis

Analysis of lateral cranial shape and size

All further analyses were restricted to the left side of the lateral skull to limit the effect of asymmetry as well as to avoid any redundancy in information. The shape MANOVA (Table 4.2) of the symmetric component of the lateral skull indicated that age, year of sampling, the interaction sex:year, and the interaction age:year were all significant predictors of lateral skull shape. However, sex, the sex:age interaction, and the sex:age:year interaction were all non-significant (Table 4.2). The size MANOVA (Table 4.2) of the symmetric component showed that sex, age, year, the sex:year interaction, and the age:year interaction were all significant predictors of lateral skull size. Only the sex:age and sex:age:year interaction factors were non-significant predictors (Table 4.2).

Table 4.2. MANOVA results of the shape and size components of the symmetric variation in the lateral skull. Values in bold are statistically significant.

Component	Effect	d.f.	MS	F	p-value
Shape	Sex	1, 140	0.0014149	1.45	0.137
	Age	**3, 140**	**0.0032126**	**3.29**	**0.001**
	Year	**4, 140**	**0.0030085**	**3.08**	**0.001**
	Sex:Age	3, 140	0.0008420	0.86	0.614
	Sex:Year	**2, 140**	**0.0014938**	**1.53**	**0.015**
	Age:Year	**8, 140**	**0.0011521**	**1.18**	**0.011**
	Sex:Age:Year	3, 140	0.0009856	1.01	0.131
Size	**Sex**	**1, 140**	**8.076**	**5.06**	**0.027**
	Age	**3, 140**	**36.859**	**23.09**	**0.001**
	Year	**4, 140**	**3.562**	**2.23**	**0.014**
	Sex:Age	3, 140	0.954	0.60	0.472
	Sex:Year	**2, 140**	**9.643**	**6.04**	**0.001**
	Age:Year	**8, 140**	**3.669**	**2.30**	**0.001**
	Sex:Age:Year	3, 140	1.883	1.18	0.092

Pairwise comparisons of homogeneity of slopes for variation in shape by age class showed that age class III differed from age classes I and II while comparisons of slopes for year showed that shape was only significantly different between specimens from 1996 and 1997. Age class IV was not significantly different from any other age classes and age classes I and II were not significantly different from each other. Specimens from 1975, 1994, and 1995 did not differ significantly in shape between each other or between specimens from 1996 and 1997.

Pairwise comparisons testing for factor interactions showed that males from 1995 differed significantly in shape from females of 1995, but the model did not identify any other significantly different pairs between sexes from any of the other years. Pairwise comparisons testing for factor interactions for the age:year interaction showed that age class I from 1996 was significantly different from age class II from 1996, from age class III from 1994, and was significantly different from age class IV from 1994. Age class I from 1995 was significantly different from age class II from 1996, age class III from 1994, and from age

class IV from 1994. However, all other age:year interactions were not significantly different from one another.

Pairwise comparisons of homogeneity of slopes for size showed that males were significantly larger than females (Table 4.2; Figure 4.9). Pairwise comparisons of homogeneity of slopes between the age classes showed that age class I differed significantly in size to age classes III and IV, and age class IV also differed significantly in size to age classes II and III (Figure 4.9). Age class IV was significantly larger than all other age classes, although size increased with increasing age classes, and only age classes II and III did not differ significantly from each other (Figure 4.9). Moreover, pairwise comparisons of homogeneity of slopes for year of sampling showed that specimens from 1994 differed significantly to specimens from 1996 and specimens from 1997. Specimens from 1995 differed significantly from specimens from 1996 and those from 1997 (Figure 4.9). Only specimens from 1975 were not significantly different from any other year.

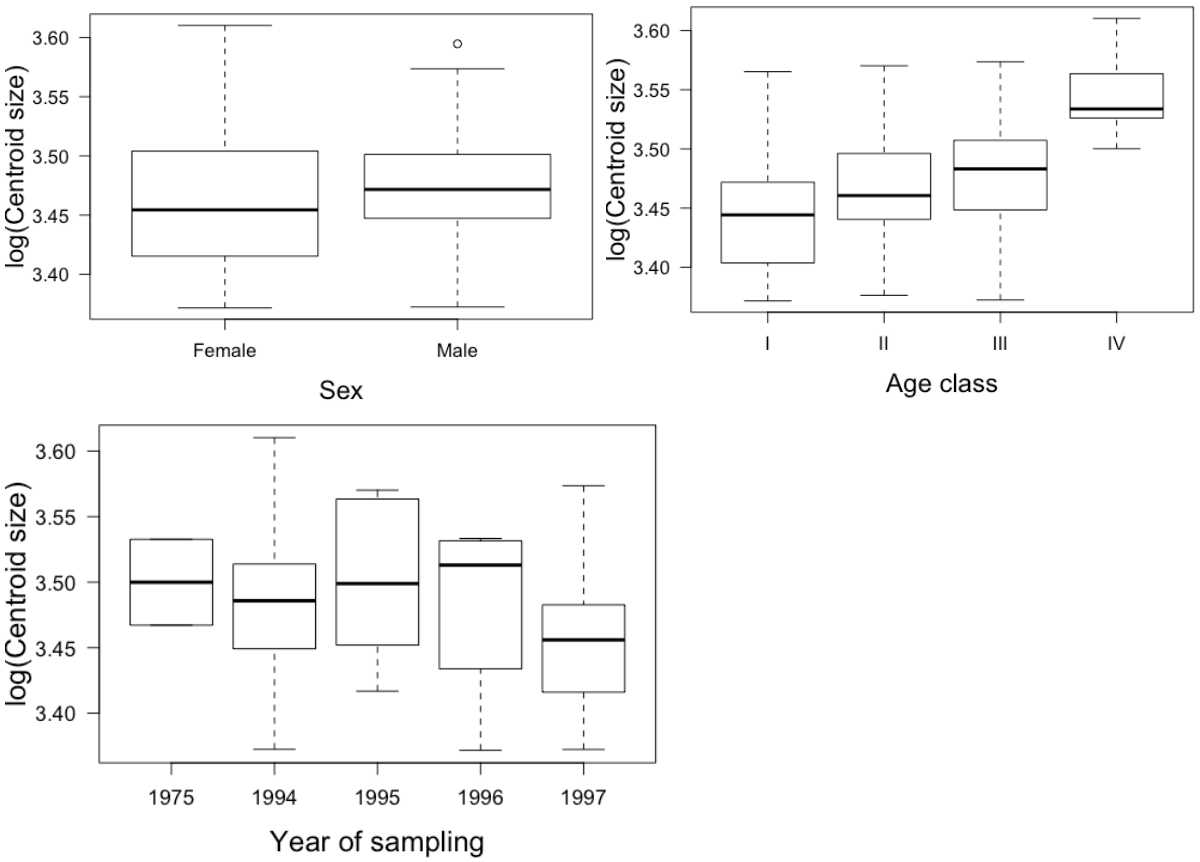


Figure 4.9. Variation in log-centroid size of the ventral skull between the sexes (top-left), age class (top-right), and year of sampling (bottom). The box represents the interquartile range from the 1st quartile (bottom of box) to the 3rd quartile (top of box) with the median indicated as a black line within the box. The horizontal ends of the whiskers indicate the minimum (bottom) and maximum (top) values. Open circles indicate outliers.

Pairwise ANOVA comparisons testing factor interactions showed that females from 1995 differed significantly in shape from males of 1995, although all other interaction terms were not significantly different from each other (Figure 4.10). Pairwise ANOVA comparisons testing the interaction for the age:year factor showed that age class I from 1996 was significantly different to age class II from 1996. Age class I from 1996 was also statistically different to age class III from 1994 and was statistically different to age class IV from 1994 (Figure 4.11). Age class I from 1995 was different to age class IV from 1995, age class II from 1996, age class III from 1994, and age class IV from 1994 (Figure 4.11).

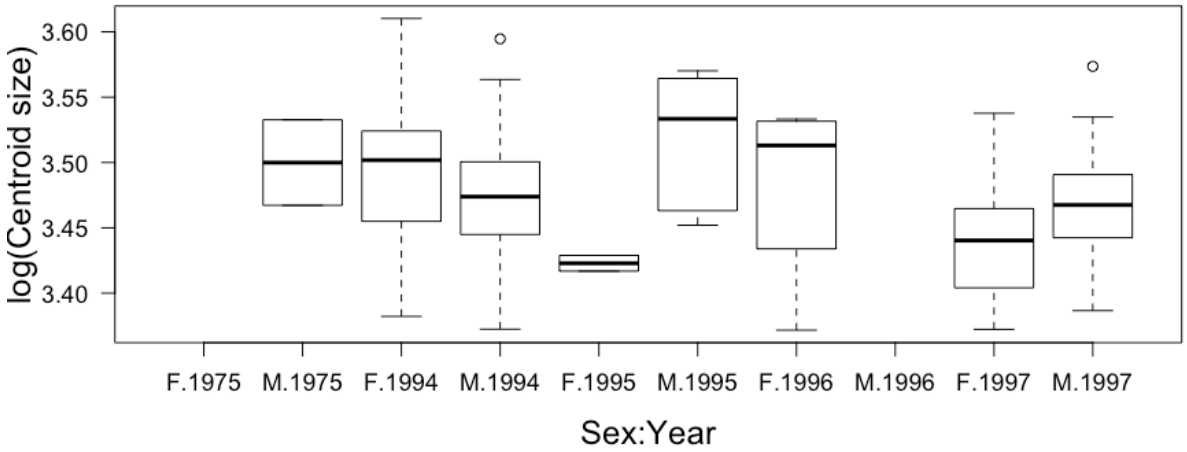


Figure 4.10. Variation in log-centroid size of the lateral skull for the sex:year of sampling interaction. The boxes represent the interquartile range from the 1st quartile (bottom of box) to the 3rd quartile (top of box) with the median indicated as a black line within each box. The horizontal ends of the whiskers indicate the minimum (bottom) and maximum (top) values. Open circles indicate outliers.

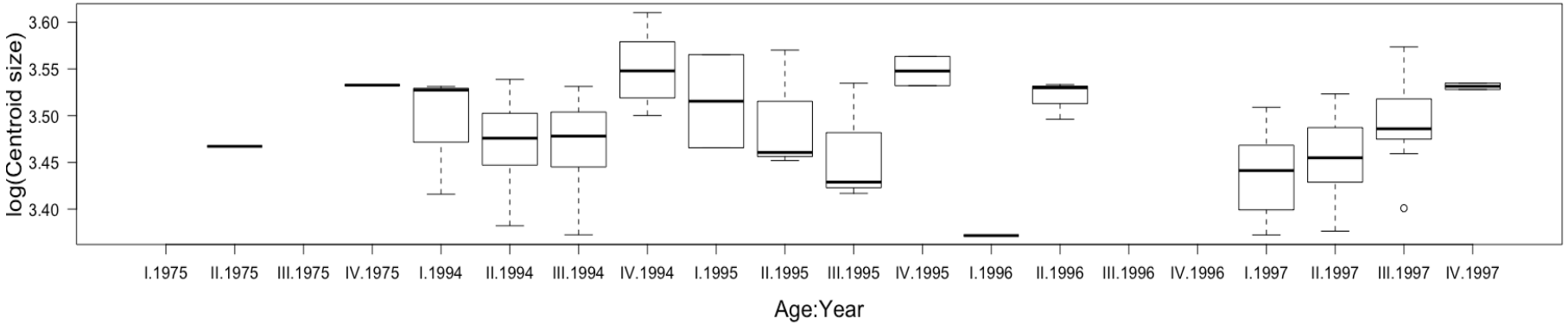


Figure 4.11. Variation in log-centroid size of the lateral skull for the age:year of sampling interaction. The boxes represent the interquartile range from the 1st quartile (bottom of box) to the 3rd quartile (top of box) with the median indicated as a black line within each box. The horizontal ends of the whiskers indicate the minimum (bottom) and maximum (top) values. Open circles indicate outliers.

Allometry of the lateral skull

A multivariate regression of size (as log-centroid size) on shape (the shape regression scores) showed that size was a highly significant (F=13.79; d.f.= 1, 154; p<0.001) predictor of lateral skull shape (Figure 4.12), although the multivariate regression explained very little of the variation (R^2=0.08). Age (Figure 4.13) and year of sampling (Figure 4.14) show positive parallel allometry. Sex (Figure 4.15), however, showed negative allometry.

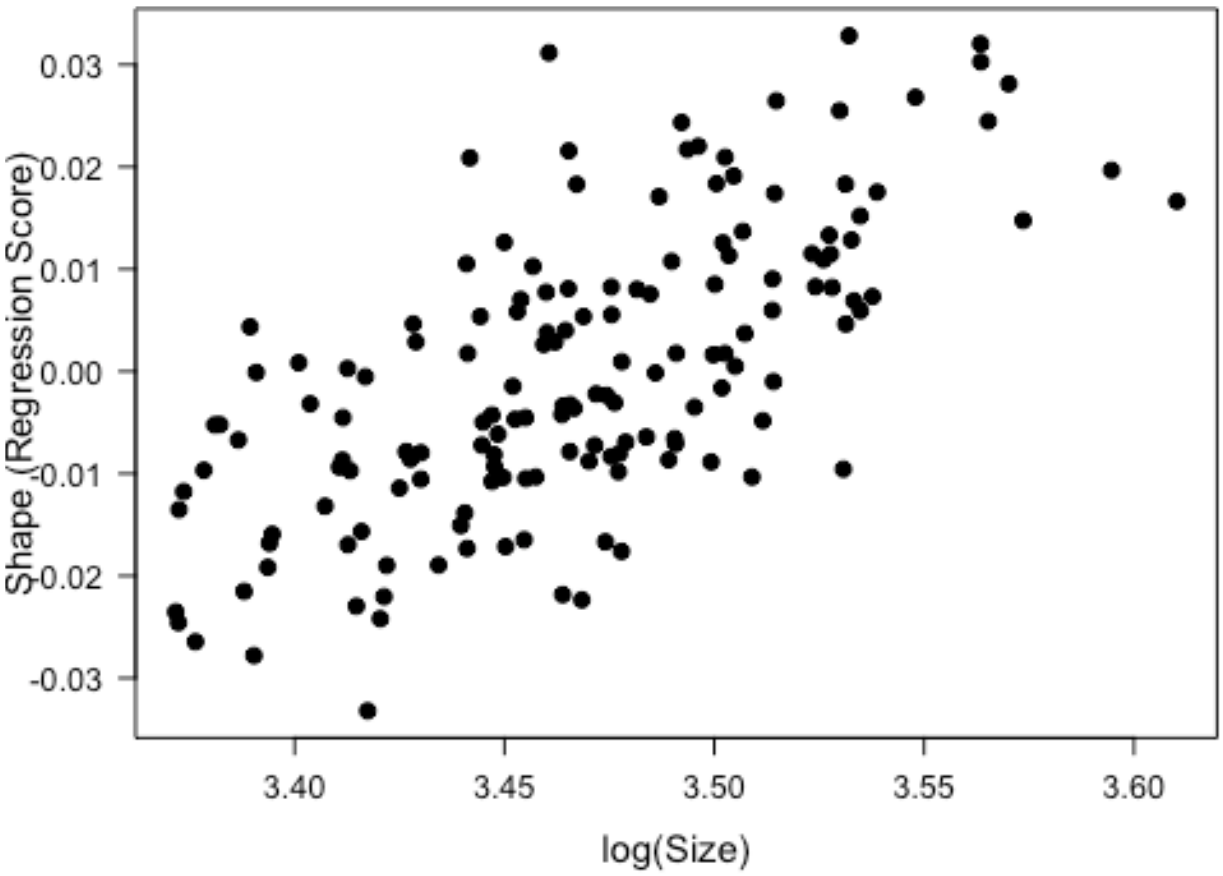


Figure 4.12. Multivariate regression of shape (using the regression score) on size (log-centroid size) of the lateral skull.

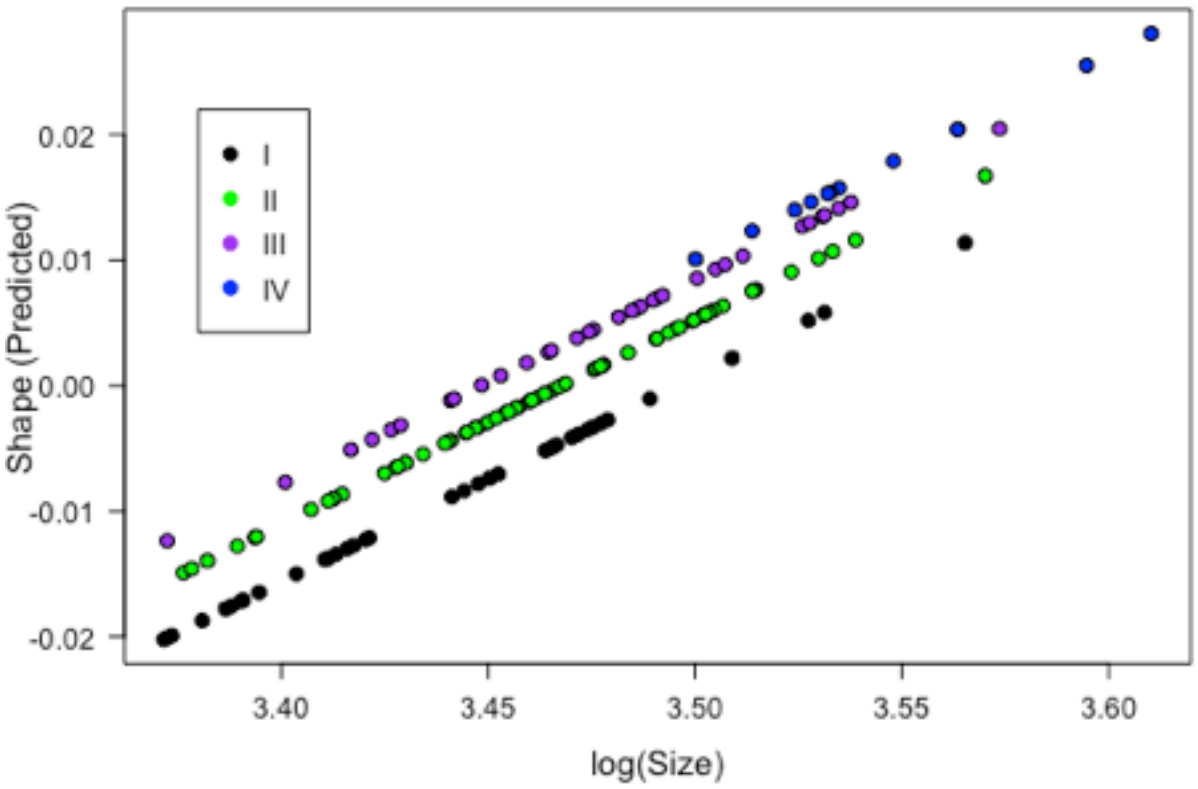


Figure 4.13. Allometric relationship between age classes for the lateral skull.

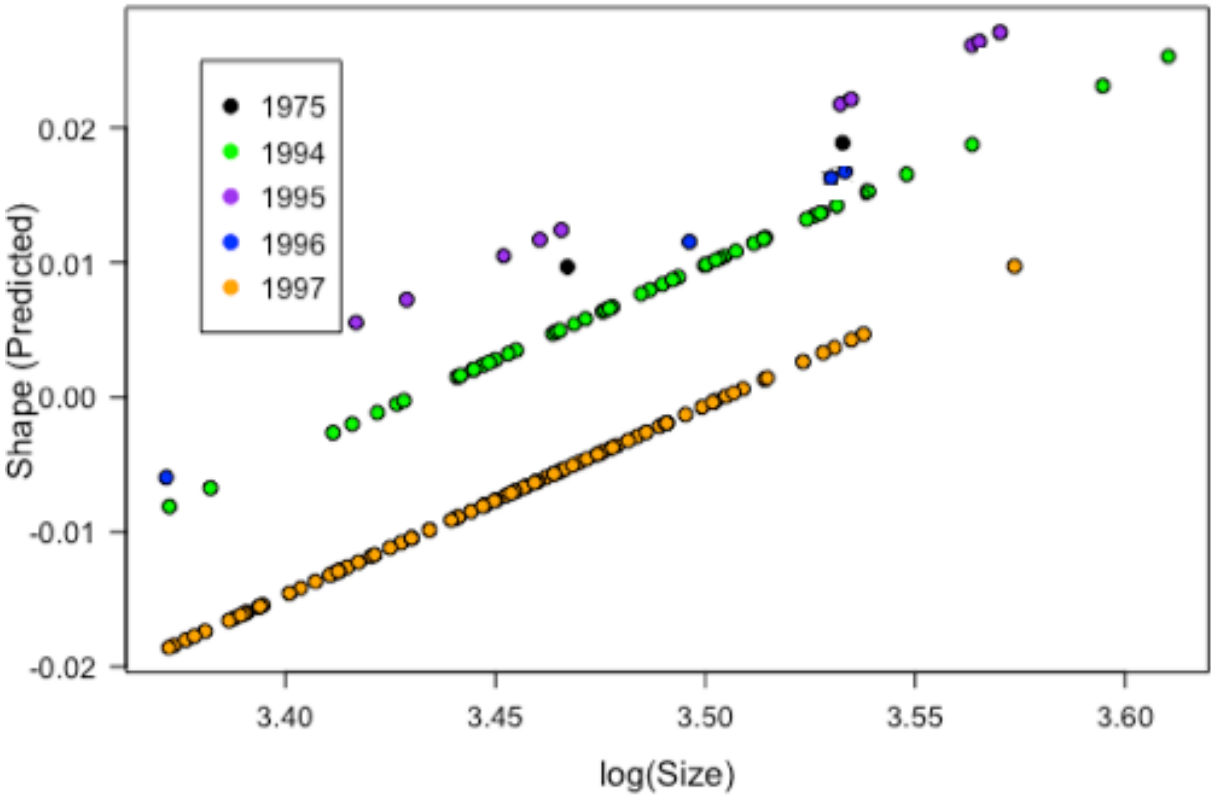


Figure 4.14. Allometric relationship between log-centroid size and the shape of the lateral skull between years of specimen collection.

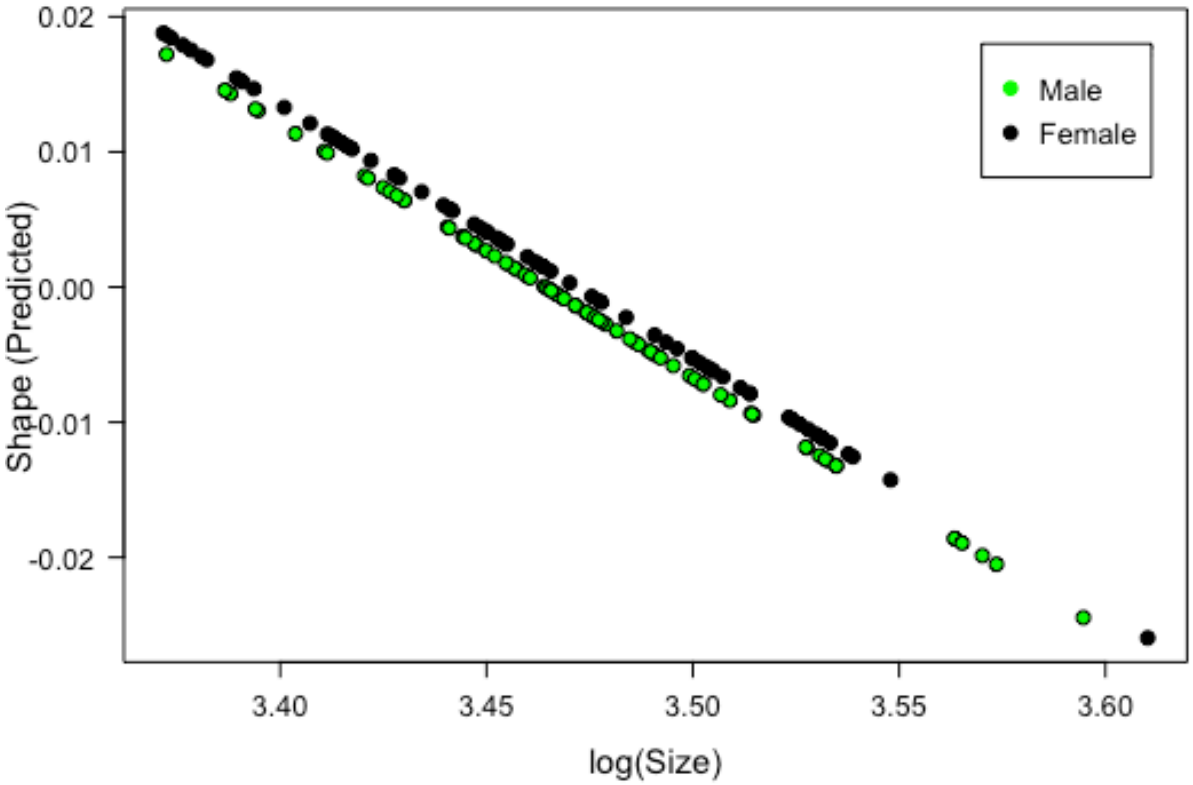


Figure 4.15**.** Allometric relationship between log-centroid size and lateral skull shape between the sexes.

Shape comparisons of the lateral skull with PCA

Given the significance of size on shape, size-corrected residuals were used to construct a PCA for lateral skull shape. The size-corrected PCA was plotted with four Relative Warp plots that illustrated the extremes along PC 1 and PC 2 (Figure 4.16). There was a large degree of overlap between the age classes (Figure 4.16), although age class III and age class IV were more centrally located, with a tighter spread. The minimum extreme of PC 1 showed landmark 9 and 10 located more anteriorly tighter spread. The minimum extreme of PC 1 showed landmark 9 and 10 located more anteriorly which made the caudal end of skull more slanted. The maximum extreme indicated a straighter vertical end to the end of the braincase with landmarks 9 and 10 located more posteriorly (Figure 4.16). The minimum extreme of PC 1 also indicated steeper jugal region with landmarks 12 and 13 located more ventrally and landmarks 14 and 15 located more dorsally than in the maximum extreme of PC 1. Landmark 11 also provided a morphological difference between the extremes of PC 1, with the dorsal surface of the skull curved more deeply at the maximum extreme, and a gentler curve with landmark 11 located more posteriorly at the minimum extreme (Figure 4.16). Landmark 2 was located more anteriorly from landmarks 1 and 3 at the minimum extreme of PC1 (Figure

4.20). The minimum extreme of PC 2 indicated a more flattened dorsal skull surface with a steeper zygomatic, while the maximum extreme of PC 2 indicated a more curved dorsal surface with a less angular zygomatic (Figure 4.16). Age classes III and IV were concentrated slightly more centrally than the wider spread of age classes I and II, and so age classes III and IV had a shape intermediate to the two extremes of PC 1.

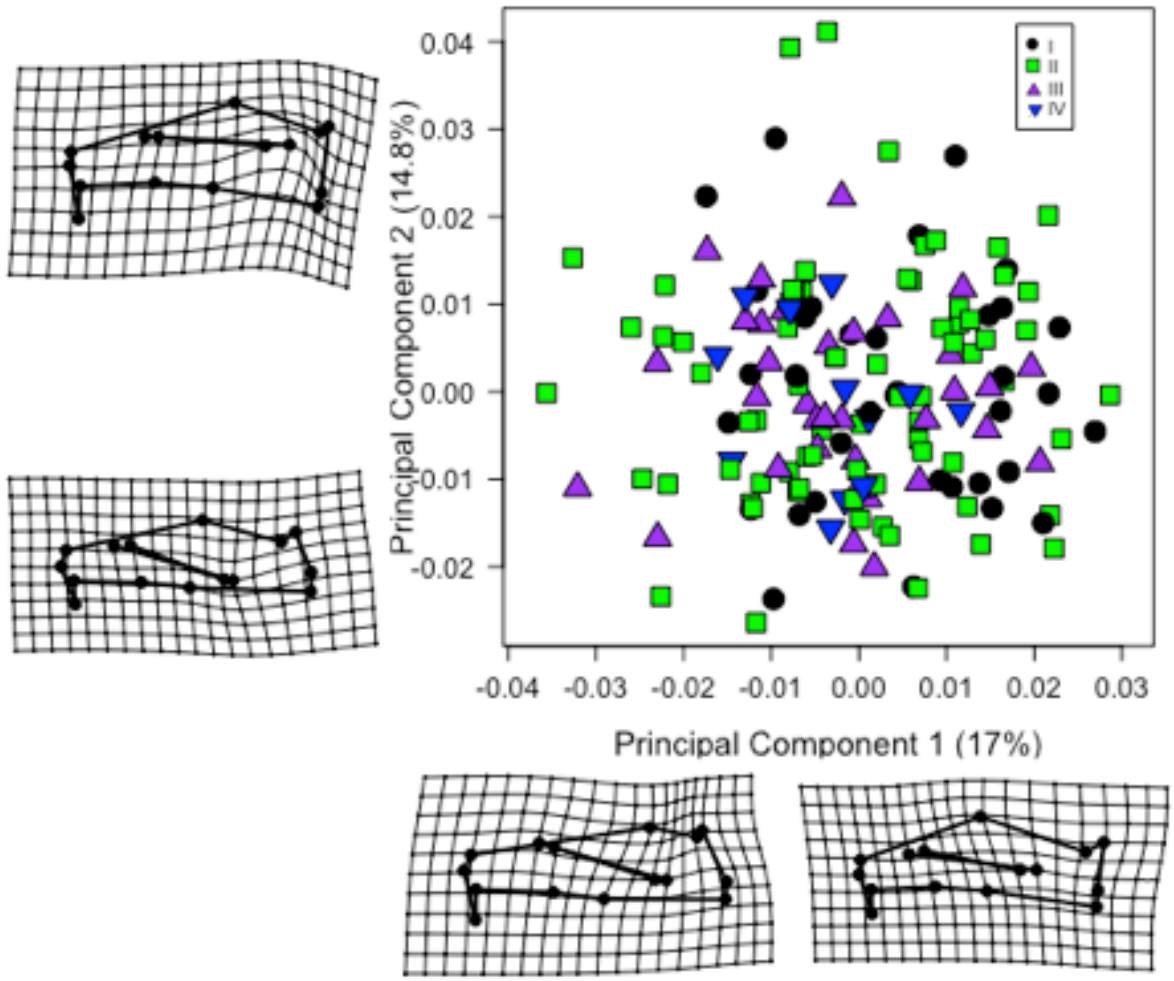


Figure 4.16. Allometry-adjusted Principal Component Analysis of the first two principal components indicating the spread of the four age classes for the lateral skull. Relative warp plots along the two axes indicate the minimum and maximum shape configurations along those axes. Relative warp plots have been magnified by a scale of three to more clearly illustrate variation.

Specimens from 1997 were more concentrated toward the maximum extreme of PC 1 with landmark 9 positioned more posteriorly and creating a more vertical end to the braincase and landmark 11 positioned more anteriorly creating a deeper curved neurocranium (Figure 4.17). Specimens from 1997 also had less steep zygomatic arches with landmarks 12 and 13

more dorsally located, and landmarks 14 and 15 more ventrally located at the maximum extreme of PC 1 (Figure 4.17). Specimens from 1994, while quite spread out along PC 1, plotted more toward the minimum end of PC 2, with landmarks 12 and 13 located closer to the ventral surface of the skull, creating a steeper zygomatic arch, and landmarks along the dorsal and ventral surfaces located closer together, creating a neurocranium shortened in height (Figure 4.17). Specimens from 1995 and 1996 were located more centrally between the two extremes of PC 1 but separated more along PC 2 (Figure 4.17). Specimens from 1995 had a wider spread along the second PC than those from 1996, with individuals with more horizontal zygomatic arches (i.e. landmarks 12, 13, 14, and 15 located closer together in height) and taller neurocrania (with the an increased distance between landmark 11 and the landmarks along the ventral surface of the skull) and individuals with more flattened skulls (i.e. landmarks that delineated the ventral and those that delineated the dorsal surfaces of the skull were closer together in height; Figure 4.17). Specimens from 1996 plotted more toward the minimum extreme of PC 2 with shorter heights of the neurocranium, but much steeper zygomatic arches (with landmarks 12 and 13 located closer to the ventral surface of the skull; Figure 4.17).

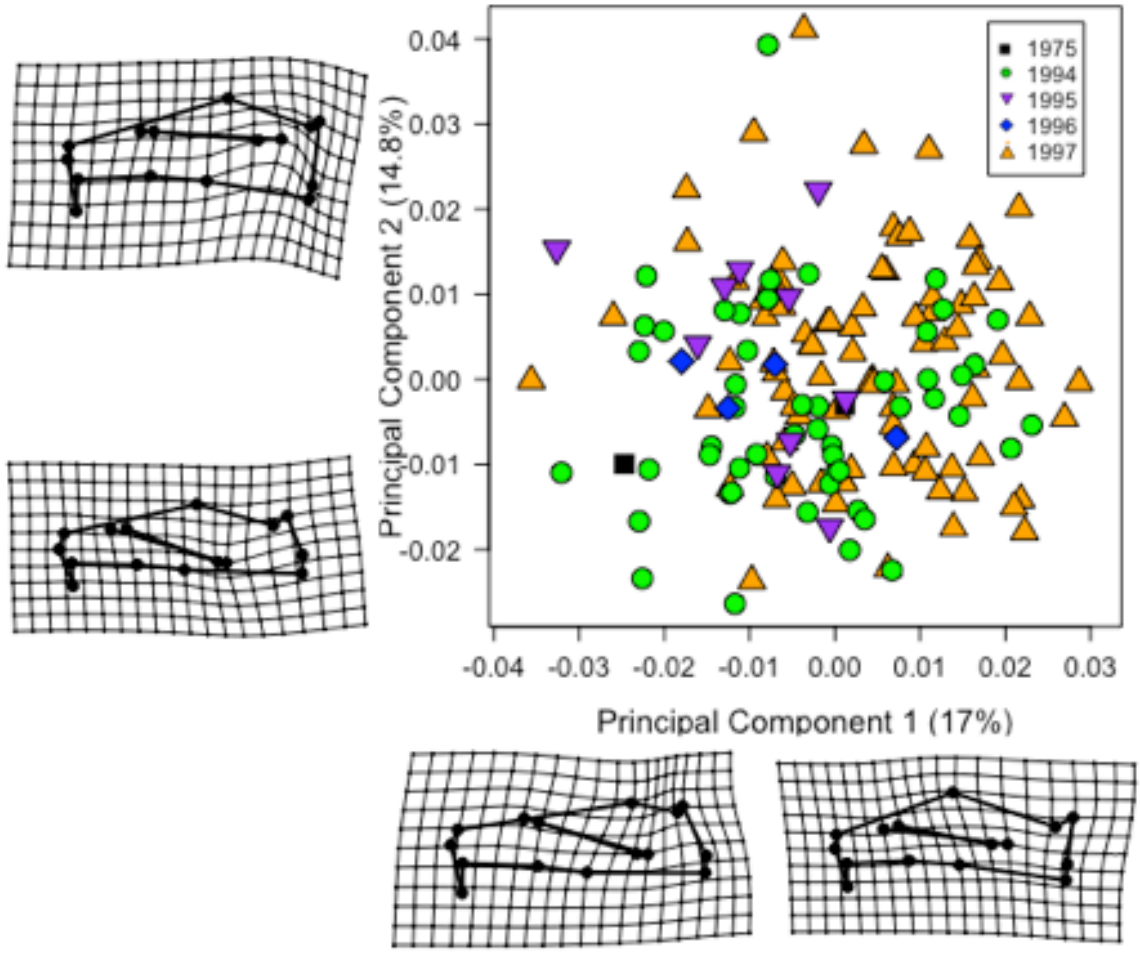


Figure 4.17. Allometry-adjusted Principal Component Analysis of the first two principal components indicating the spread across year of specimen collection for the lateral skull. The relative warp plots have been magnified by a factor of three to more clearly illustrate the differences between the two extrema of each axis.

Males and females both plotted along the extent of the two PC axes and showed no sign of clustering at all (Figure 4.18).

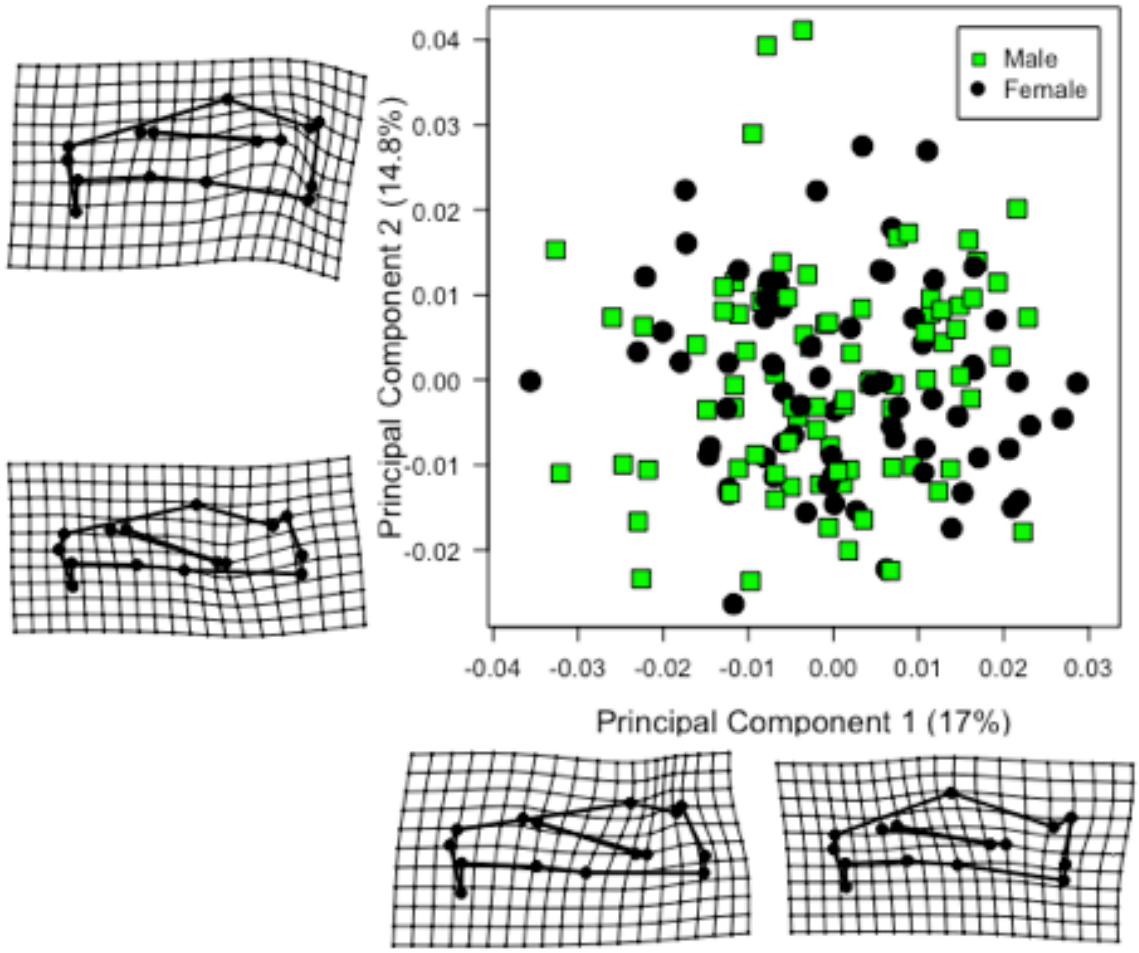


Figure 4.18. Allometry-adjusted Principal Component Analysis of the first two principal components indicating the spread for the sexes for the lateral skull. Relative Warp plots have been magnified by a scale of three to better illustrate shape differences between extrema.

4.3. Mandible landmark analysis

Analysis of mandibular shape and size

All further analyses were restricted to the left hemi-mandible to limit the effects of asymmetry and the two images of the left hemi-mandible for each individual were averaged to avoid redundancy in information. A MANOVA of the symmetric component of the mandibles showed that age, year of collection, the sex:age interaction, the age:year interaction, and the sex:age:year interaction were all significant predictors of mandibular shape (Table 4.3). Only sex and the sex:year interaction were non-significant predictors for mandibular shape (Table 4.3). Sex, age class, and year of collection were all significant predictors of mandibular size variation, while the sex:age, sex:year, age:year, and sex:age:year interactions were non-significant (Table 4.3).

Table 4.3. MANOVA results of the shape and size components of the symmetric variation in the mandible. Values in bold are statistically significant.

Component	Effect	d.f.	MS	F	P-value
Shape	Sex	1, 96	0.0013873	0.89	0.482
	Age	**3, 96**	**0.0037059**	**2.38**	**0.003**
	Year	**3, 96**	**0.0035802**	**2.30**	**0.001**
	Sex:Age	**3, 96**	**0.0027484**	**1.77**	**0.013**
	Sex:Year	3, 96	0.0014618	0.94	0.295
	Age:Year	**4, 96**	**0.0024151**	**1.55**	**0.005**
	Sex:Age:Year	**2, 96**	**0.0026192**	**1.68**	**0.013**
Size	**Sex**	**1, 96**	**8.7393**	**14.25**	**<0.001**
	Age	**3, 96**	**5.6554**	**9.22**	**<0.001**
	Year	**3, 96**	**1.5572**	**2.54**	**0.017**
	Sex:Age	3, 96	0.2589	0.42	0.613
	Sex:Year	3, 96	0.1791	0.29	0.735
	Age:Year	4, 96	0.7354	1.20	0.134
	Sex:Age:Year	2, 96	0.6851	1.12	0.170

Pairwise comparisons of homogeneity of slopes for the age class factor showed that age class IV differed significantly in shape from age classes I, II, and III, and that age class II differed significantly from age class III. Only age classes I and III were not found to be significantly different from one another. For the year of sampling, specimens from 1994 differed significantly from those caught in 1995, 1996, and 1997. Additionally, specimens from 1997 also differed significantly to those caught in 1995 and 1996. Only specimens from 1995 and 1996 were not significantly different from one another.

Pairwise comparisons of homogeneity of slopes for size showed that females were significantly smaller than males (Figure 4.19). Pairwise comparisons of slopes amongst age classes showed that specimens from age class IV were significantly larger in size than those in all the other age classes although none of the other age classes differed significantly from each other (Figure 4.19). Pairwise comparisons of slopes between years of sampling showed that specimens caught in the year 1997 were significantly smaller than those caught in 1994

and 1996 (Figure 4.19). Specimens from 1994, 1995, and 1996 were not significantly different from one another.

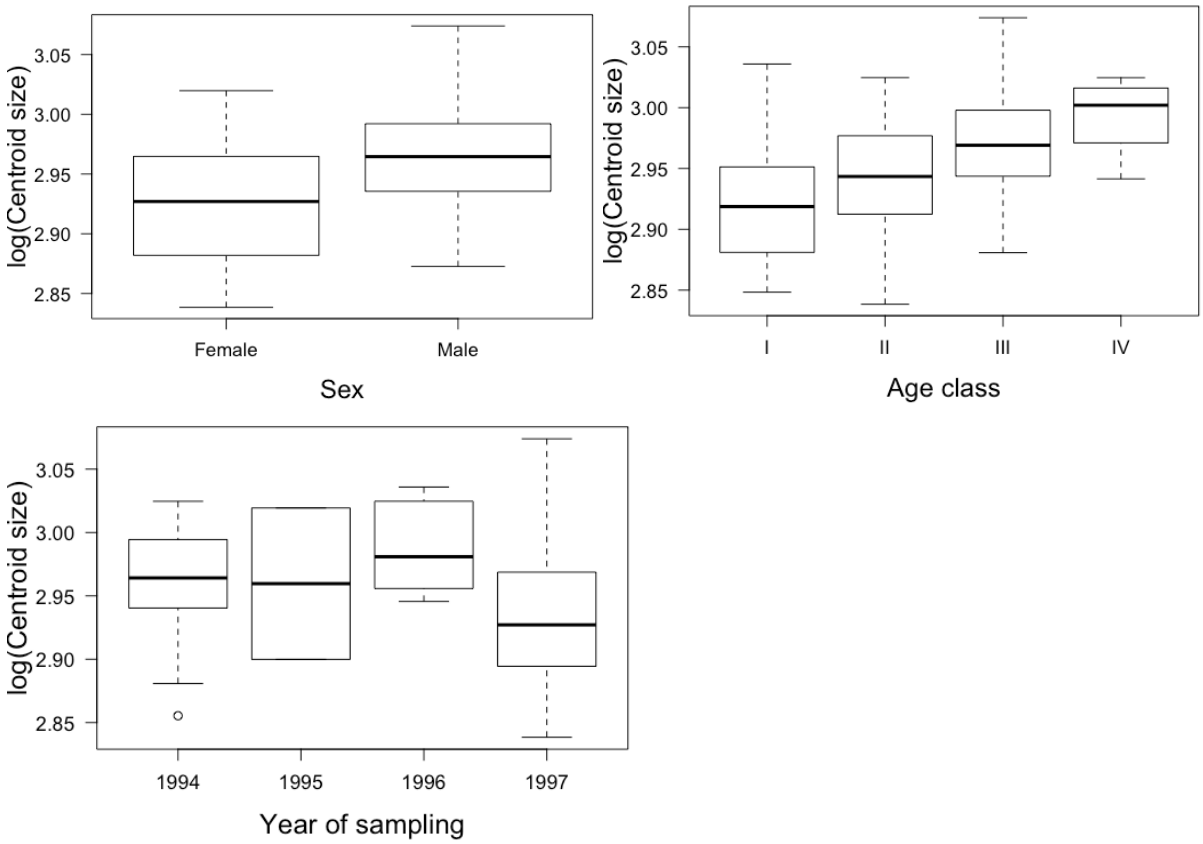


Figure 4.19. Variation in log-centroid size of the left mandible between the sexes (top-left), age classes (top-right), and years of sampling (bottom). The box represents the interquartile range from the 1st quartile (bottom of box) to the 3rd quartile (top of box) with the median indicated as a black line within the box. The horizontal ends of the whiskers indicate the minimum (bottom) and maximum (top) values.

Allometry of the mandible

A multivariate regression of size (using log-centroid size) on mandibular shape (the regression scores) showed that size was a highly significant predictor (Figure 4.20)) of shape, although the model explained very little of the variation (R^2=0.04). The age classes showed negative allometry (Figure 4.21), while year of sampling (Figure 4.22) and sex showed positive allometry (Figure 4.23).

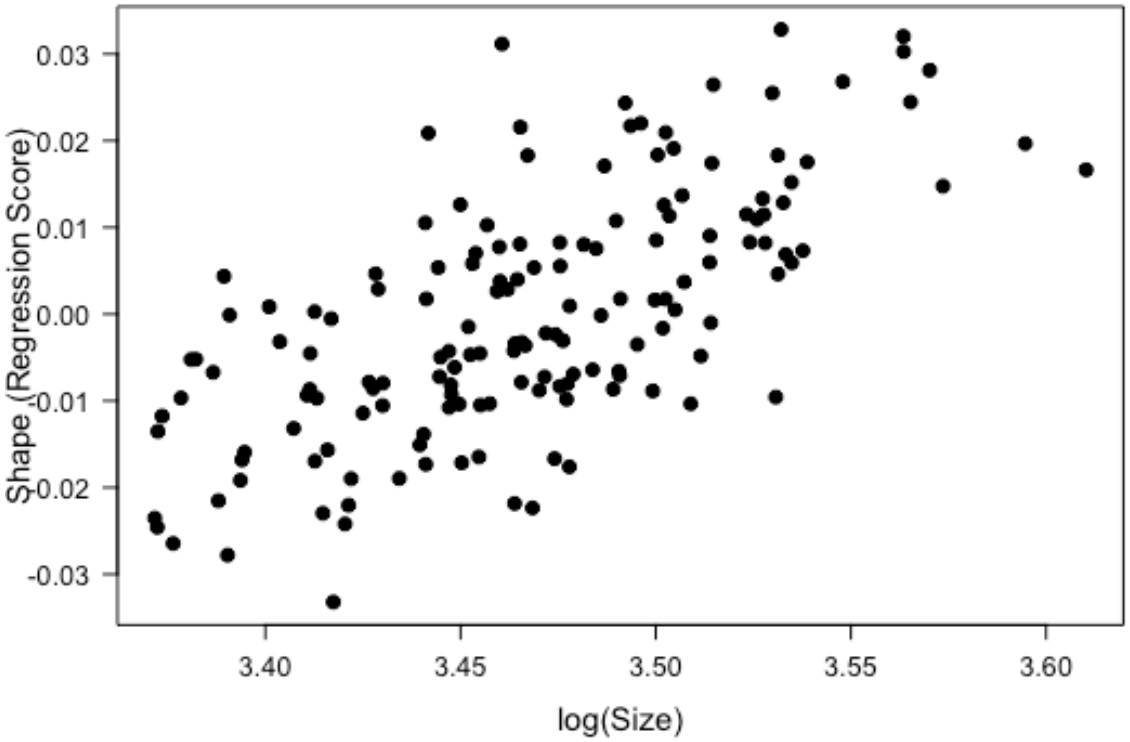


Figure 4.20. Multivariate regression of shape (using the regression score) on size (log-centroid size) of the mandible.

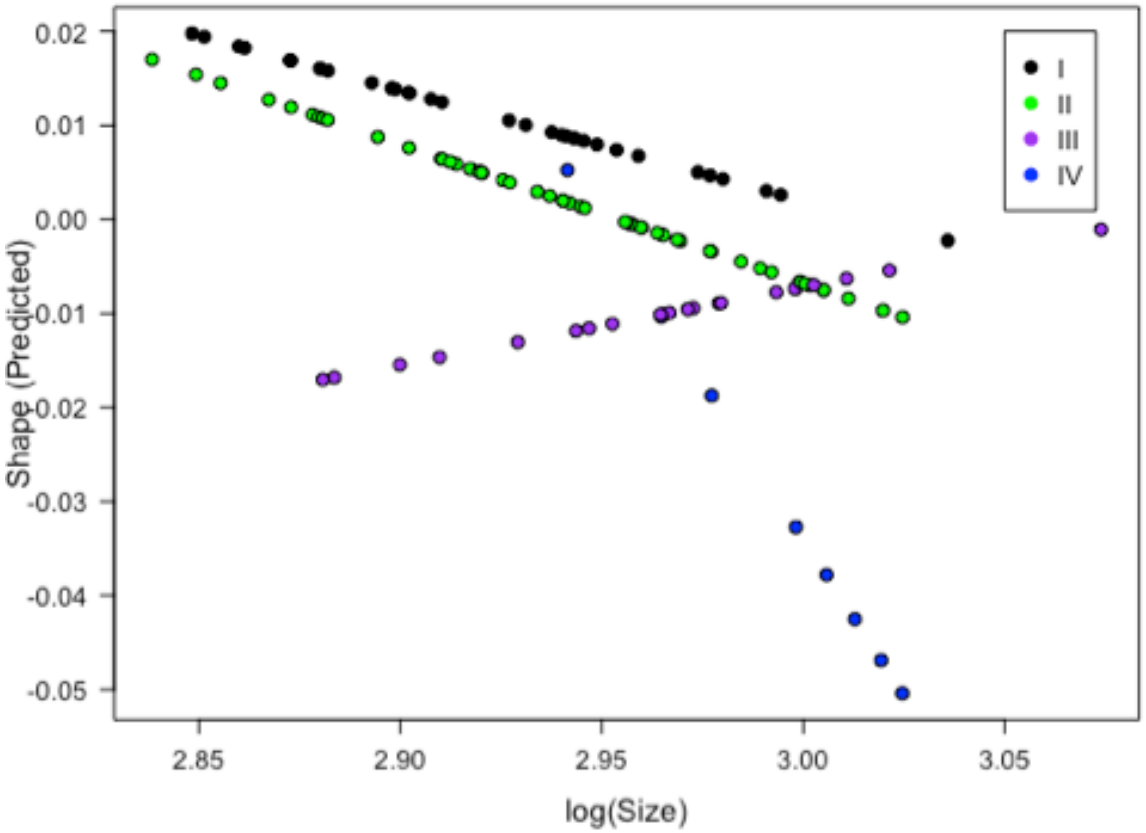


Figure 4.21. Allometric relationship between log-centroid size and the shape of the mandible for age classes.

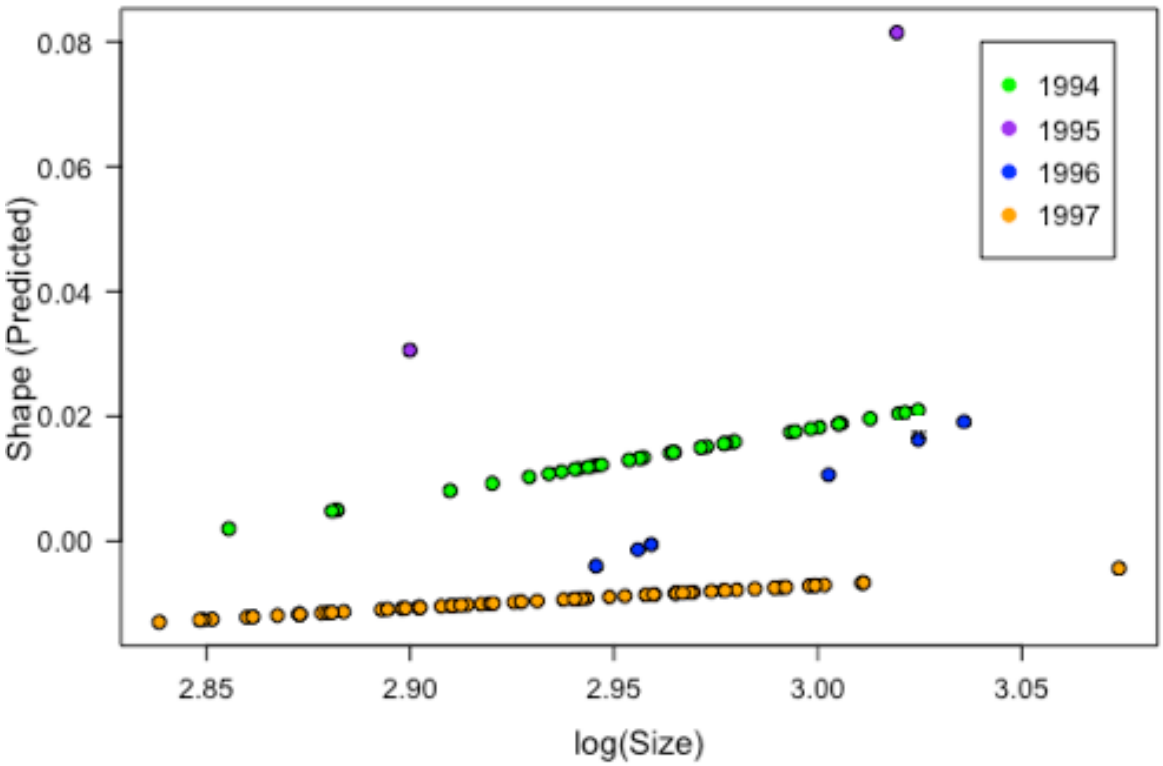


Figure 4.22. Allometric relationship between log-centroid size and the shape of the mandible for years of specimen collection.

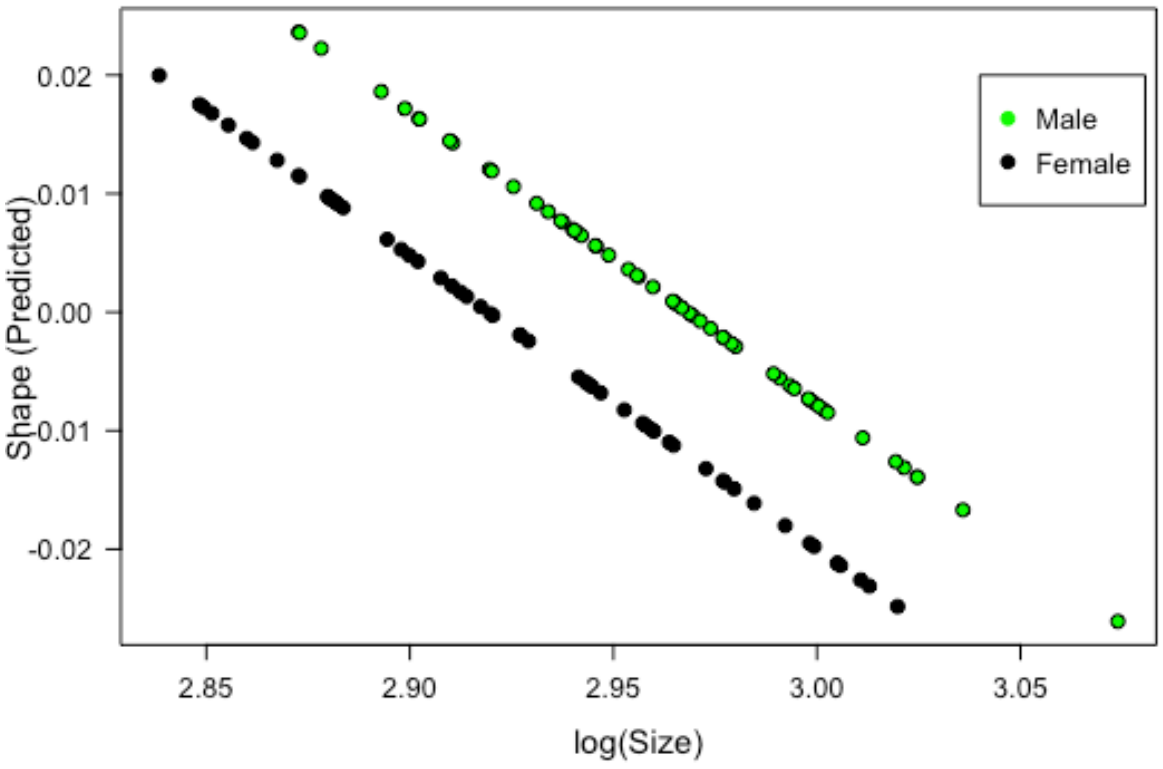


Figure 4.23. Allometric relationship between log-centroid size and the shape of the mandible for the sexes.

Shape comparisons of the mandible with PCA

Given the significance of size on shape, a PCA was constructed for the mandibles using size-corrected residuals. The age classes overlapped to a large degree and plotted along both PCs (Figure 4.24). Age class IV separated along the negative side of PC 1; specimens from age class IV had a more anteriorly-located landmark 7 (with a more curved posterior ventral border and thus a more curved ventral border of the angular process (Figure 4.24.

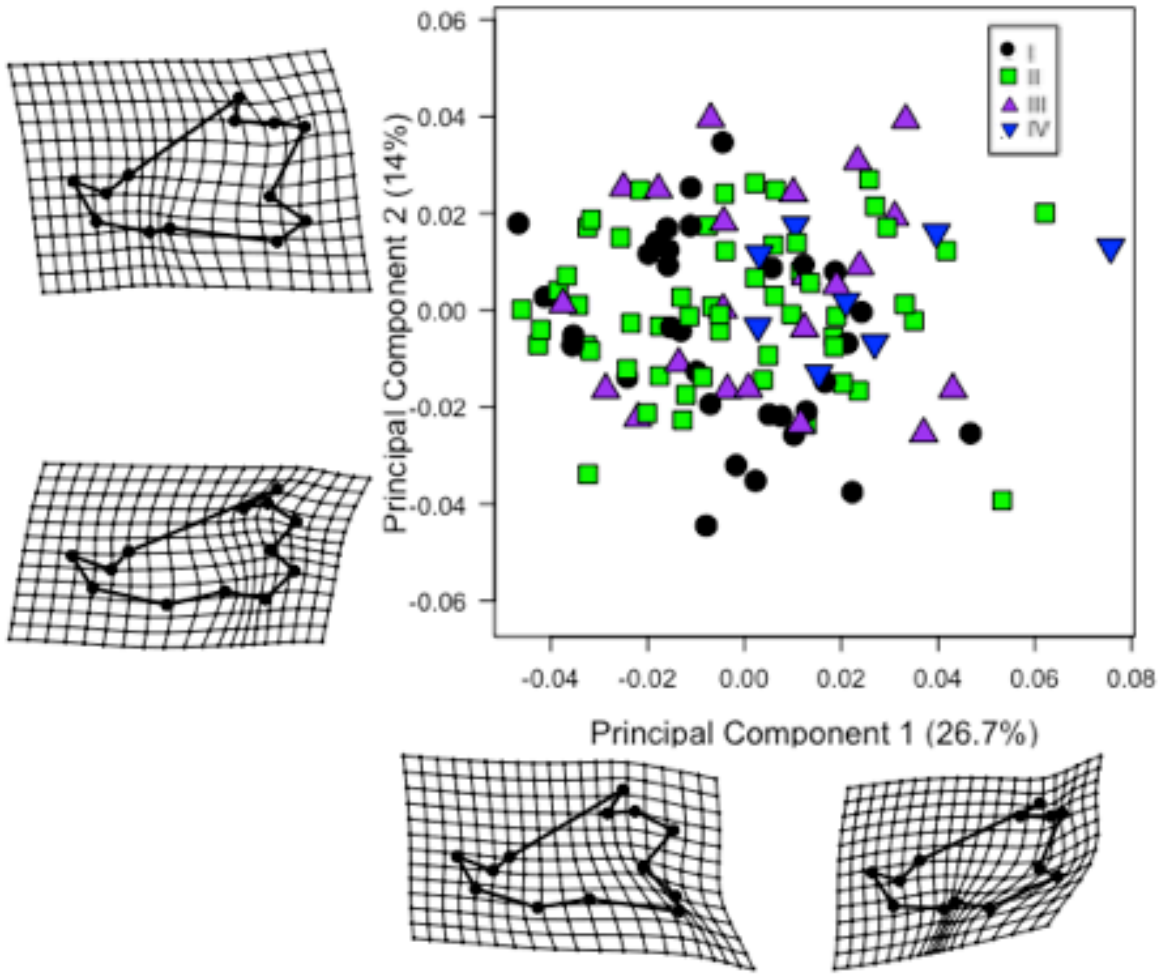


Figure 4.24. Allometry-adjusted Principal Component Analysis of the first two principal components indicating the spread of the four age classes for the mandible. Relative warp plots along the two axes indicate the minimum and maximum shape configurations along those axes. Relative warp plots have been magnified by a scale of three to more clearly illustrate variation.

The 1994 samples had a much looser spread than specimens sampled from the other years, although specimens sampled in 1997 also plotted quite loosely (Figure 4.25).

Specimens from 1994 and 1997 plotted along both PC axes indicating the specimens from those years had variable shapes (Figure 4.25). Specimens collected in 1996 plotted along the positive side (maxima) of PC1, indicating these specimens had a squarer angular process with landmarks 6 and 7 located closer together and landmark 7 located more posteriorly (Figure 4.25). The two specimens from 1995 plotted on the negative side (minimum) of PC 1 and indicated specimens in which the posterior curve (landmark seven) along the ventral border was located more anteriorly (closer to landmark 8 than landmark 6). This created a more ventrally curved angular process at the minimum of PC 1. These specimens also plotted on the positive side (maximum) of PC 2 and indicated a deeper posteriorly curved coronoid process as landmark one and two shifted more posteriorly and anteriorly, respectively, at the maximum of PC 2 (Figure 4.25).

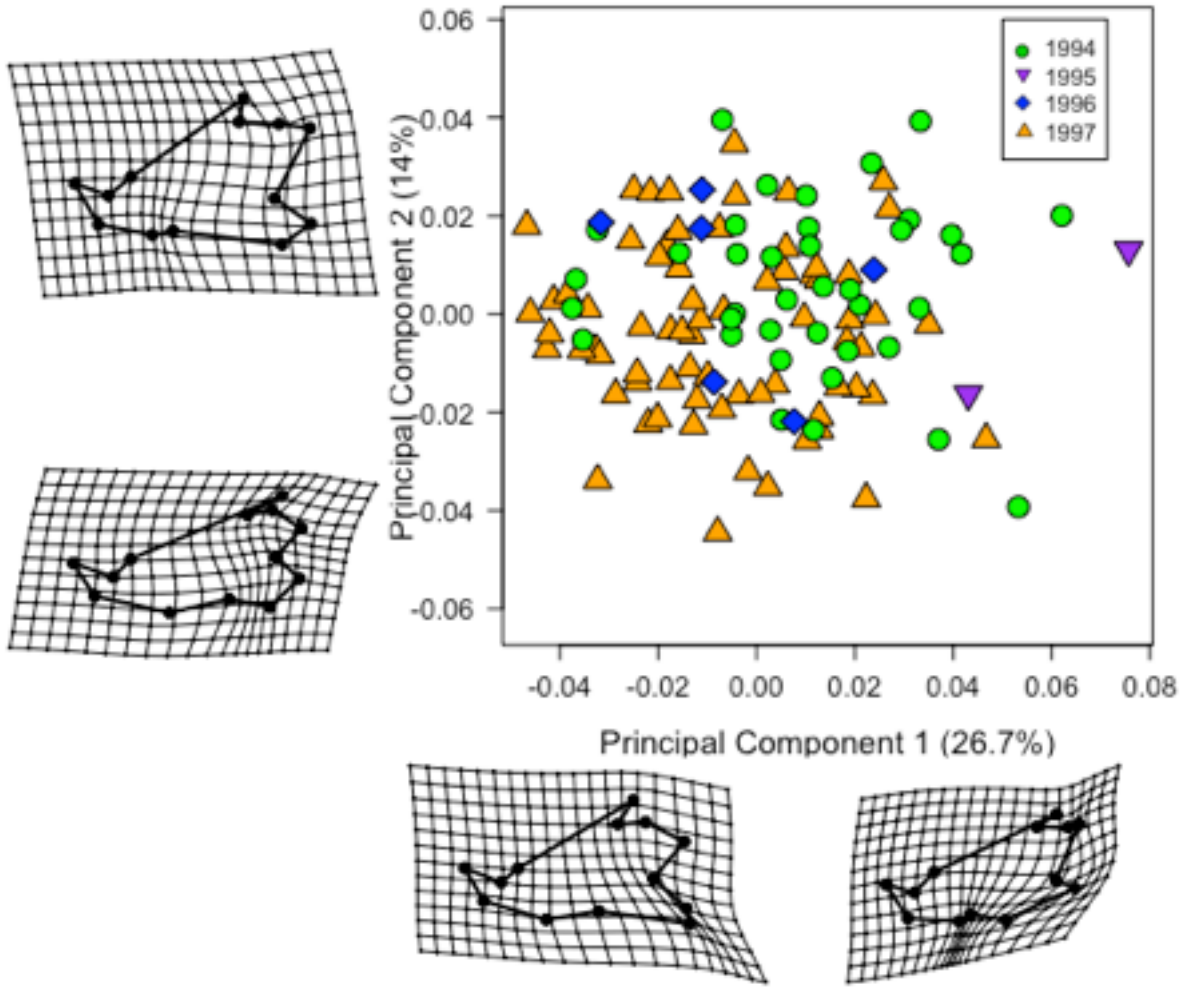


Figure 4.25. Allometry-adjusted Principal Component Analysis of the first two principal components indicating the spread across year of specimen collection for the mandible. The relative warp plots have been magnified by a factor of 3 to more clearly illustrate the differences between the two extrema of each axis.

The sexes did not appear to cluster in any way, as were spread across the ranges of both PC axes (Figure 4.26), displaying a wide morphological variance.

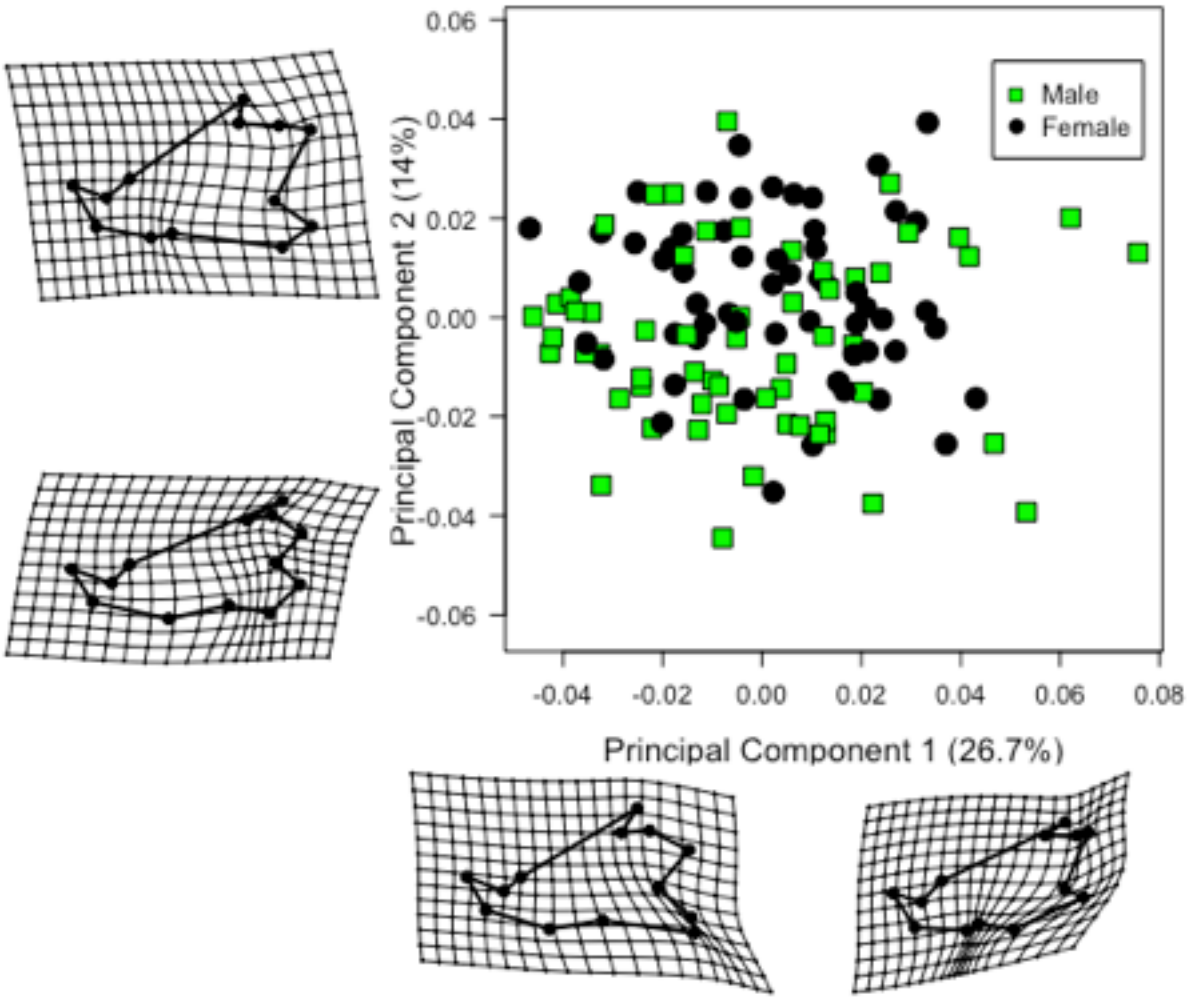


Figure 4.26. Allometry-adjusted Principal Component Analysis of the first two principal components indicating the spread for the sexes for the mandible. Relative Warp plots have been magnified by a scale of three to better illustrate shape differences between extrema.

4.4. Mandible landmark and semi-landmark curve analyses

Analysis of mandibular curve shape and size

All further analyses were restricted to the left hemi-mandible and the two left hemi-mandible images for each individual were averaged to avoid redundancy of information and to limit the effect of asymmetry on the data analysis. A MANOVA of the symmetric shape component showed that only age class was a significant predictor of mandibular shape (Table 4.4). Sex, year of sampling, the sex:age, the sex:year, the age:year, and the sex:age:year interactions were all non-significant for the shape component. The MANOVA for the size component showed that sex (Figure 4.27), and age class (Figure 4.27) were the only significant

predictors of mandible size, however year of sampling (Figure 4. 35), the sex:age interaction, the sex:year interaction, the age:year interaction, and the sex:age:year interaction were not significant predictors of size (Table 4.4).

Table 4.4. MANOVA results of the shape and size components of the symmetric variation in the mandible using semi-landmark analysis. Values in bold are statistically significant.

Component	Effect	d.f.	MS	F	P-value
Shape	Sex	1, 96	0.00100437	1.10	0.352
	Age	**3, 96**	**0.00144053**	**1.58**	**0.029**
	Year	1, 96	0.00133153	1.44	0.104
	Sex:Age	3, 96	0.00091452	1.00	0.402
	Sex:Year	3, 96	0.00121421	1.32	0.143
	Age:Year	4, 96	0.00113094	1.23	0.085
	Sex:Age:Year	2, 96	0.00092687	1.01	0.238
Size	**Sex**	**1, 96**	**27.4666**	**16.83**	**<0.001**
	Age	**3, 96**	**15.8590**	**9.72**	**<0.001**
	Year	3, 96	2.268	0.87	0.149
	Sex:Age	3, 96	0.9982	0.61	0.438
	Sex:Year	3, 96	0.6556	0.40	0.611
	Age:Year	4, 96	1.0018	0.61	0.433
	Sex:Age:Year	2, 96	2.0118	1.23	0.154

Pairwise tests for homogeneity of slopes for the significant shape factors showed that only age classes III and IV were significant different. Neither age class III nor IV differed significantly from age classes I and II. Age classes I and II did not differ significantly from each other either. No other factors were significant predictors of mandibular shape.

Males were larger than females (Figure 4.27). Pairwise tests for homogeneity of slopes for significant size factors detected significant differences between the age classes. Age class I differed significantly from age class III and age class IV, and age class II differed significantly to age class III and age class IV. Age class I did not differ significantly to age class II, and age class III did not differ significantly from age class IV (Figure 4.27).

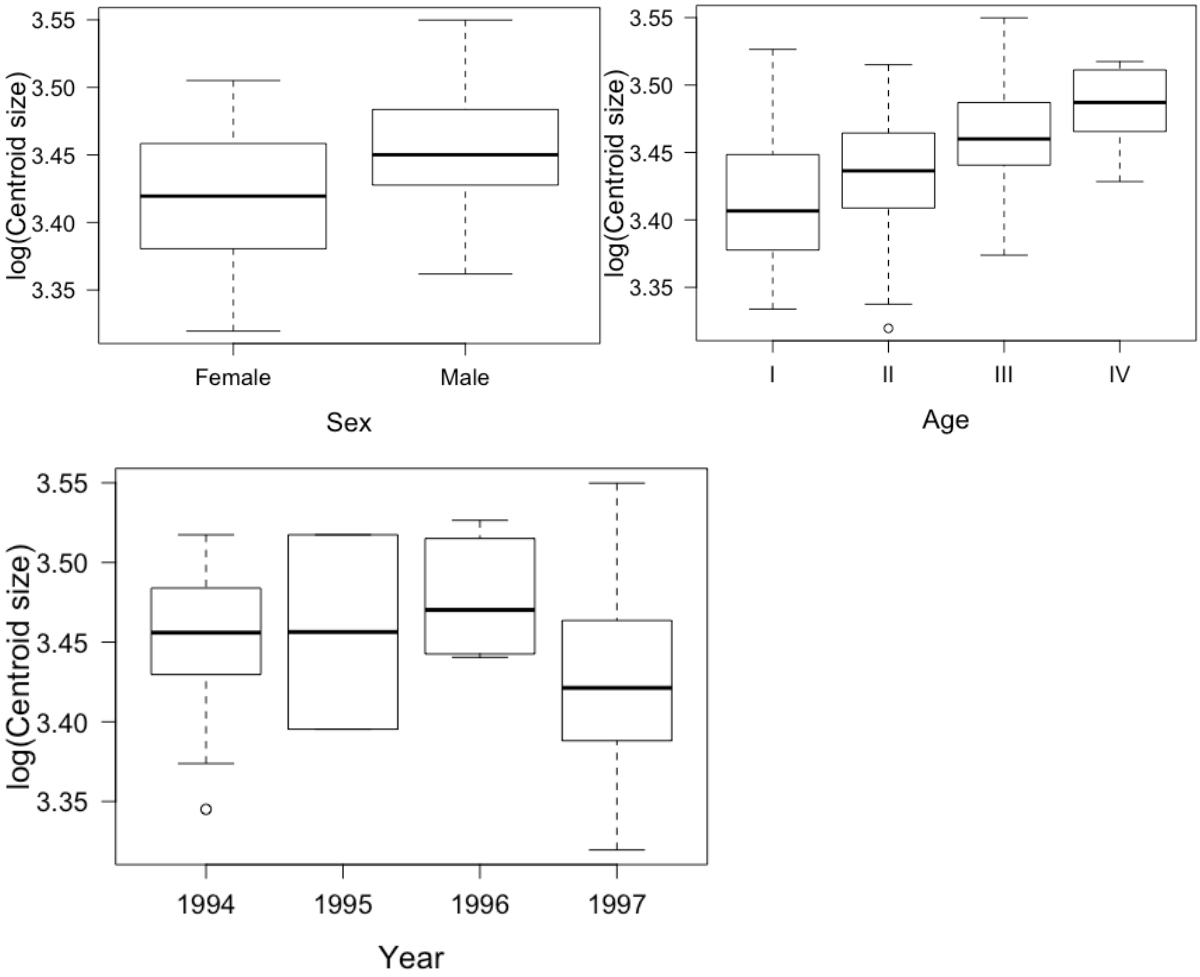


Figure 4.27. Variation in log-centroid size of the left mandible sampled using landmarks and semi-landmarks between sex (top-left), age class (top-right), and year of sampling (bottom). The box represents the interquartile range from the 1st quartile (bottom of box) to the 3rd quartile (top of box) with the median indicated as a black line within the box. The horizontal ends of the whiskers indicate the minimum (bottom) and maximum (top) values.

Allometry of mandibular curves

A multivariate regression of size (using log-centroid size as a proxy) on mandibular shape (using regression scores) showed that size was a highly significant predictor (Figure 4.28) of shape ($F= 3.926$; $d.f.= 1, 114$; $p<0.001$), although the model explained very little of the variation ($R^2=0.08$). The age classes demonstrated positive allometry (Figure 4.29). Year of sampling was positively allometric for 1996, and negatively allometric for 1994, 1995, and 1997 (Figure 4.30). Both sexes displayed parallel, negative allometry (Figure 4.31).

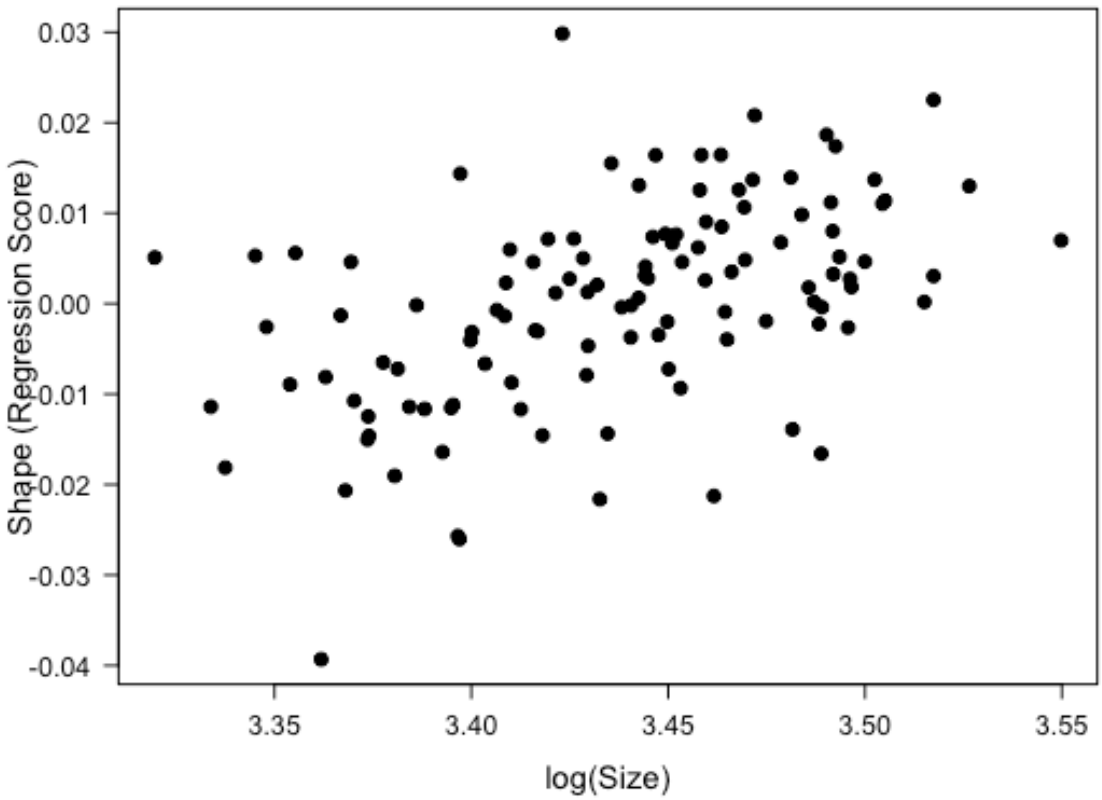


Figure 4.28. Multivariate regression of shape (using the regression score) on size (log-centroid size) of the mandibular curves.

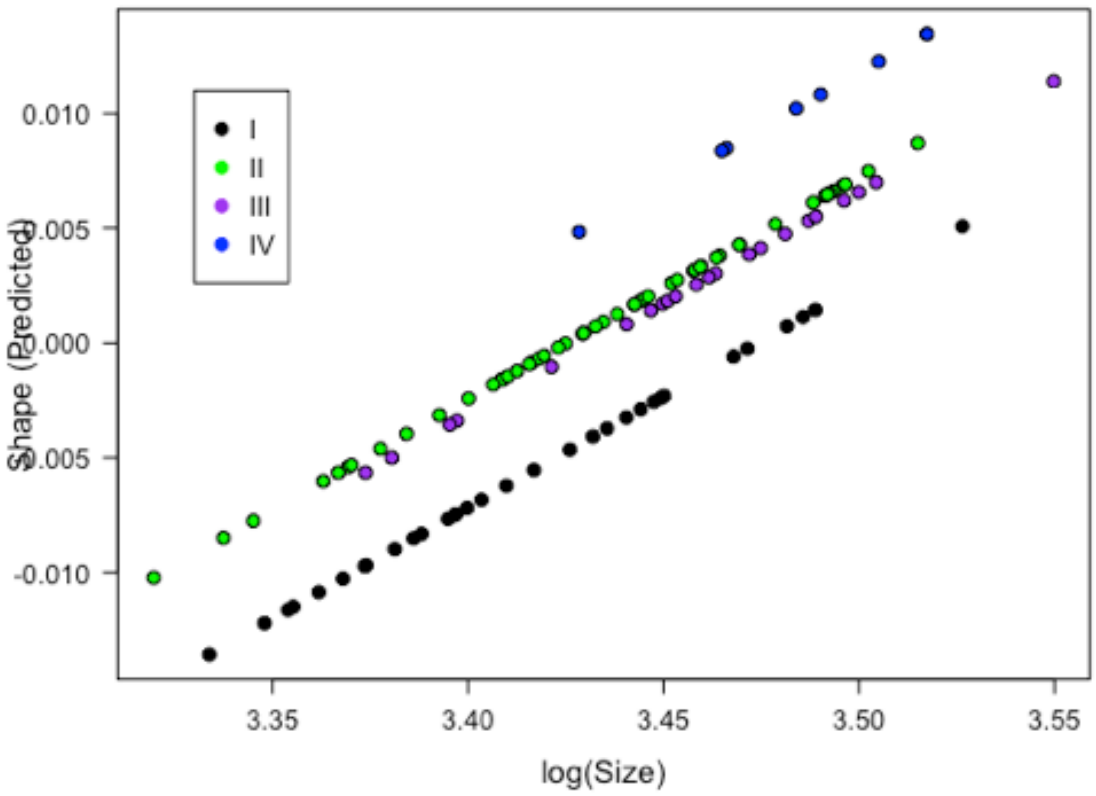


Figure 4.29. Allometric relationships of age classes for the mandible, sampled using semi-landmarks.

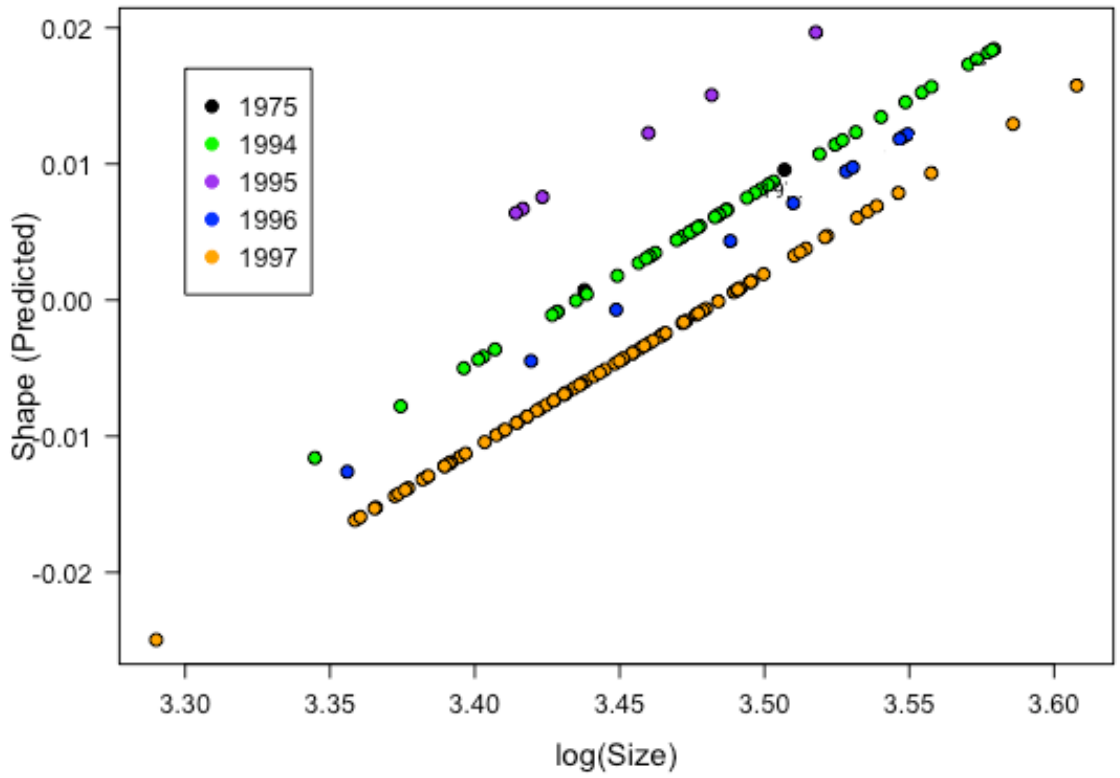


Figure 4.30. Allometric relationships between log-centroid size and the shape of the mandible, sampled using semi-landmarks for years of specimen collection.

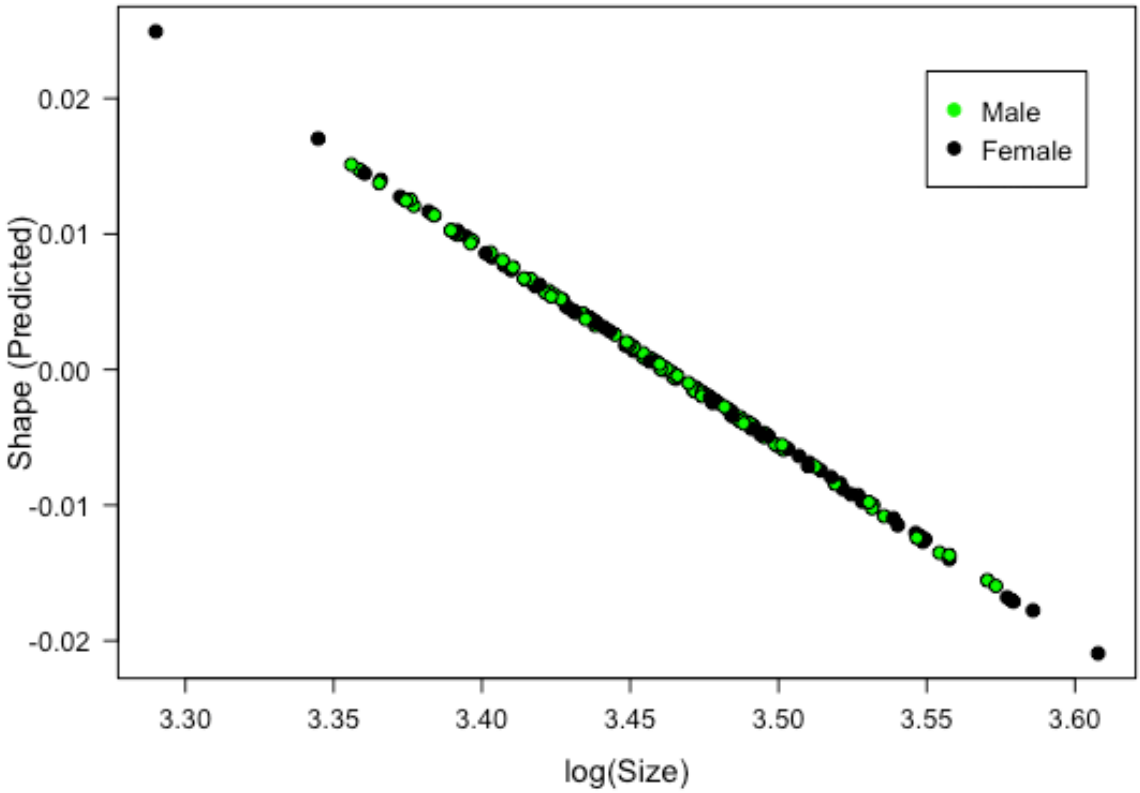


Figure 4.31. Relationship of allometry between log-centroid size and the shape of the mandible, sampled using semi-landmarks for the sexes.

Shape comparisons of the mandibular curves with PCA

Given the significance of size on shape, a PCA was constructed for the left hemi-mandibles using size-corrected residuals with the factor groups plotted onto the PCA. All age classes clustered loosely together, although the first three age classes were far more spread along both PC axes (Figure 4.32). The wide scatter of individuals from the first three age classes indicated a wide variety of shapes for individuals in those classes, including individuals with both ventrally shortened coronoids, a shallower curve between landmarks 1 and 2, and a shortened curve between landmarks 3 and 4 along the minimum extreme of PC 1. While the maximum of PC 1 (Figure 4.32) indicated a more dorso-ventrally enlarged ascending ramus, with more dorsally projected coronoid and condylar processes, a less concave curve between landmarks 3 and 4, and an overall shorter mandible (Figure 4.32). Along the second PC, individuals also displayed more anteriorly reduced coronoid processes, wider condylar and angular processes, smaller and less deeply curved region between landmarks three and four along the minimum extreme of PC 2 (Figure 4.32). Age class IV, however, plotted more along the maximum extreme of PC 2 and displayed a more posteriorly elongated coronoid process (defined by landmark one and the semi-landmarks between landmarks 1 and 2). Age class IV also displayed more posteriorly elongated condylar process with a more reduced surface for articulation (defined by the more posterior location of landmark two and the reduced distance between the second and third landmark), and a deeper and wider curve of the semi-landmarks between landmarks 4 and 5. The angular process was also narrower in age class IV (location of landmark 4 compared to the surrounding semi-landmarks; Figure 4.32).

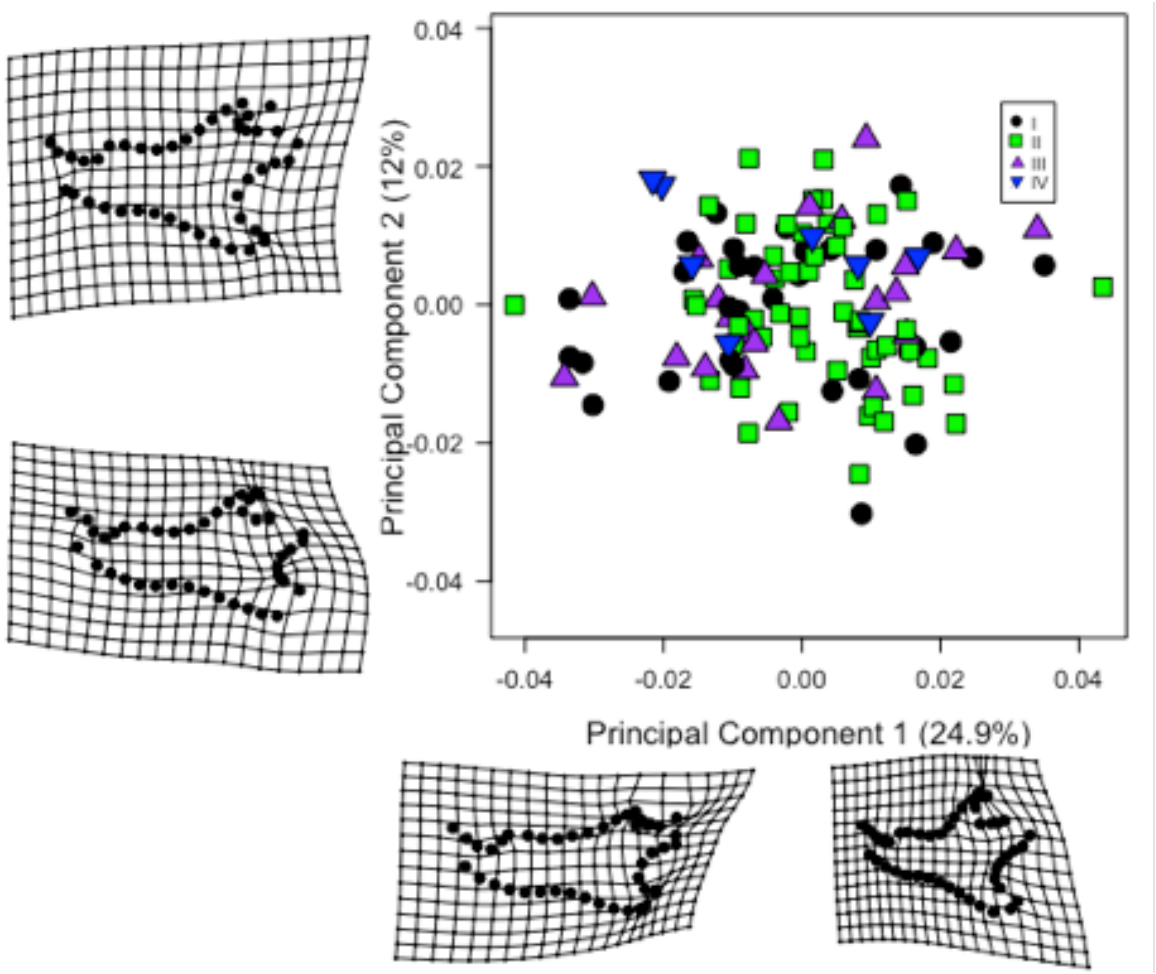


Figure 4.32. Allometry-adjusted Principal Component Analysis of the first two principal components indicating the spread of the four age classes for the mandibular curves. Relative warp plots along the two axes indicate the minimum and maximum shape configurations along those axes. Relative warp plots have been magnified by a scale of three to more clearly illustrate variation.

Specimens collected from 1994 and 1997 clustered loosely throughout the PCA along both PC axes, which indicated individuals with a broad variety of shapes (Figure 4.33). The two specimens from 1995 plotted at the minimum of PC 1 and the maximum of PC 2. These specimens demonstrated antero-posterior elongation of the mandible and shortened condylar and angular processes (PC 1) and a more posteriorly elongated coronoid process. These specimens form 1995 had wider angular processes and a deeper curve between the condylar and angular processes (Figure 4.33). The specimens sampled from 1996 plotted more centrally along PC 1, but along most of PC 2. The specimens from 1996 thus displayed a more intermediate shape between the PC 1 extremes but varied in the degree of coronoid posterior curvature (semi-landmarks on the dorsal curve before landmark 1), and the depth of

the curvature between the coronoid and condyle (semi-landmarks between landmarks 1 and 2). The breadth of the angular process and the extreme concavity of the curve between the condylar and angular processes (semi-landmarks between landmarks 3 and 4; Figure 4.33) was also highly variable.

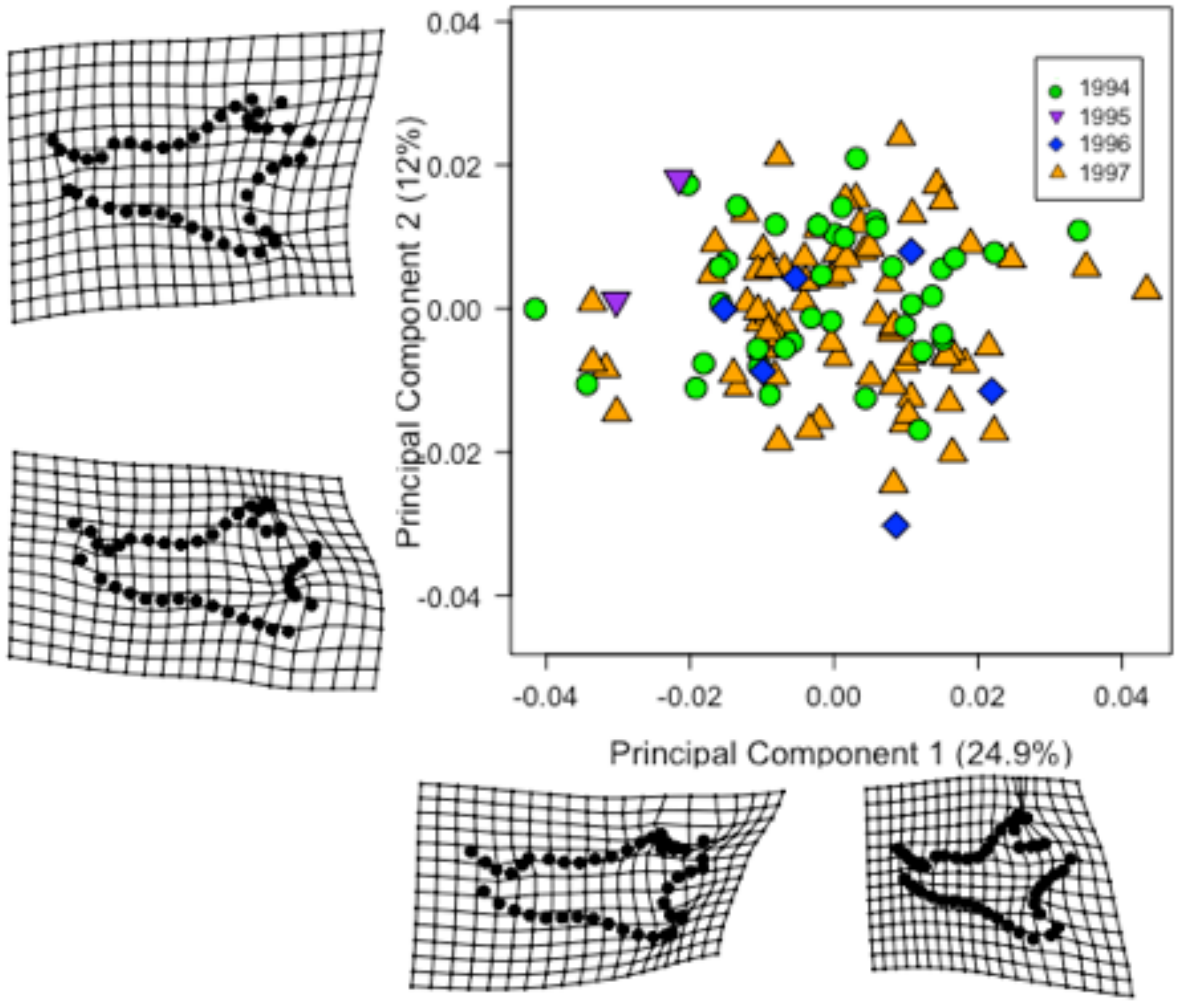


Figure 4.33. Allometry-adjusted Principal Component Analysis of the first two principal components indicating the spread for year of specimen collection for the mandibular curves. The relative warp plots have been magnified by a factor of 3 to more clearly illustrate the differences between the two extrema of each axis.

The sexes, while clustering loosely together, separated slightly on average, as females had a slightly more curved ascending ramus located in the top-left half of the PCA (PC 1 maximum and PC 2 minimum and males had slightly more protruding processes and plotted in the bottom-right half (PC 1 minimum and PC 2 maximum) of the PCA (Figure 4.34).

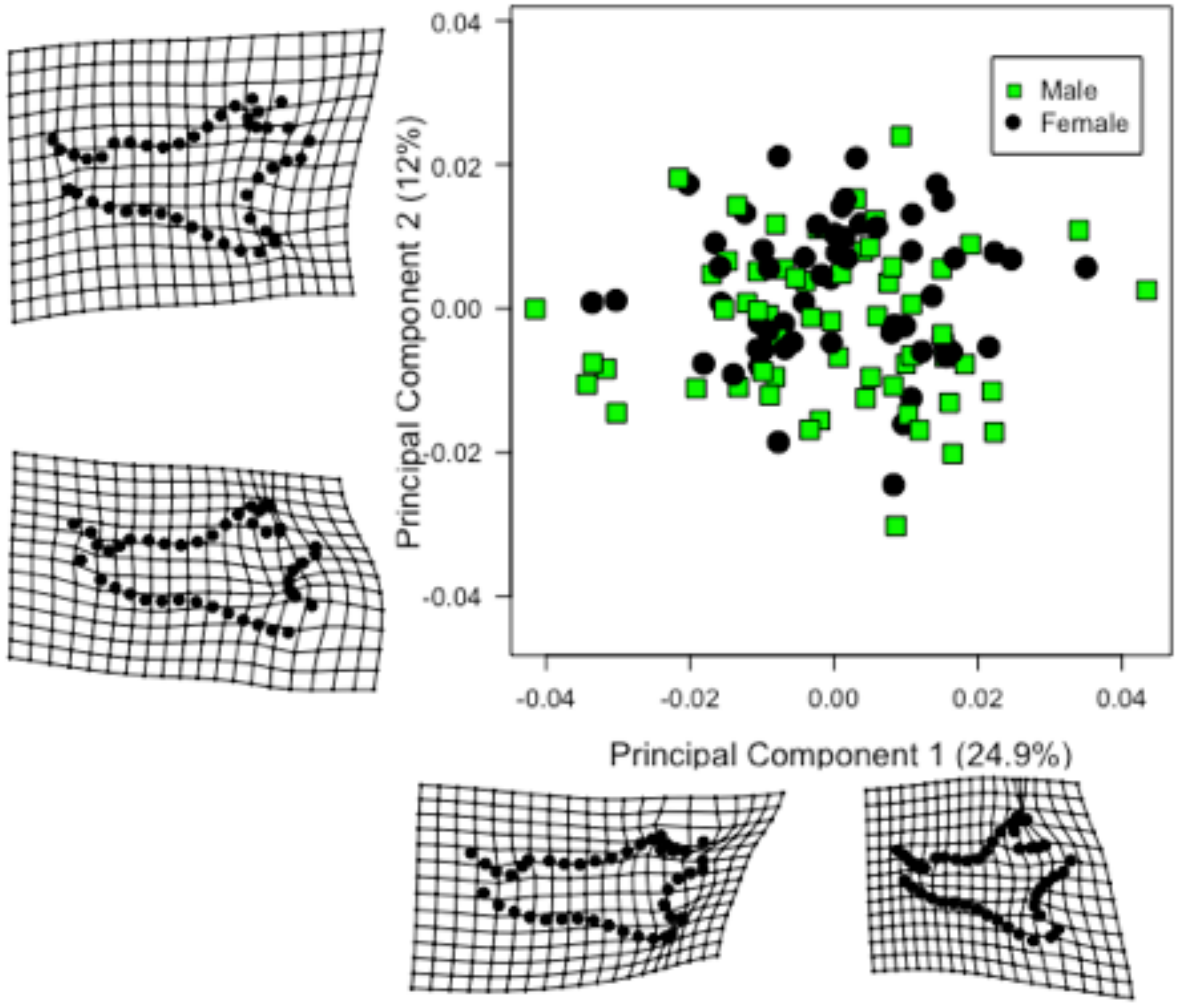


Figure 4.34. Allometry-adjusted Principal Component Analysis of the first two principal components indicating the spread for the sexes for the mandibular curves. Relative Warp plots have been magnified by a scale of three to better illustrate shape differences between extrema.

4.5. Outline analysis of Molars

Analysis of shape and size of the first upper molar

The shape MANOVA (Table 4.5) of the first upper molar showed that age class and year of sampling were significant predictors of shape variation, while sex, and the interactions between sex, age class, and year of sampling were not significant predictors of shape. The size MANOVA (Table 4.5) showed that age (Figure 4.43) was a significant predictor of size, while sex (Figure 4.44), year of sampling (Figure 4.45), and the interactions between sex, age, and year of sampling were not significant predictors of size for the first upper molar.

Table 4.5. MANOVA results of the shape and size components of the symmetric variation in the first upper molar. Values in bold are statistically significant

Component	Effect	d.f.	MS	F	P-value
Shape	Sex	1, 140	0.0015037	1.29	0.233
	Age	**3, 140**	**0.0051871**	**4.45**	**0.001**
	Year	**4, 140**	**0.0037481**	**3.21**	**0.001**
	Sex:Age	3, 140	0.0012223	1.05	0.389
	Sex:Year	3, 140	0.0009370	0.80	0.690
	Age:Year	9, 140	0.0015239	1.31	0.081
	Sex:Age:Year	4, 140	0.0012359	1.06	0.338
Size	Sex	1, 140	0.00008	0.001	0.969
	Age	**3, 140**	**0.32374**	**4.40**	**0.009**
	Year	4, 140	0.07961	1.08	0.377
	Sex:Age	3, 140	0.13647	1.85	0.147
	Sex:Year	3, 140	0.06487	0.88	0.434
	Age:Year	9, 140	0.13840	1.88	0.066
	Sex:Age:Year	4, 140	0.05921	0.80	0.498

A pairwise comparison of the homogeneity of slopes for significant shape factors detected significant differences only between age classes I and II although not between these age classes and age classes III and IV. Age class III did not differ significantly from age class IV. Significant shape differences were found between the following years of sampling: 1994 and 1995, 1994 and 1997, 1995 and 1996, and 1995 and 1997. However, specimens from 1975 and 1996 did not differ significantly from specimens from 1994 and 1997, nor from each other.

A pairwise comparison of size in the age classes showed that age class I was significantly smaller than age classes II, III, and IV, age class II was significantly smaller than age class IV, and age class three was significantly smaller than age class IV (Figure 4.43). Only age classes II and III did not differ significantly from each other.

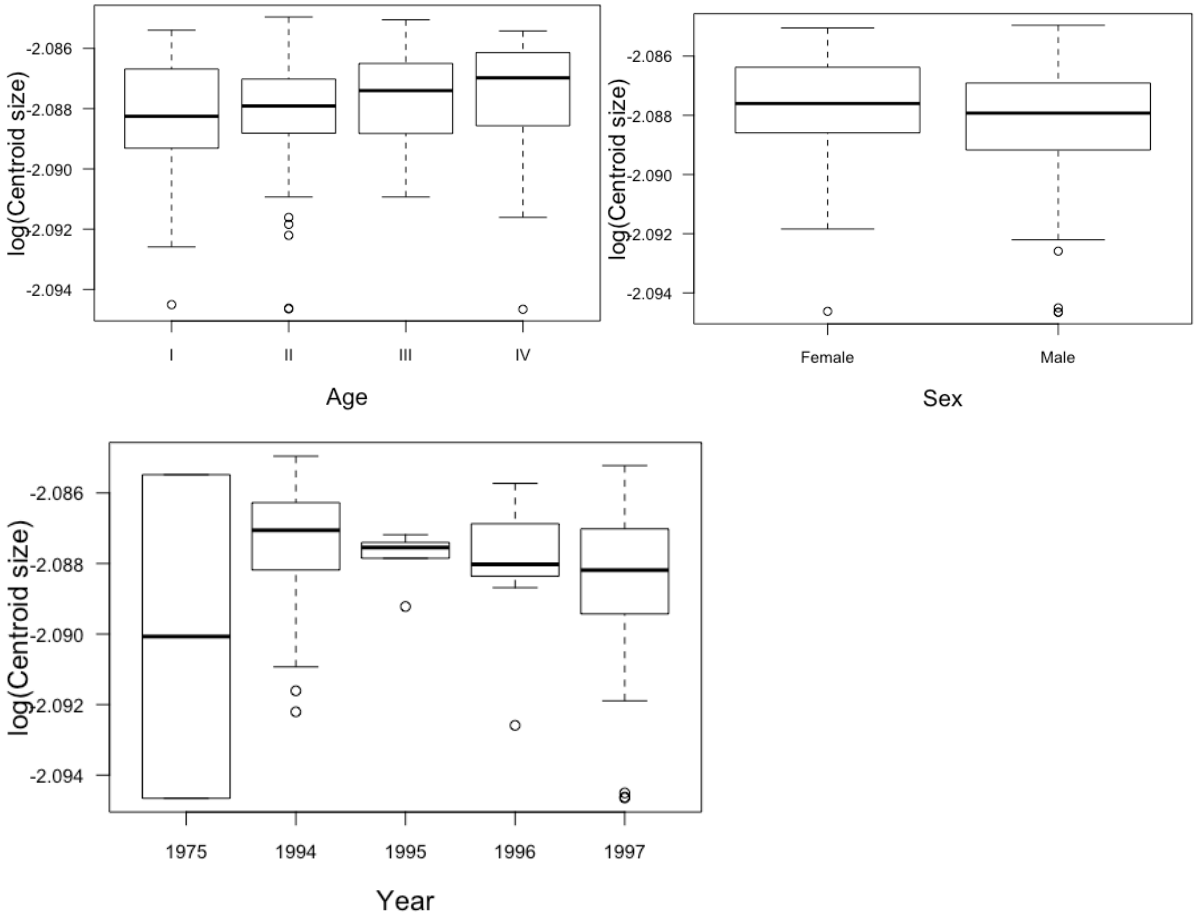


Figure 4.35. Variation in log-centroid size of the first upper molar between age classes (top-left), sex (top-right), and year of sampling (bottom). The box represents the interquartile range from the 1st quartile (the bottom of the box) to the 3rd quartile (the top of the box) with the median indicated as a black line within the box. The end of the whiskers indicates the minimum (bottom) and maximum (top) values. Open circles indicate outliers.

Allometry of the first upper molar

A multivariate regression of the shape scores on log-centroid size showed that size was a highly significant predictor of shape F=3.62; d.f.= 1, 166; p = 0.003) in the first upper molar (Figure 4.36), although the multivariate regression did not explain very much of the variability (R^2=0.02). A multivariate regression of shape on log-centroid size showed that age (Figure 4.37) was negatively allometric for 1994 and 1997 and positively allometric for 1975, 1995, and 1996. Year of sampling (Figure 4.38) was negatively allometric with different ontogenetic trajectories, and sex (Figure 4.39) showed a negative allometric relationship for females and a positive allometric relationship between shape and log-centroid size for males.

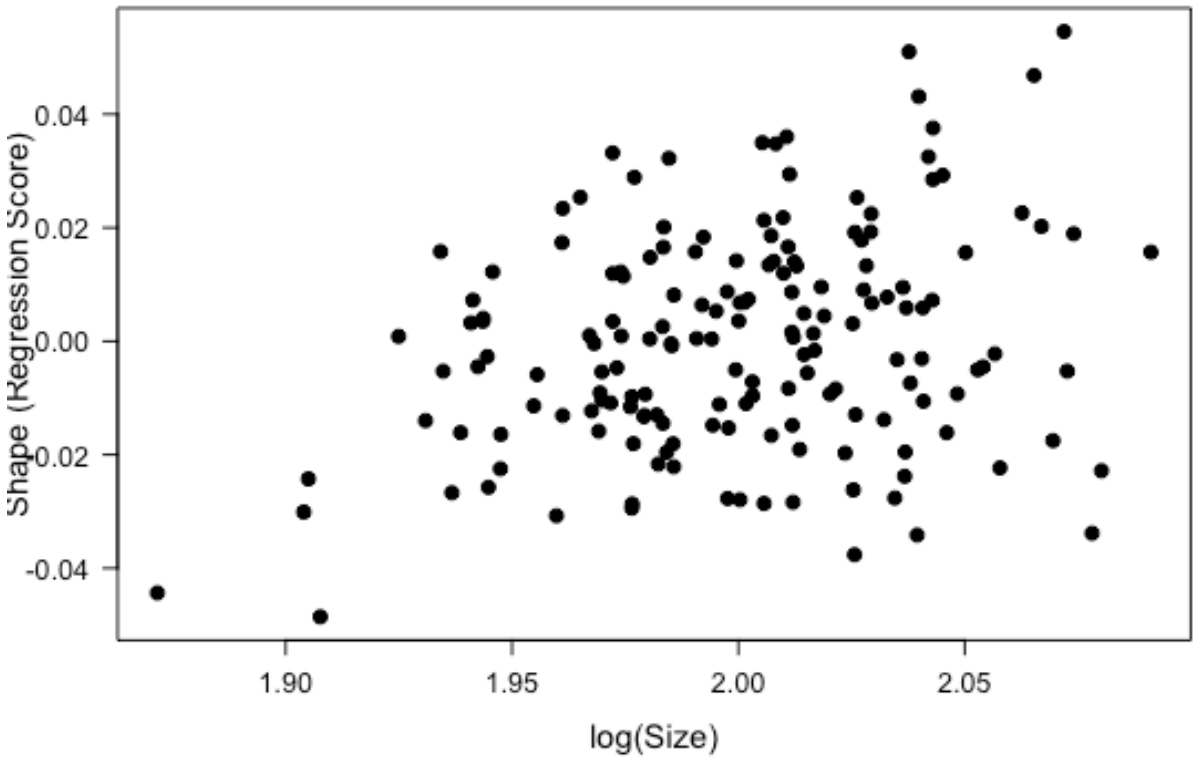


Figure 4.36. Multivariate regression of shape (using the regression score) on size (log-centroid size) of the first upper molar.

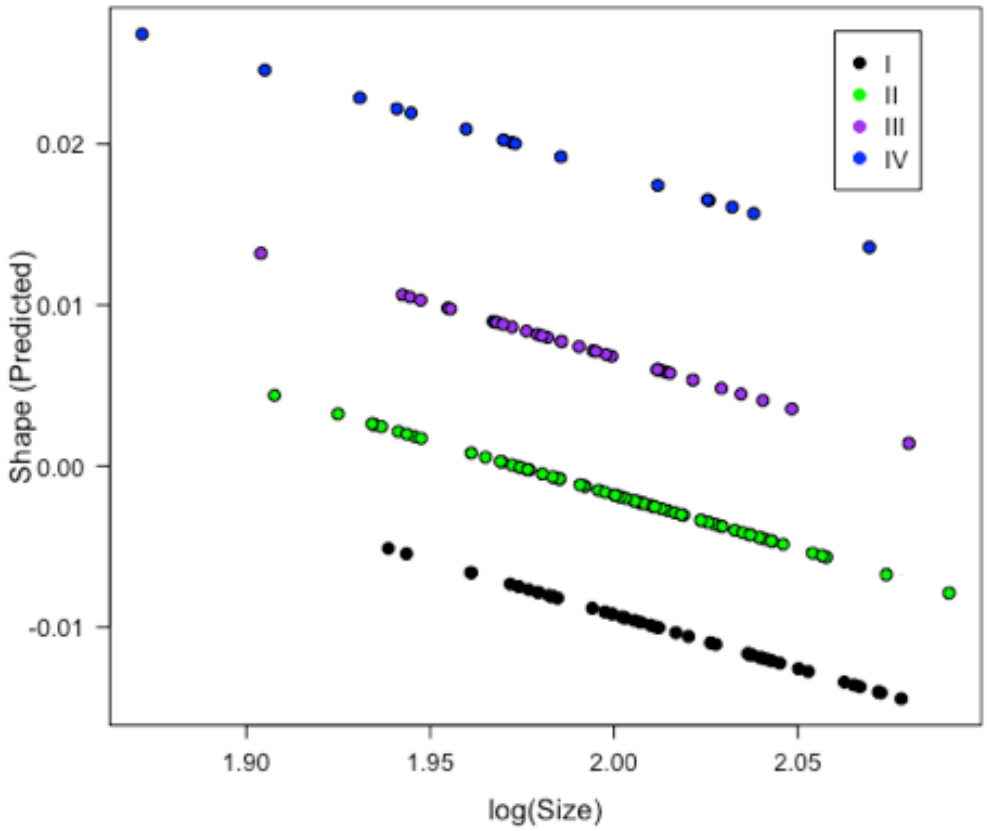


Figure 4.37. Allometric relationship between log-centroid size and first upper molar shape in the four age classes.

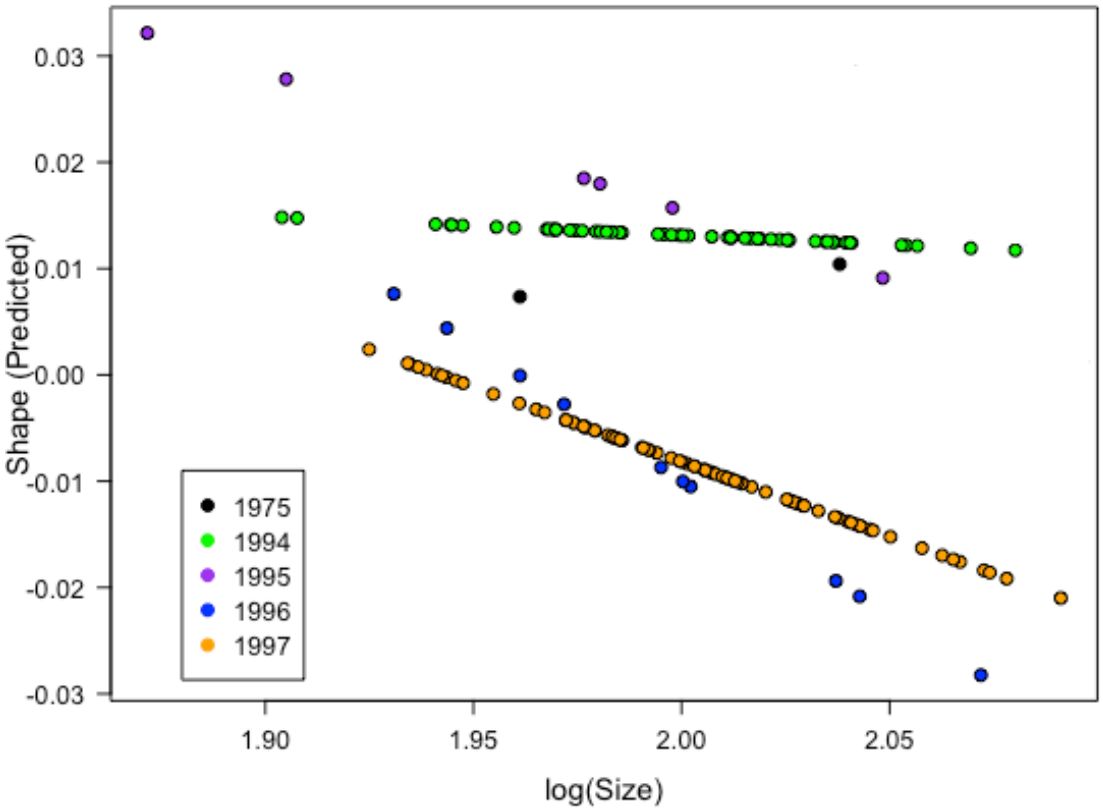


Figure 4.38. Allometric relationship between log-centroid size and first upper molar shape among years of specimen collection.

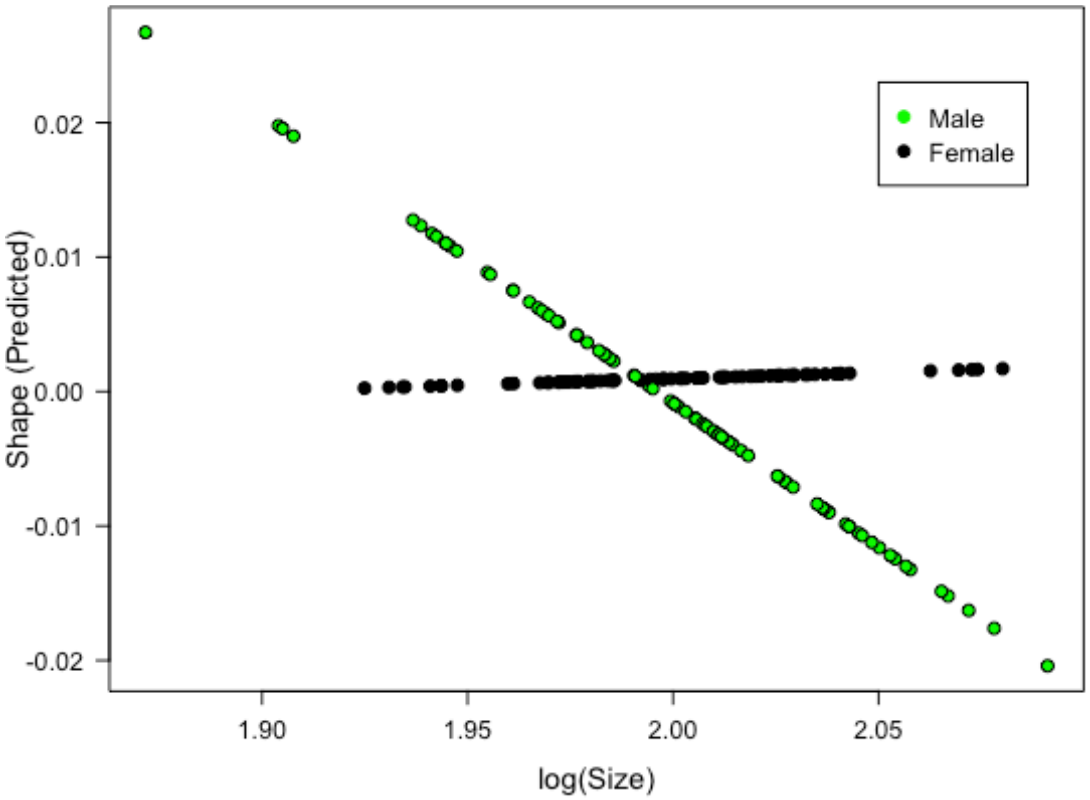


Figure 4.39. Allometric relationship between log-centroid size and first upper molar shape between the sexes.

Shape comparisons of the first upper molar with PCA

Due to the large effect of size on shape, I calculated allometry-free residuals using a multivariate linear regression and used these residuals to construct an allometry-free Principal Component Analysis (PCA). The size-corrected PCA was plotted with four Relative Warp plots to illustrate the extremes along the first two principal component axes (Figures 4.40, 4.41, 4.42). The PCA supported the shape MANOVA results as the first two age classes separated out the most, with the first molars of age class I located primarily at the negative extreme of PC 1, and the first molars of the age class II located further along the positive extreme of PC 1 (Figure 4.40). Age class I thus displayed more defined cusp outlines as well as more elongate molars, while age class II displayed cusps that were more antero-posteriorly compressed (Figure 4.40). Age classes III and IV were clustered together toward the end of PC 1, with most of the shape variation spread along PC 2. Age class IV plotted toward the negative extreme of PC 2 indicating a more medio-laterally widened and antero-posteriorly compressed shape with little cusp definition, while age class III plotted more toward the positive extreme of PC 2 with less defined cusps and an antero-posteriorly elongated and medio-laterally compressed shape (Figure 4.40).

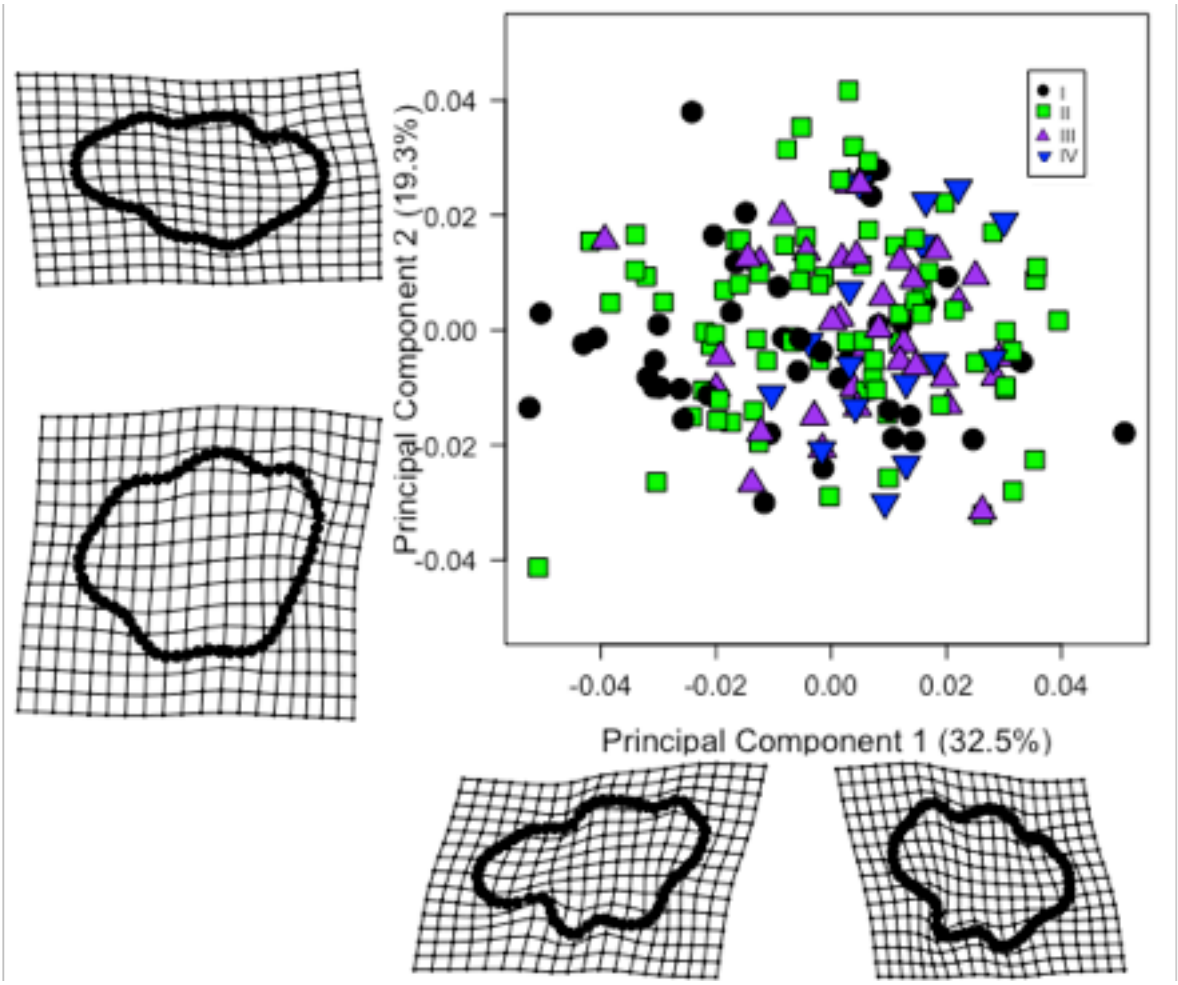


Figure 4.40. Allometry-adjusted Principal Component Analysis of the first two principal components indicating the spread of the four age classes for the first upper molar. Relative warp plots along the two axes indicate the minimum and maximum shape configurations along those axes. Relative warp plots have been magnified by a scale of three to more clearly illustrate variation.

While there was considerable overlap between years of sampling overall, clear patterns were distinguishable and provided support for the shape MANOVA results. Molars from specimens collected in 1975, 1994 and 1995 were located more toward the positive extreme of PC 1, indicating more antero-posteriorly compressed, rounded first molars (Figure 4.41). Specimens from 1997 and 1996 plotted closer to the negative extreme of PC 1 indicating anteroposterior elongation with defined cusp outlines. All years plotted along the length of PC 2, and as such PC 2 did not provide much shape variation to what was shown to be significant by the shape MANOVA (Figure 4.41; Table 4.5).

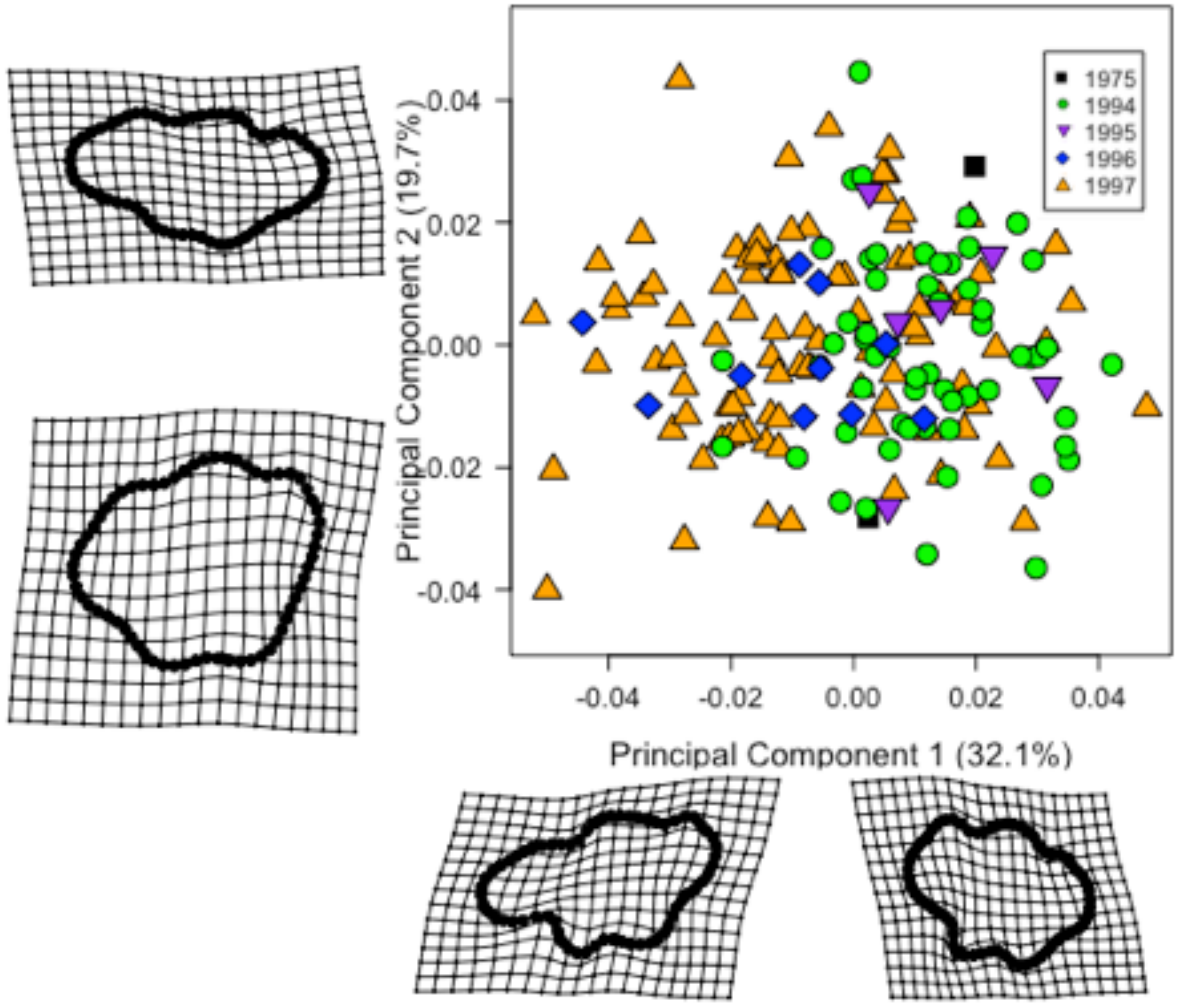


Figure 4.41. Allometry-adjusted Principal Component Analysis of the first two principal components indicating the spread across year of specimen collection for the first upper molar. The relative warp plots have been magnified by a factor of three to more clearly illustrate the differences between the two extrema of each axis.

As with all previous anatomical structures, sexual shape dimorphism in the first upper molar was not evident in the PCA, supporting shape MANOVA results (Figure 4.42; Table 4.5). Both sexes clustered together along both PC axes.

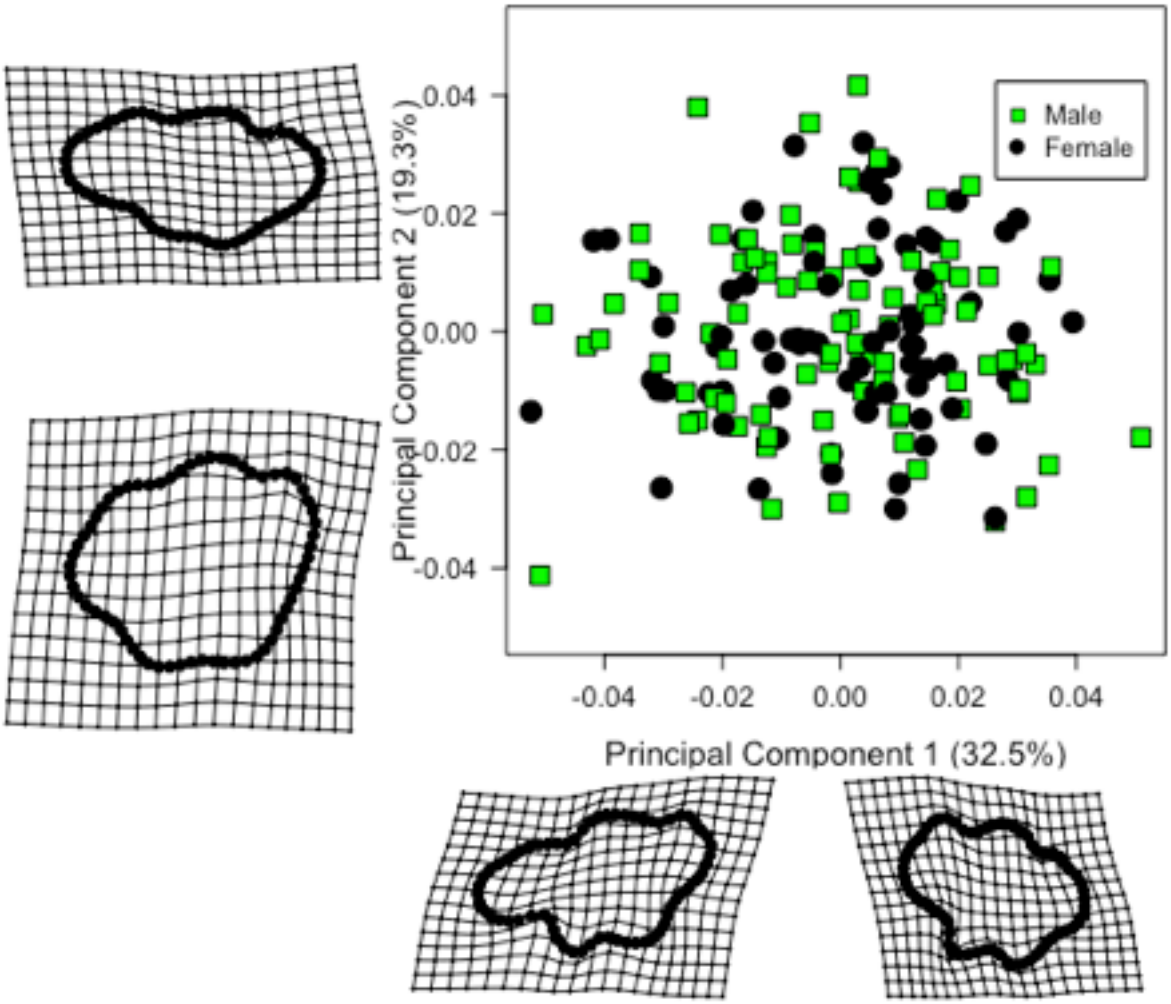


Figure 4.42. Allometry-adjusted Principal Component Analysis of the first two principal components indicating the spread for the sexes for the first upper molar. Relative Warp plots have been magnified by a scale of three to better illustrate shape differences between extrema.

Analysis of shape and size of the second upper molar

The shape MANOVA (Table 4.6) for the second upper molar showed that only age was a significant predictor of shape variation, while sex, year, and the interactions between sex, age, and year were not significant shape predictors. The size MANOVA conducted on log-centroid size showed that age (Figure 4. 53) and year (Figure 4.54) were significant predictors of size of the second upper molar, although sex (Figure 4.55) and the interactions between sex, age, and year were not significant (Table 4.6).

Table 4.6. MANOVA results of the shape and size components of the symmetric variation in the second upper molar. Values in bold are statistically significant

Component	Effect	d.f.	MS	F	P-value
Shape	Sex	1, 140	0.00100437	1.10	0.853
	Age	**3, 140**	**0.00144053**	**1.58**	**0.001**
	Year	4, 140	0.00133153	1.44	0.066
	Sex:Age	3, 140	0.00091452	1.00	0.085
	Sex:Year	3, 140	0.00121421	1.32	0.064
	Age:Year	9, 140	0.00113094	1.23	0.276
	Sex:Age:Year	4, 140	0.00092687	1.01	0.708
Size	Sex	1, 140	0.000088	0.002	0.970
	Age	**3, 140**	**0.198374**	**4.19**	**0.011**
	Year	4, 140	**0.133020**	**2.81**	**0.027**
	Sex:Age	3, 140	0.056809	1.20	0.307
	Sex:Year	3, 140	0.055903	1.18	0.327
	Age:Year	9, 140	0.063850	1.35	0.224
	Sex:Age:Year	4, 140	0.037797	0.80	0.532

A pairwise comparison of the homogeneity of slopes showed significant shape differences only between age class II and age class III, although not between age classes I and IV. Age classes I and IV were not significantly different from age classes II and III either.

A pairwise comparison of the homogeneity of slopes for size indicated that age class I and age class II were the only age classes not significantly different from one another (Figure 4.43). Age classes I and II were the largest in second molar size, age class III was smaller than the first two age classes, and age class IV displayed the smallest second upper molars compared to the first three age classes (Figure 4.43). Pairwise comparisons of the homogeneity of slopes across years of sampling indicated that the second molars from specimens collected in 1994 were significantly different from the second molars of specimens collected in 1995 and 1997. Specimens from 1995 had the smallest second molars of all years, while those from 1994 had the largest, and those from 1997 had the second largest second upper molars (Figure 4.43). Specimens from 1975 and 1996 were not

significantly different from any of the other years, and nor were they significantly different from each.

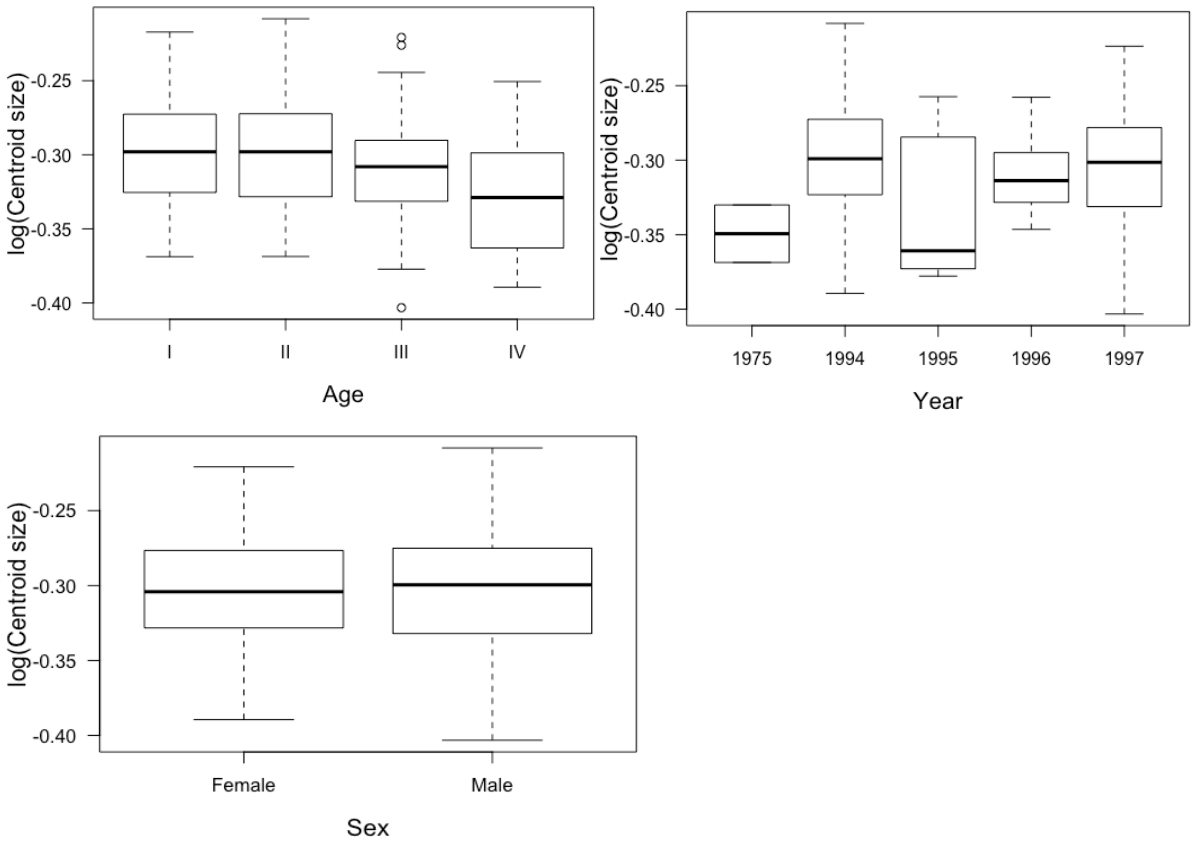


Figure 4.43. Variation in log-centroid size of the second upper molar between age classes (top-left), year of sampling (top-right), and sex (bottom). The box represents the interquartile range from the 1st quartile (the bottom of the box) to the 3rd quartile (the top of the box) with the median indicated as a black line within the box. The end of the whiskers indicates the minimum (bottom) and maximum (top) values. Open circles indicate outliers.

Allometry of the second upper molar

The multivariate regression of shape on log-centroid size showed that size was a significant predictor of shape ($F = 3.26$; d.f. = 1, 166; $p=0.017$) in the second upper molar (Figure 4.44), although the multivariate regression did not explain very much of the variability ($R^2=0.02$). The multivariate regression of shape on log-centroid size showed that age was parallel and negatively allometric (Figure 4.45), year of sampling demonstrated various proportions of size-shape change as 1994 and 1997 were negatively allometric and 1975, 1995, and 1996 were highly positively allometric (Figure 4.46), and sex (Figure 4.47) was parallel and positively allometric.

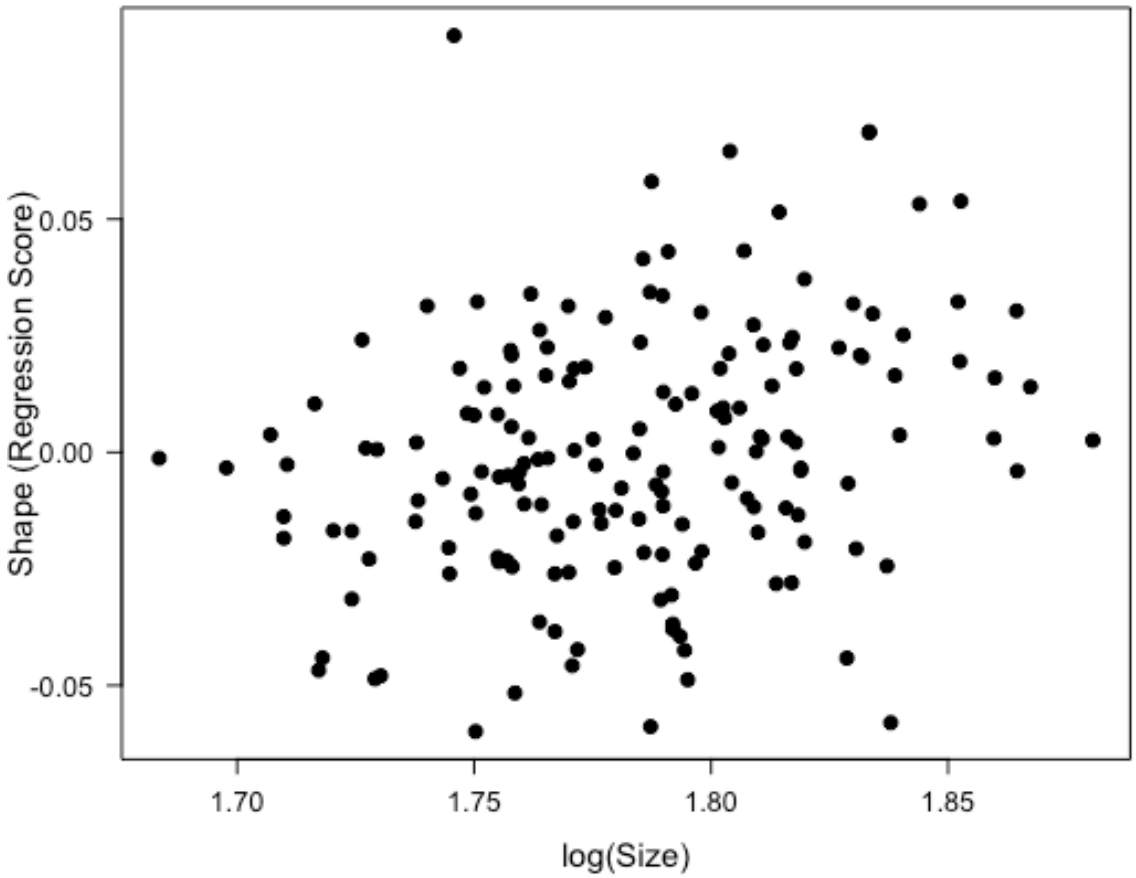


Figure 4.44. Multivariate regression of shape (using the regression score) on size (log-centroid size) of the second upper molar.

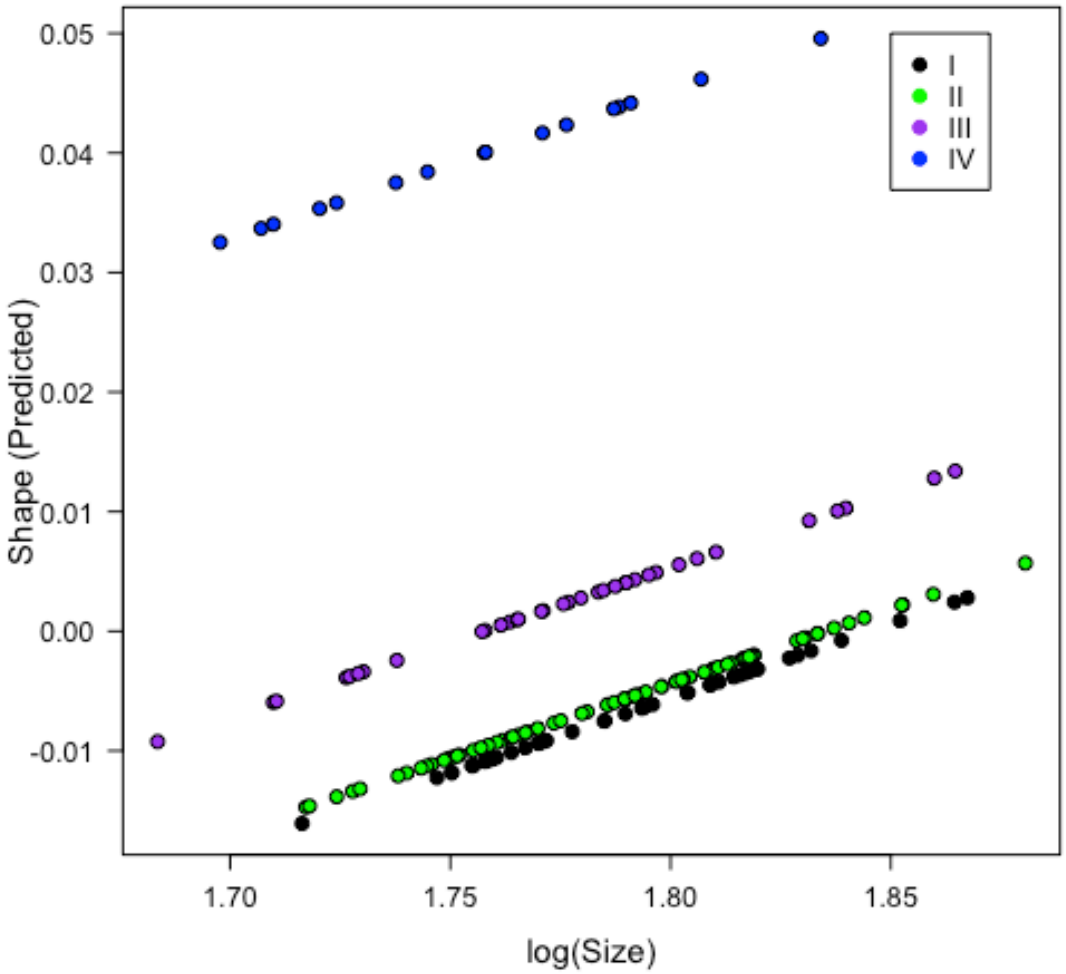


Figure 4.45. Allometric relationship between log-centroid size and second upper molar shape in the four age classes.

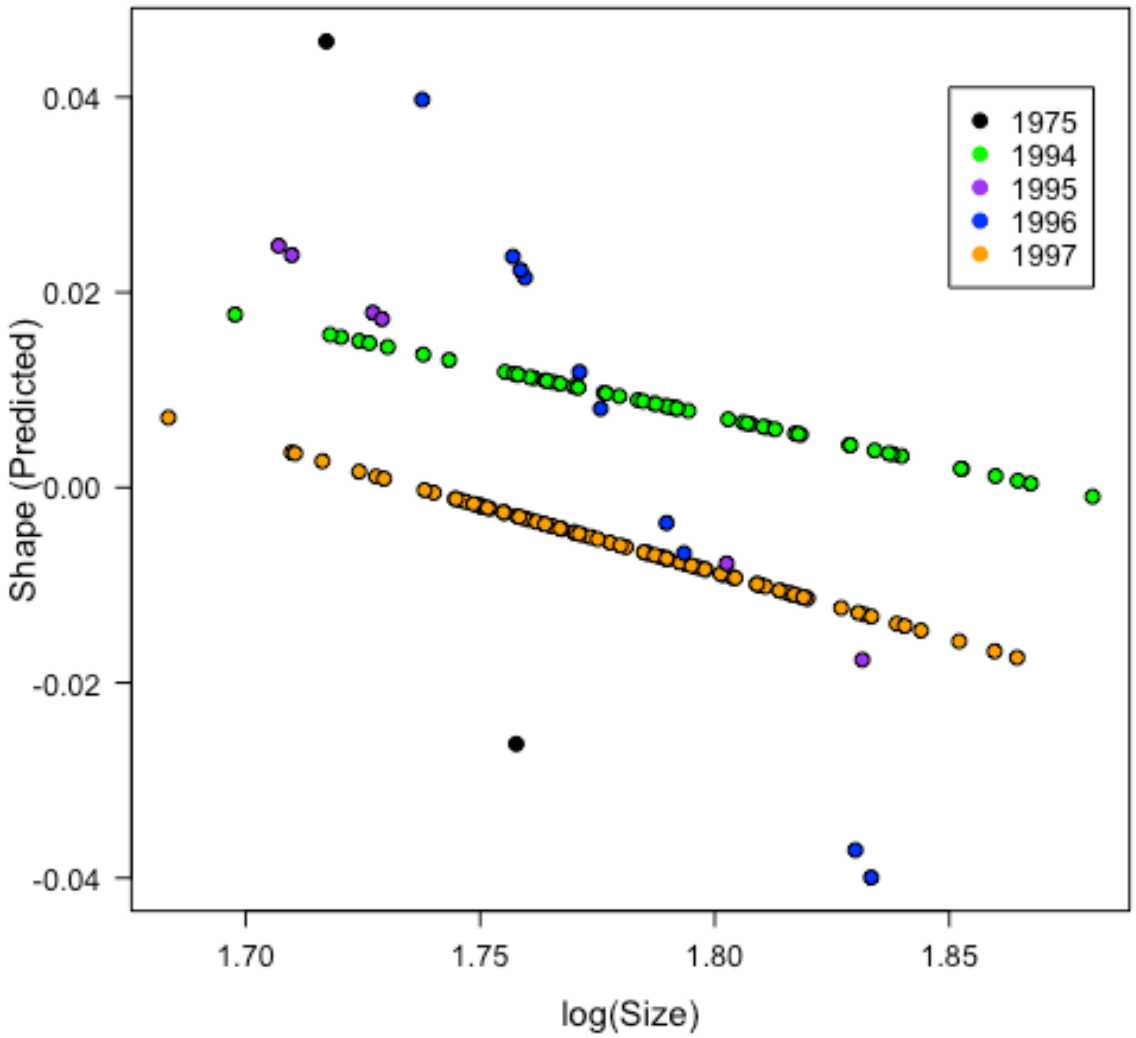


Figure 4.46. Allometric relationship between log-centroid size and second upper molar shape among years of specimen collection.

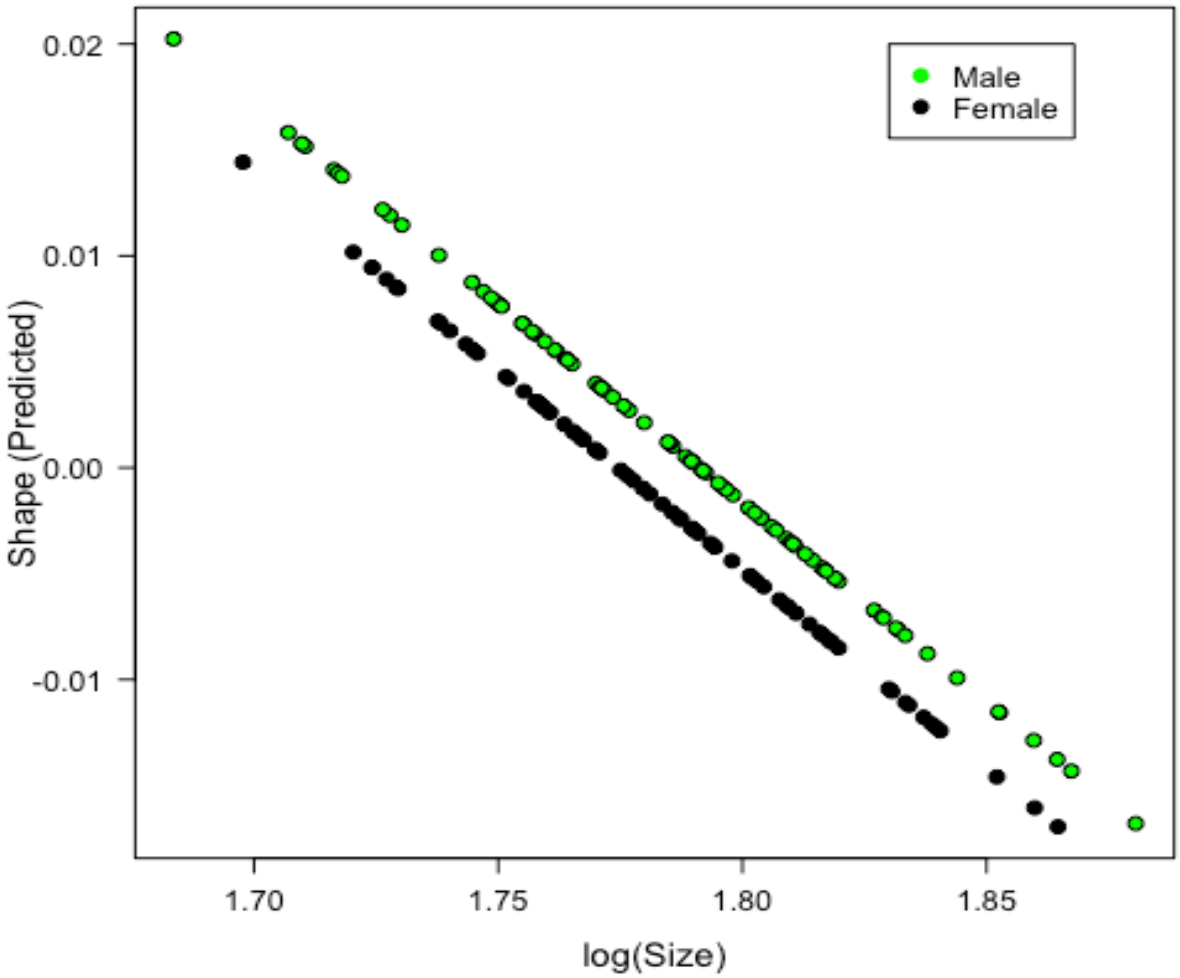


Figure 4.47. Allometric relationship between log-centroid size and second upper molar shape between the sexes.

Shape comparisons of the second upper molar with PCA

The effects of size were removed from the shape data by way of multivariate linear regression given the significant effect of size on shape, and a PCA was constructed from the size-free residuals. The PCA was plotted with relative warps of the minimum and maximum extremes of the first two PC axes (Figure 4.48, 4.49, 4.50). Shape MANOVA results were partially supported by the PCA as some clustering was evident between age classes (Figure 4.48). Age class IV was the most clearly distinguishable of the age classes; age class IV plotted at the positive extreme of PC 2 with a more rounded shape and little evidence of cusp outlines. Age class III also separated out, although still displayed clear overlap with the first two age classes; its form was more intermediate between age classes I and II and age class IV, plotting at the central point of PC 1. A large amount of overlap was clearly visible

between the first two age classes (Figure 4.48), although this relationship was not supported in the shape MANOVA results (Table 4.6).

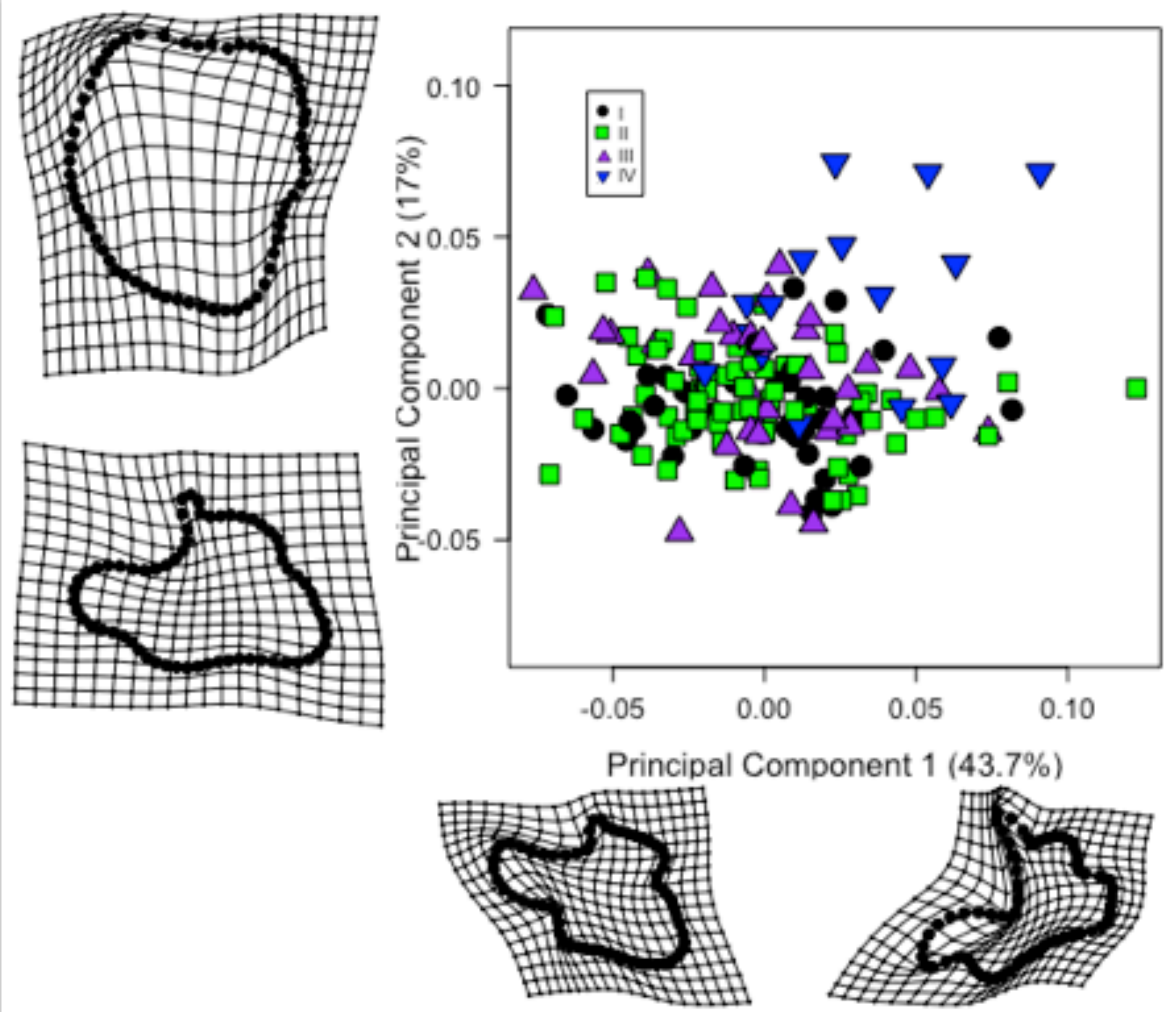


Figure 4.48. Allometry-adjusted Principal Component Analysis of the first two principal components indicating the spread of the four age classes for the second upper molar. Relative warp plots along the two axes indicate the minimum and maximum shape configurations along those axes. Relative warp plots have been magnified by a scale of three to more clearly illustrate variation.

Little clustering was evident between years of sampling with all five years spread throughout the plot along PC 1 (Figure 4.49). Specimens from 1996 displayed second molars that plotted a little closer to the negative extreme of PC 1, although all specimens plotted centrally along the second PC axes.

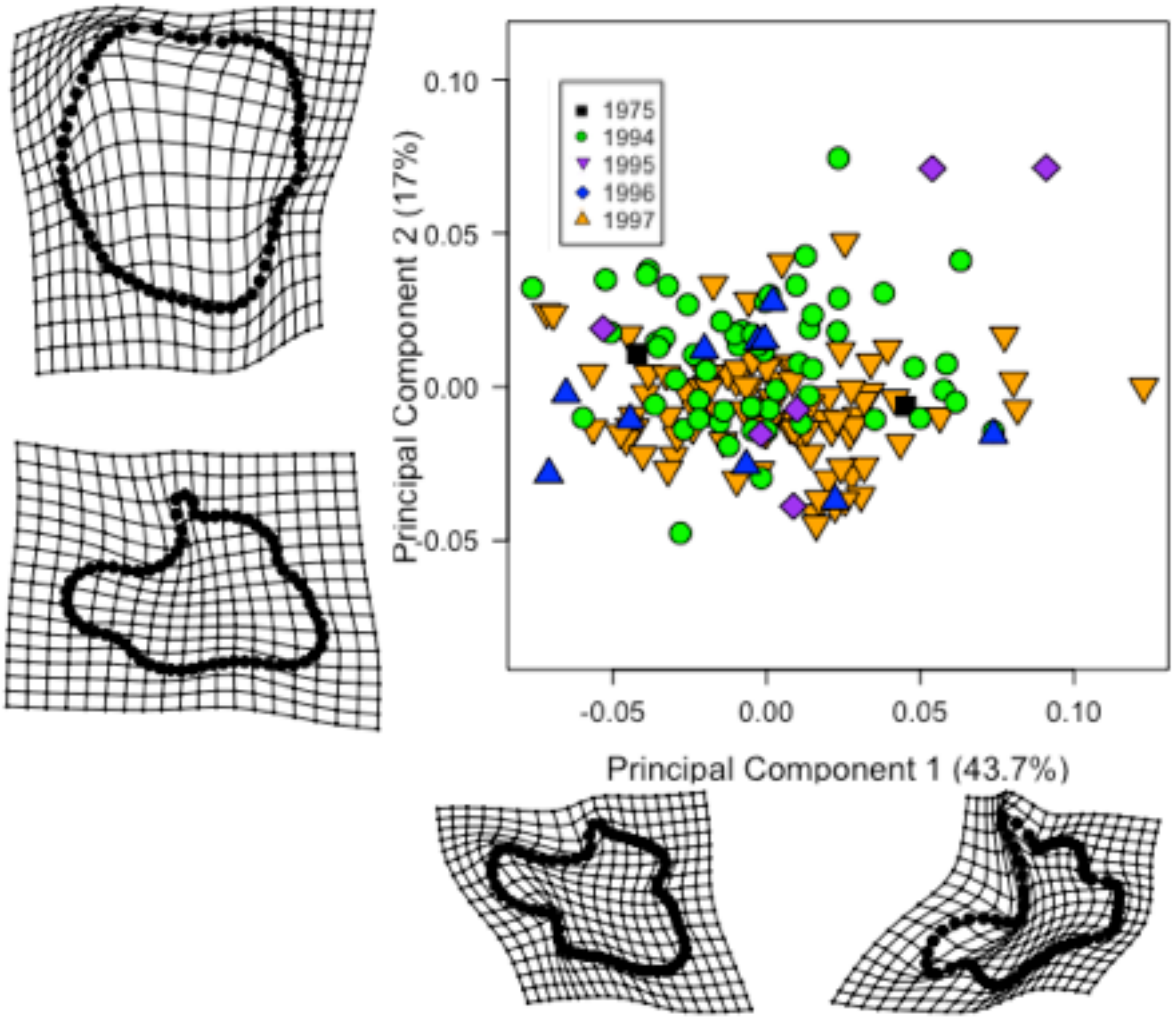


Figure 4.49. Allometry-adjusted Principal Component Analysis of the first two principal components indicating the spread across year of specimen collection for the second upper molar. The relative warp plots have been magnified by a factor of three to more clearly illustrate the differences between the two extrema of each axis.

As with the first upper molar, no clear sexual shape dimorphism was apparent in the second upper molar (Figure 4.50).

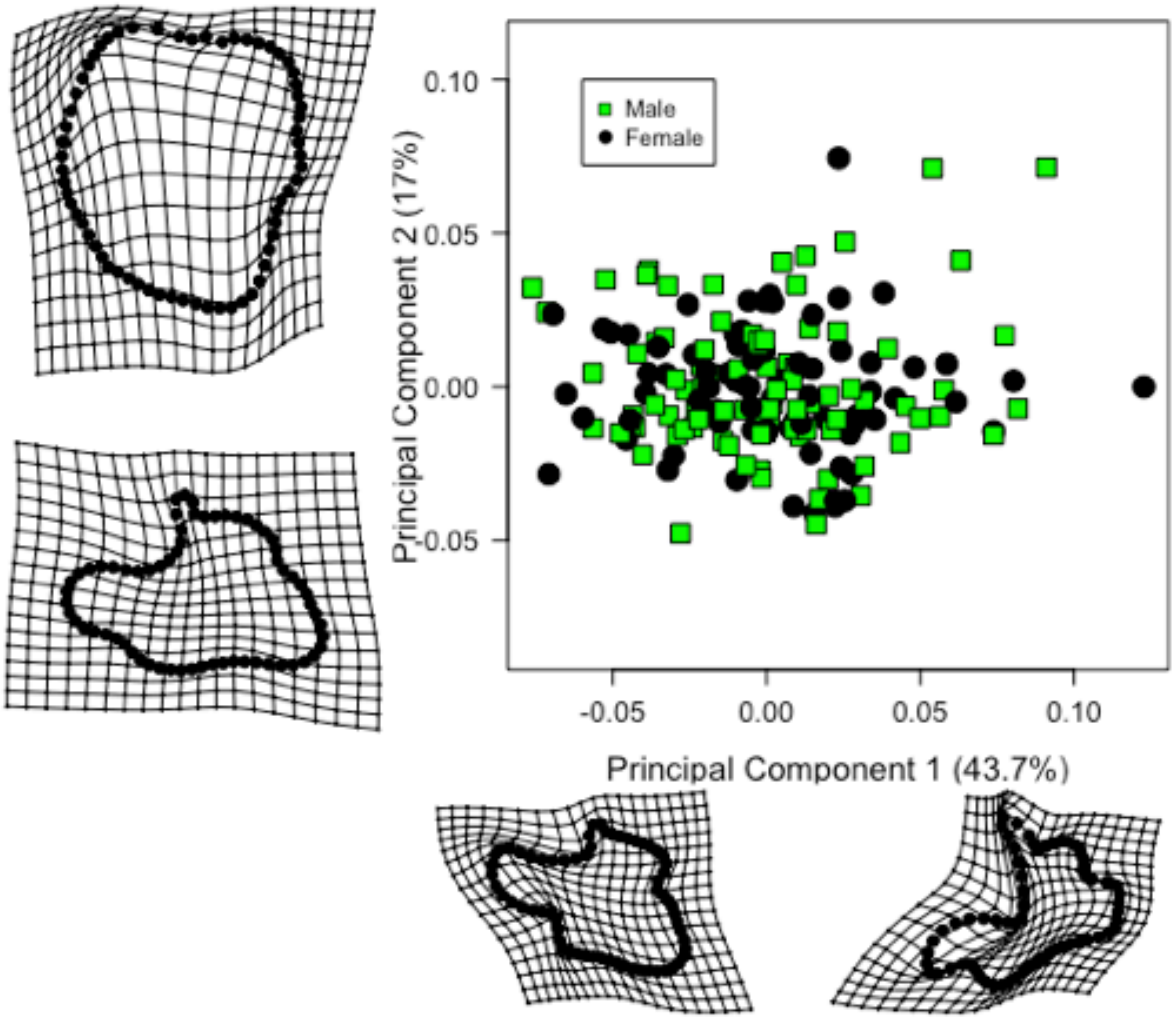


Figure 4.50. Allometry-adjusted Principal Component Analysis of the first two principal components indicating the spread for the sexes for the second upper molar. Relative Warp plots have been magnified by a scale of three to better illustrate shape differences between extrema.

Analysis of shape and size of the third upper molar

The shape MANOVA (Table 4.7) for the third upper molar showed that age and year of sampling were significant predictors of shape variation, while sex, and the interactions between sex, age, and year of sampling were not significant predictors. The size MANOVA on log-centroid size (Table 4.7) showed only year of sampling (Figure 4.51) was a significant predictor of size variation in the third upper molar, while sex (Figure 4.51), age (Figure 4.51), and the interactions between sex, age, and year of sampling were not significant predictors.

Table 4.7. MANOVA results of the shape and size components of the symmetric variation in the third upper molar. Values in bold are statistically significant

Component	Effect	d.f.	MS	F	P-value
Shape	Sex	1, 140	0.0035058	0.87	0.459
	Age	**3, 140**	**0.0227263**	**5.67**	**0.001**
	Year	**4, 140**	**0.0072248**	**1.80**	**0.036**
	Sex:Age	3, 140	0.0020266	0.51	0.954
	Sex:Year	3, 140	0.0056286	1.40	0.142
	Age:Year	9, 140	0.0035574	0.89	0.656
	Sex:Age:Year	4, 140	0.0025321	0.63	0.876
Size	Sex	1, 140	0.018284	0.30	0.583
	Age	3, 140	0.118642	1.95	0.105
	Year	**4, 140**	**0.194777**	**3.20**	**0.007**
	Sex:Age	3, 140	0.091424	1.50	0.220
	Sex:Year	3, 140	0.005639	0.09	0.967
	Age:Year	9, 140	0.095099	1.56	0.126
	Sex:Age:Year	4, 140	0.046367	0.76	0.582

Pairwise comparisons of the homogeneity of slopes for significant shape variation in the third upper molar failed to detect any significant differences between age classes but showed the third molars from 1995 to be significantly different in shape from those specimens collected in 1996 and 1997. Specimens from 1975 and 1994 were not significantly different from each other, nor from specimens from 1995, 1996, and 1997.

Pairwise comparisons of the homogeneity of slopes for significant size factors failed to detect any significant differences between years of sampling statistically although clear differences in median sizes of the third molar are visible between visual comparisons of 1995 and 1975, 1994, and 1997 although not from 1996 (Figure 4.51).

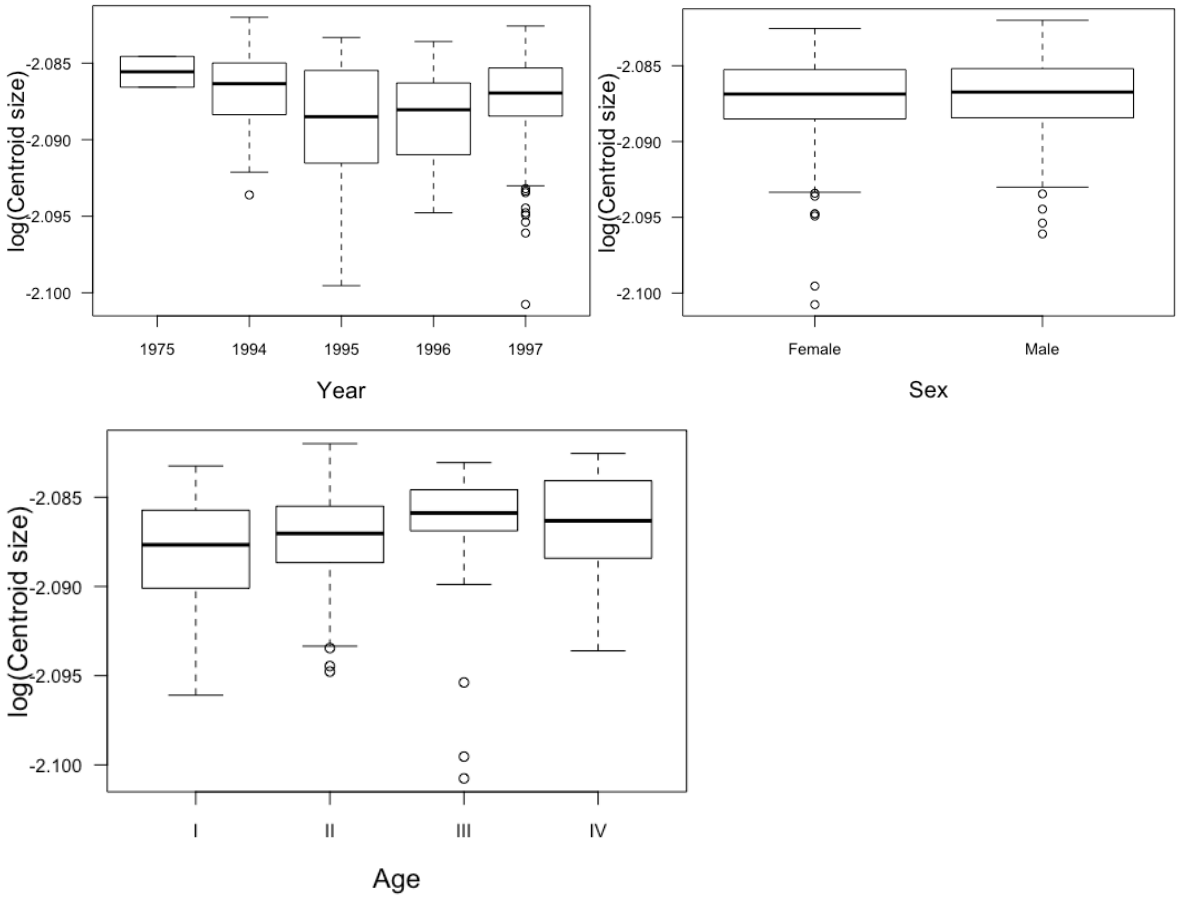


Figure 4.51. Variation in log-centroid size of the third upper molar between years of sampling (top-left), sex (top-right), and age class (bottom). The box represents the interquartile range from the 1st quartile (bottom of box) to the 3rd quartile (top of box) with the median indicated as a black line within the box. The horizontal ends of the whiskers indicate the minimum (bottom) and maximum (top) values. Open circles indicate outliers.

Allometry of the third upper molar

A multivariate regression of shape on log-centroid size showed that size was not a highly significant predictor of shape F=1.97; d.f.= 1, 166; p = 0.075) in the third upper molar (Figure 4.52) and the multivariate regression did not explain very much of the variability (R^2=0.01). A multivariate regression of shape on log-centroid size showed that age (Figure 4.53) and year (Figure 4.54) were approximately parallel and negatively allometric, while sex (Figure 4.55) was approximately parallel and positively allometric.

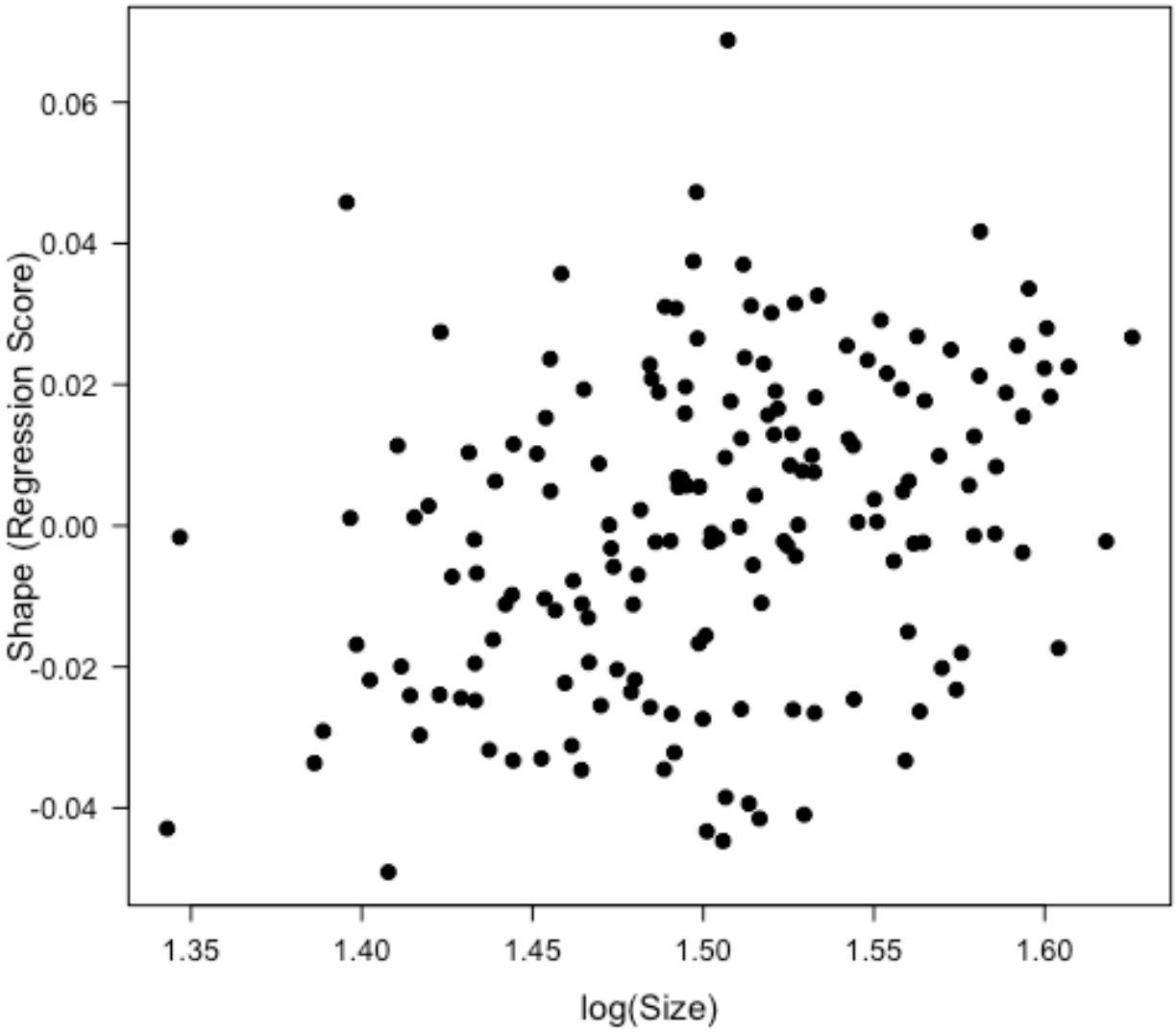


Figure 4.52. Multivariate regression of shape (using the regression score) on size (log-centroid size) of the third upper molar.

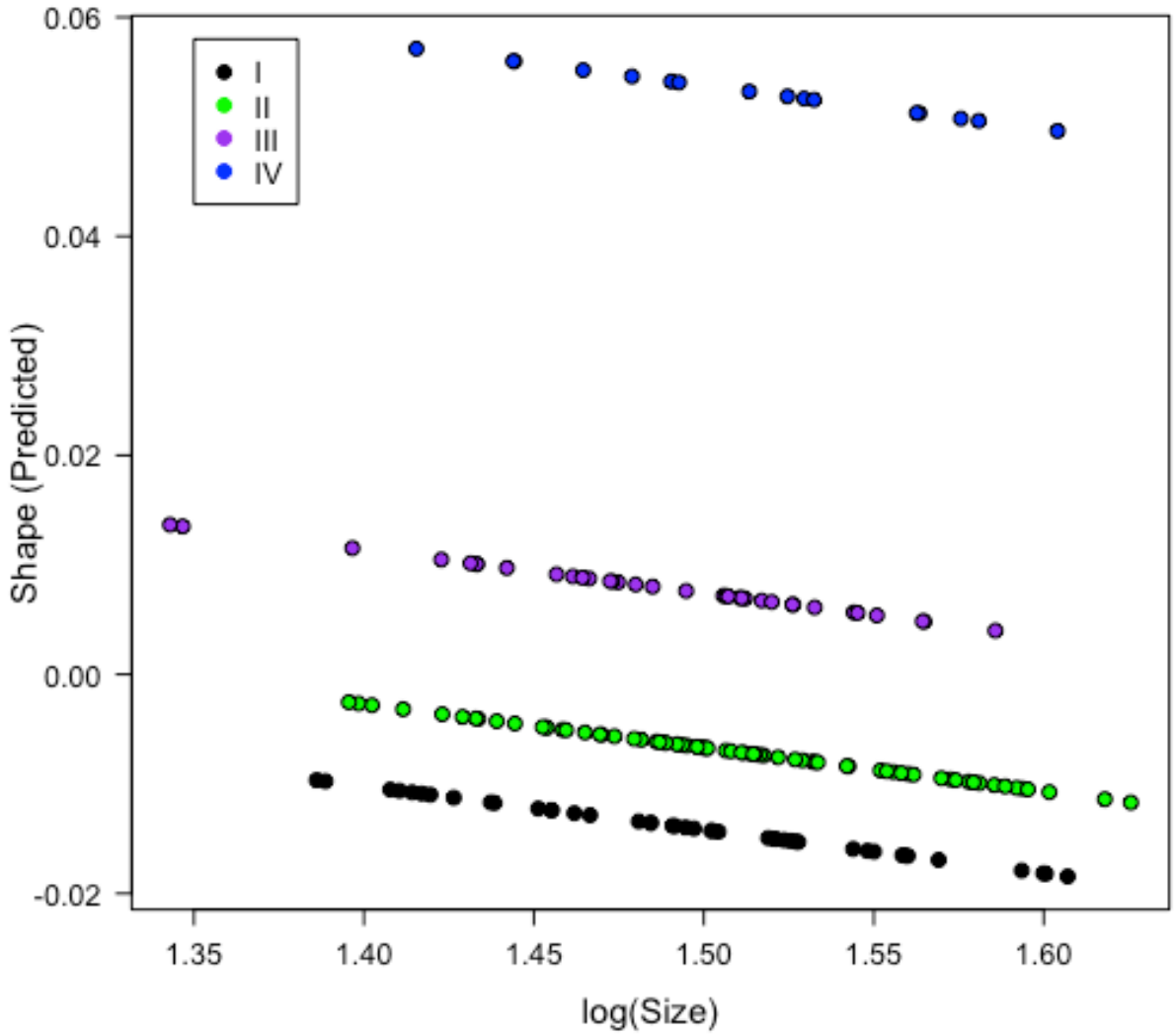


Figure 4.53. Allometric relationship between log-centroid size and third upper molar shape in the four age classes.

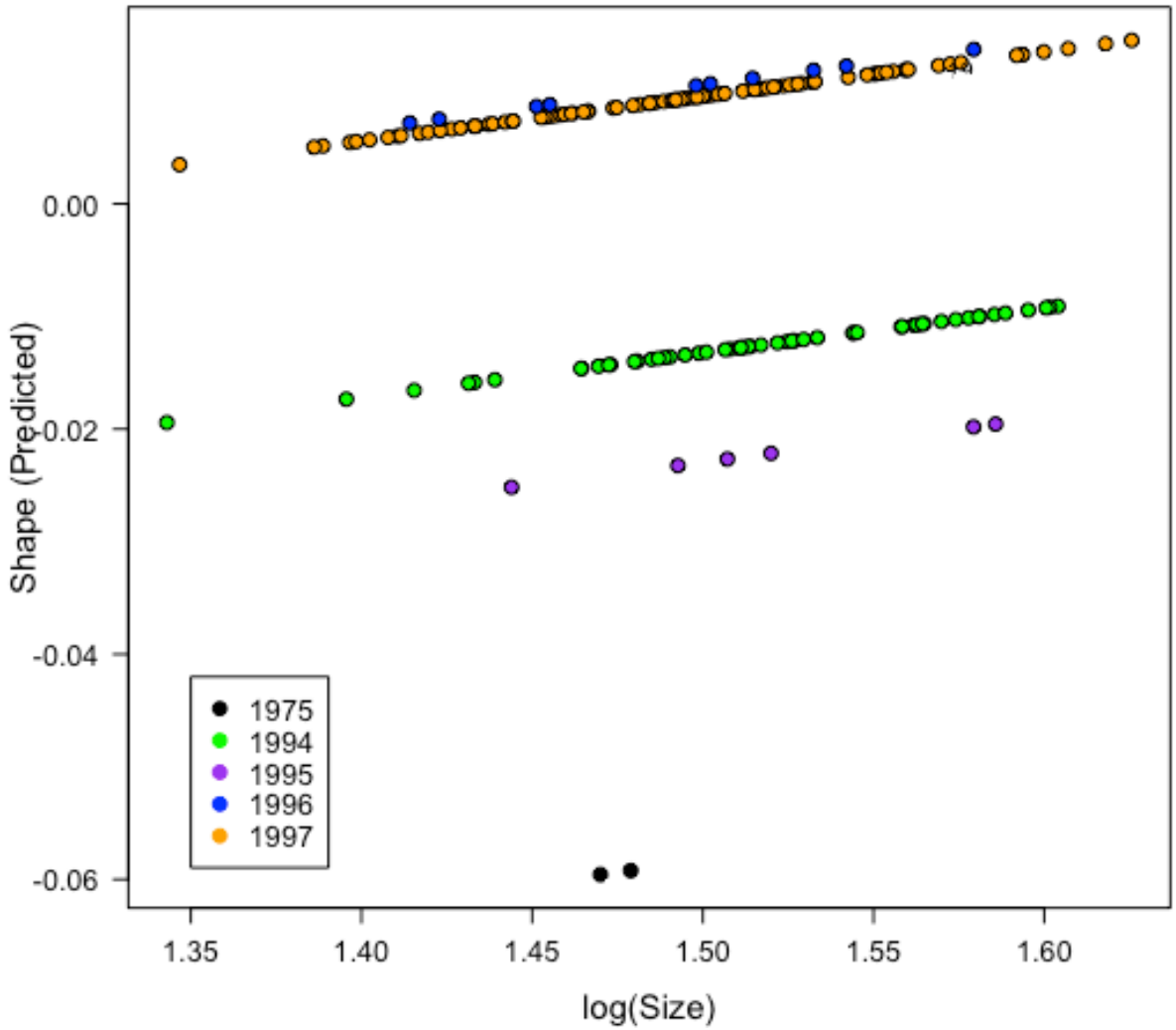


Figure 4.54. Allometric relationship between log-centroid size and third upper molar shape among years of specimen collection.

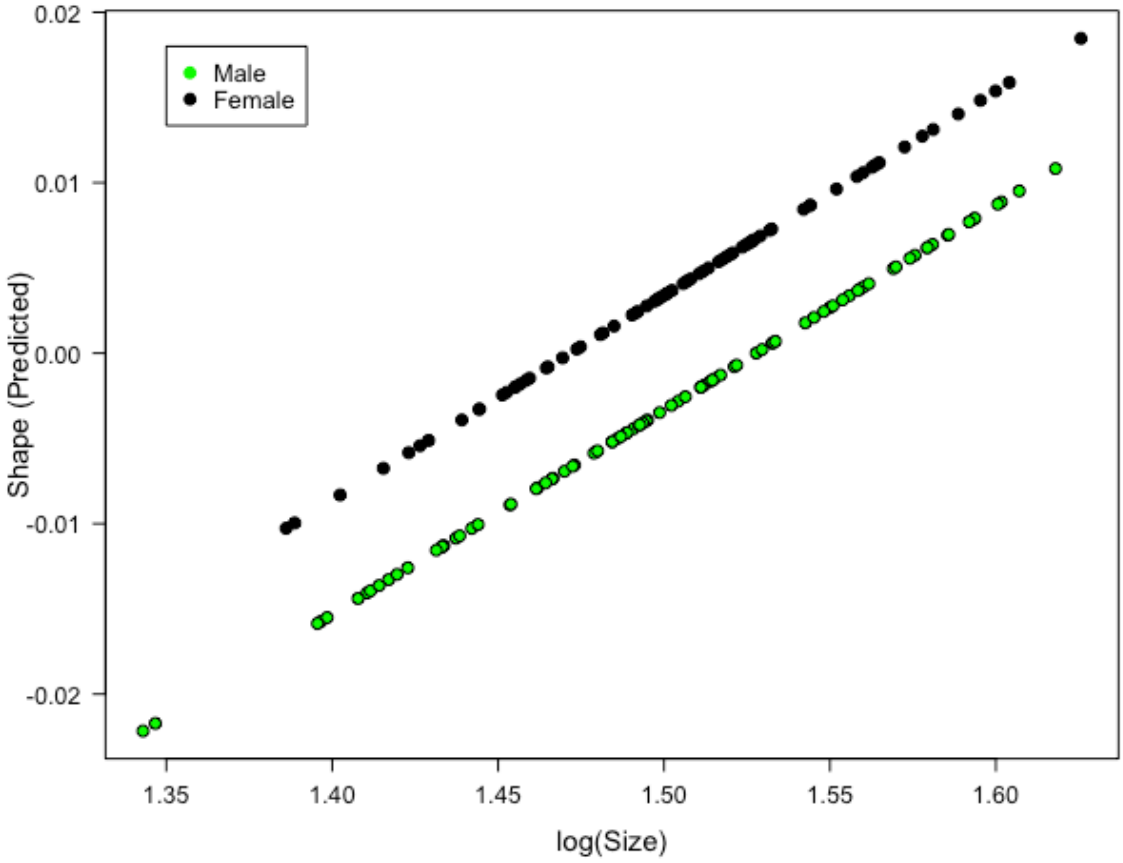


Figure 4.55. Allometric relationship between log-centroid size and third upper molar shape between the sexes.

Shape comparisons of the third upper molar with PCA

The size-corrected PCA was plotted with relative warps delineating the maximum and minimum extremes of the first two PC axes. While the shape MANOVA failed to detect significant differences between age classes (Table 4.7), the PCA indicated that age class IV had a somewhat more shortened lingual edge (Figure 4.56) than the first three age classes. The first three age classes displayed a large amount of overlap in their spread along PC 1, and most specimens for all four age classes plotted centrally along PC 2.

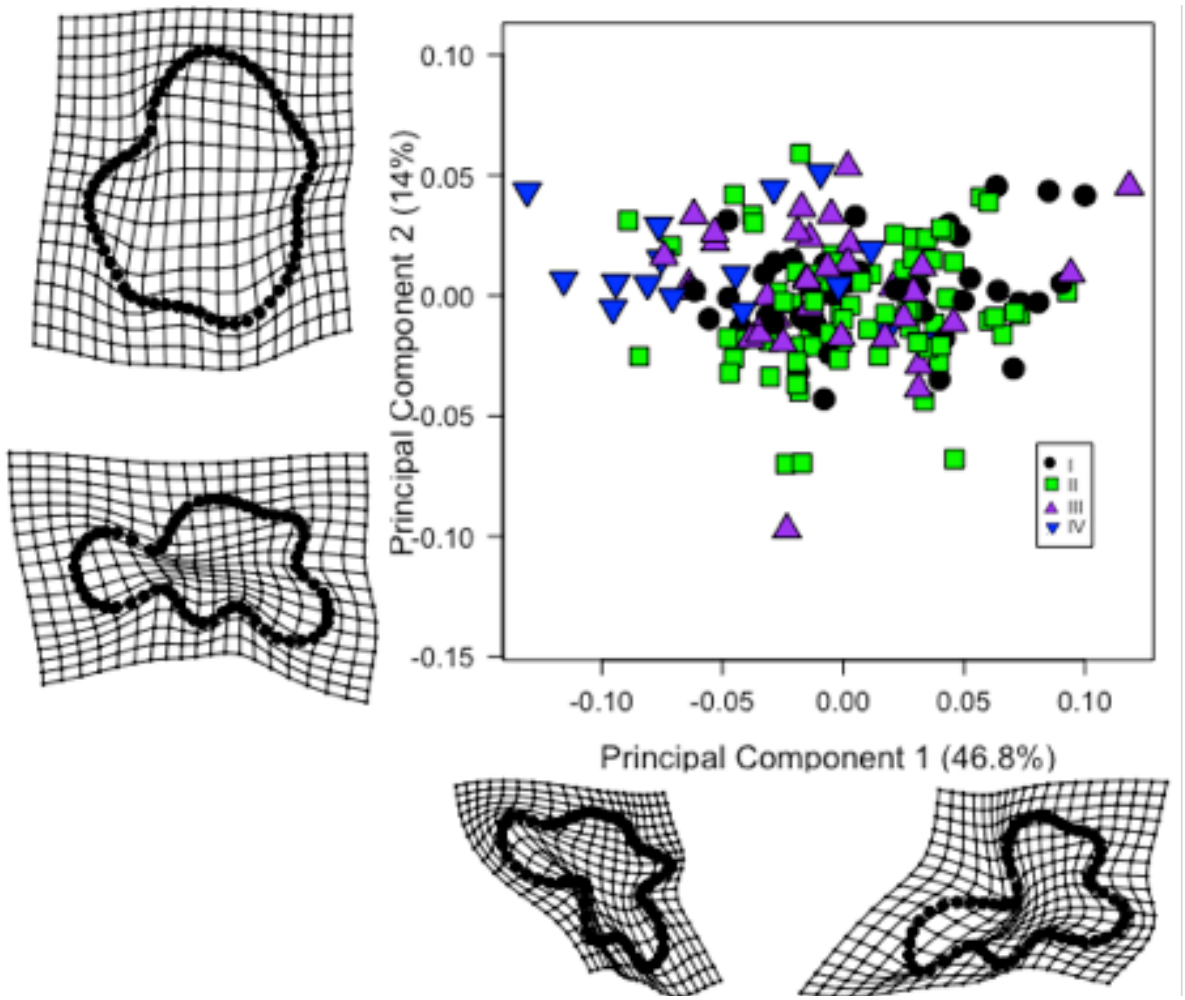


Figure 4.56. Allometry-adjusted Principal Component Analysis of the first two principal components indicating the spread of the four age classes for the third upper molar. Relative warp plots along the two axes indicate the minimum and maximum shape configurations along those axes. Relative warp plots have been magnified by a scale of three to more clearly illustrate variation.

Results from the shape MANOVA were not supported by the PCA (Figure 4.57) since clustering among years was not readily apparent. Overall, however, specimens from 1994 and 1997 plotted along the extent of PC 1, only loosely clustering and thus displayed a variety of shapes. Specimens from 1975, 1995, and 1996 clustered only slightly tighter.

Sexual shape dimorphism was not apparent in the PCA as in the shape MANOVA (Figure 4.58).

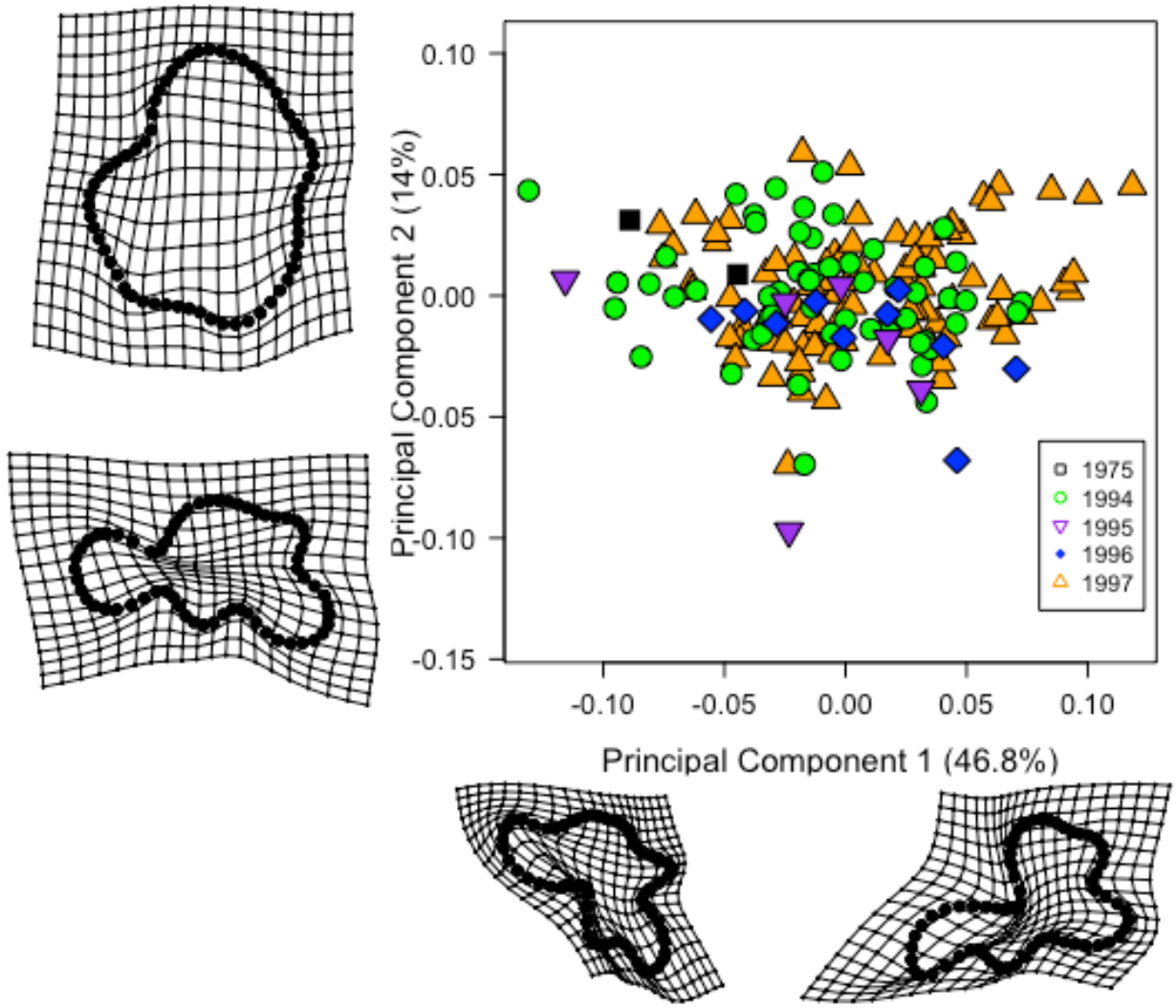


Figure 4.57. Allometry-adjusted Principal Component Analysis of the first two principal components indicating the spread across year of specimen collection for the third upper molar. The relative warp plots have been magnified by a factor of three to more clearly illustrate the differences between the two extrema of each axis.

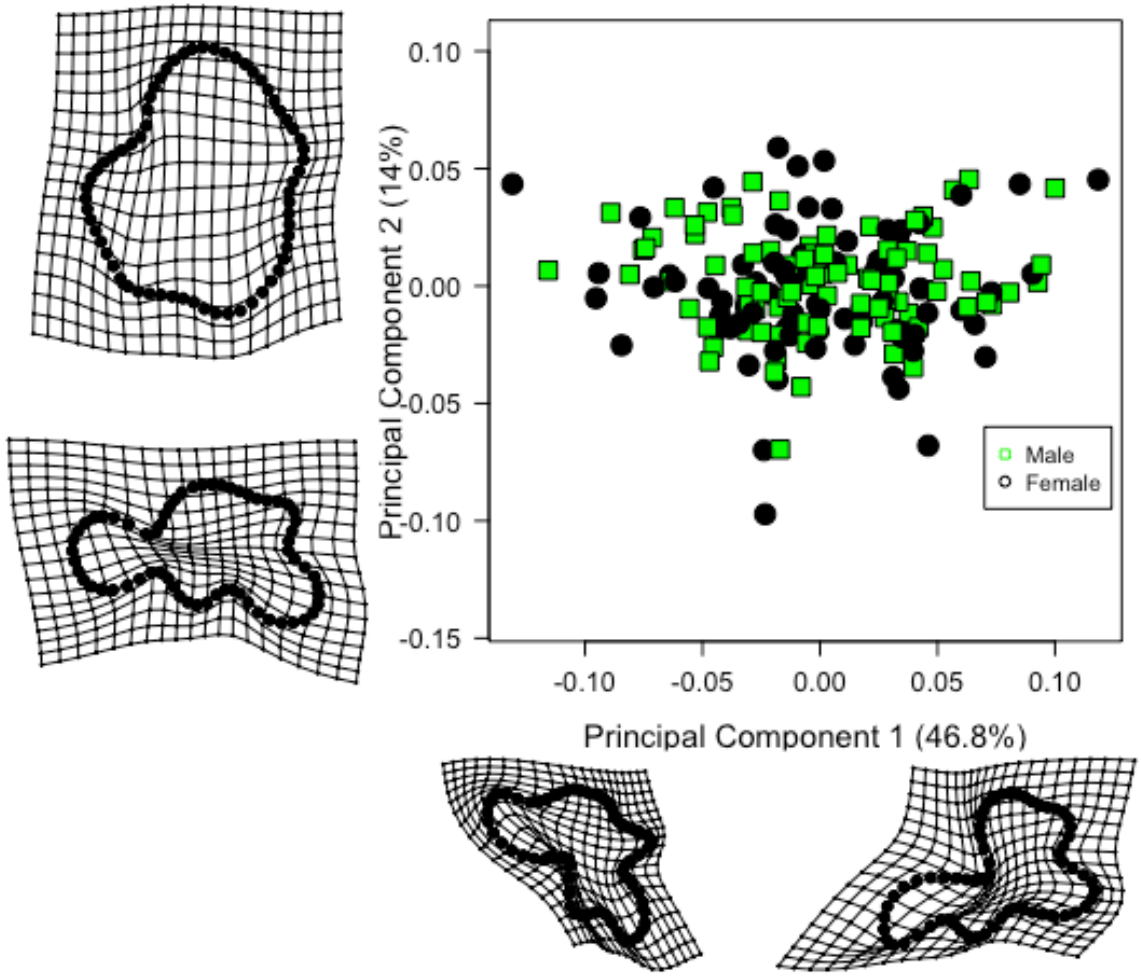


Figure 4.58. Allometry-adjusted Principal Component Analysis of the first two principal components indicating the spread for the sexes for the third upper molar. Relative Warp plots have been magnified by a scale of three to better illustrate shape differences between extrema.

4.5. Descriptive comparison of climate data and form across years

Rainfall decreased between 1975 and 1994, while maximum and minimum temperatures were higher in 1994 than in 1975 (Table 4.8). The ventral aspect of the skull and the second upper molar increased in size between 1975 and 1994. The lateral aspect of the skull and the third upper molar were smaller between 1975 and 1994 while the mandible and the first upper molar retained similar sizes between the two years. Similar shapes were retained in the lateral aspect of the skull (Figure 4.21), the mandible (Figure 4.31 & 4.41), and the first two upper molars (Figure 4.51 & Figure 4.61, respectively). Shape varied only in the ventral aspect of the skull (more reduced facial regions in 1975 and more antero-posteriorly enlarged

neurocrania in 1994; Figure 4.9) and the third upper molar (greater outline definition and complexity; Figure 4.71) from 1975 to 1994 (Table 4.8).

Table 4.8. Mean annual rainfall and temperatures from the Welkom weather station in different years of specimen sampling obtained from the South African Weather Service (2018) and associated relative form change in each of the traits. Relative size and shape changes are separated using slash signs, an absence of change is indicated using a dash, and upward and downward facing arrows indicate direction of change.

Year	Mean Annual Rainfall (mm)	Maximum Temperature (°C)	Minimum Temperature (°C)	Traits	Relative change size/shape
1975	616	23.9	9.5	Ventral Skull	- / -
				Lateral Skull	- / -
				First Upper Molar	- / -
				Second Upper Molar	- / -
				Third Upper Molar	- / -
1994	351	25.5	9.7	Ventral Skull	↑ / ↑
				Lateral Skull	↓ / -
				Mandible	- / -
				First Upper Molar	- / -
				Second Upper Molar	↑ / -
				Third Upper Molar	↓ / ↑
1995	424	26.3	10.2	Ventral Skull	↓ / -
				Lateral Skull	↑ / -
				Mandible	- / ↓
				First Upper Molar	- / ↓
				Second Upper Molar	↓ / -
				Third Upper Molar	↓ / ↓
1996	692	24.6	9.8	Ventral Skull	↑ / ↑
				Lateral Skull	↑ / ↓
				Mandible	↑ / ↑
				First Upper Molar	- / ↑
				Second Upper Molar	↑ / -
				Third Upper Molar	- / ↑
1997	463	24.9	9.6	Ventral Skull	↓ / -
				Lateral Skull	↓ / ↑
				Mandible	↓ / ↓
				First Upper Molar	- / -
				Second Upper Molar	↑ / -
				Third Upper Molar	↑ / -

Both rainfall and temperature increased from 1994 to 1995 (Table 4.8) with an associated increase in size in the lateral aspect of the skull. The ventral aspect of the skull and the second and third upper molar was reduced in size between years while the mandible and first upper molar retained a similar size to the previous year. The mandible (Figure 4.31 & Figure 4.41) had smaller processes and a more gracile structure in 1995 than in 1994, while the first (Figure 4.51) and third (Figure 3.61) upper molars had less defined and less complex outlines in 1995 (Table 4.8).

Rainfall was higher, and temperatures were cooler in 1996 than in 1995. Specimens from 1996 had a corresponding increase in cranial, mandibular and second molar size, with a medio-lateral lengthening (Figure 4.9) and a dorso-ventral shortening (Figure 4.21) of the cranium, an enlargement of muscular attachment points and reduction in the angles of articulations of the mandibular processes (Figure 4.31 & 4.41) and an increased complexity to the first (Figure 4.51) and third (Figure 4.71) upper molar shape. The first and third upper molar retained similar sizes from 1995 to 1996, while the second upper molar (Figure 4.61) retained a similar shape (Table 4.8).

Rainfall was the only climatic variable considered here that changed from 1996 to 1997, with a decrease of over 230mm in rainfall. The skull and mandible were smaller and the second and third upper molars were bigger in 1997 than in 1996. Shape in the 1996 specimens differed from the 1997 specimens only in the lateral aspect of the skull (with a dorso-ventrally compressed neurocranium and elongated facial region; Figure 4.21) and the mandible (with larger angles between mandibular processes and larger points of insertion in specimens from 1996; Figure 4.31 & 4.41). The first upper molar retained a similar size from 1996 in 1997, while the ventral aspect of the skull (Figure 4.9), and all three upper molars (Figures 4.51, 4.61, 4.71) retained similar shapes in 1997 from those in 1996 (Table 4.8).

4.6. Summary

Table 4.9. Summary of main experimental results

Structure	Component	Allometry	Age	Sexual Dimorphism	Year
Ventral Skull	Shape	Shape was significantly influenced by size; Age and year of sampling were positively allometric; Sex was negatively allometric; All factors showed parallel trends	Age classes I and II had variable shapes; Age class III had broader rostra, more protruding jugal; Age class IV had narrow rostra, less protruding jugal	Shape was not significantly different between sexes	1995 specimens had longer, narrower neurocrania and rostra; 1996 specimens had broader long, broad neurocrania; shorter, broader rostra; 1997 specimens were more variable; 1975 and 1995 were not significantly different from other years
	Size		Age class I < Age class II; Age class I < Age class III; Age class I < Age class IV; Age class II < Age class IV; Age class III < Age class IV	Males > Females	1994 > 1997; 1996 > 1997
Lateral Skull	Shape	Shape was significantly influenced by size; Age and year of sampling were positively allometric; Sex was negatively allometric;	Age classes I and II had variable shapes along both extremes; Age class III and IV had shapes intermediate to the two extremes	Shape was not significantly different between sexes	1996 more dorso-ventrally compressed neurocrania, steeper zygomatic arches; 1997 specimens had more abrupt, vertical ends to their neurocrania, less steep zygomatic arches;

Structure	Component	Allometry	Age	Sexual Dimorphism	Year of sampling
Lateral Skull	Shape	All factors showed parallel trends			1975, 1994, and 1995 specimens were not significantly different from any other years
	Size		Age class I < Age class III Age class I < Age class IV Age class II < Age class IV Age class III < Age class IV	Males > Females	1994 < 1996; 1994 < 1997; 1995 < 1996; 1995 > 1997
Mandible	Shape	Shape was significantly influenced by size; Age class was negatively allometric (but not parallel); Year of sampling (not parallel) and sex (parallel) were positively allometric	Age class IV had more curved posterior ventral border, particularly the angular process Other age classes were highly variable in shape	Shape was not significantly different between sexes	1995 specimens had more ventrally curved angular process 1996 specimens had a squarer angular process 1994 and 1997 specimens had variable shapes
	Size		Age class I < Age class IV; Age class II < Age class IV; Age class III < Age class IV	Males > Females	1994 > 1997; 1996 > 1997
First Upper Molar	Shape	Shape was significantly influenced by size; Age was negatively allometric for 1994 and 1997, and positively allometric for 1975, 1995, and 1996;	Age class I more defined cusp outlines and more elongate first molars; Age class II more antero-posteriorly compressed cusps	Shape was not significantly different between sexes	1994 and 1995 displayed more antero-posteriorly compressed, rounded first molars; 1996 and 1997 displayed anteroposterior elongation with defined cusp outlines;

Structure	Component	Allometry	Age	Sexual Dimorphism	Year of sampling
First Upper Molar	Shape	Year of sampling was negatively allometric (non-parallel); Females had negative allometric trajectories, males had positive allometric trajectories	Age classes III and IV were not significantly different		1975 more variable molar shape and so did not differ significantly from other years
	Size		Age class I < Age class II; Age class I < Age class III; Age class I < Age class IV; Age class II < Age class IV; Age class III < Age class IV	Size was not significantly different between sexes	Size was not significantly different between years of sampling
Second Upper Molar	Shape	Shape was significantly influenced by size; Age was negatively (parallel) allometric; 1994 and 1997 were negatively allometric, 1975, 1995, and 1996 were positively allometric; Sex was positively allometric	Age class II clearly defined cusps; Age class III had more variably defined cusps; Age classes I and IV were not significantly different	Shape was not significantly different between sexes	Shape was not significantly different between years of sampling
	Size		Age class I > Age class III; Age class II > Age class III; Age class I > Age class IV; Age class II > Age class IV; Age class III > Age class IV	Size was not significantly different between sexes	1994 > 1995; 1994 > 1997

Structure	Component	Allometry	Age	Sexual Dimorphism	Year of sampling
Third Upper Molar	Shape	Shape was not significantly influenced by size; Age and year were negatively allometric; Sex was positively allometric	Age classes I, II, and III had variable and widespread shapes; Age class IV displayed a shortened lingual edge	Size was not significantly different between sexes	1995 had highly variable shape; 1996 slightly more clearly defined cusps; 1997 displayed a wide variety of shapes; Specimens from 1975 and 1994 were not significantly different from any years
	Size		Size was not significantly different between age classes	Shape was not significantly different between sexes	1975 > 1995 1994 > 1995 1995 < 1997

Chapter 5

Discussion

In establishing the patterns of intraspecific variation present in a population of *Rhabdomys dilectus chakae* from the Willem Pretorius Nature Reserve, I found that allometric patterns of shape variation for the third upper molar varied only between age groups, and in the curves of the mandible, and all three upper molars between years of sampling. Age-related variation was present in the shape and size components for the skulls, mandibles, and dentition in accordance with my prediction that the skulls and mandibles would vary with changing age classes. I predicted that this age variation would result from differences in food hardness (Anderson *et al.* 2014), and this is likely the case, especially in the dental variation where abrasion of the occlusal surface would alter the shape of the outline. Shape change in the mandible due to age mostly consisted of a relative dorso-ventral expansion and antero-posterior compression with a more enlarged ascending ramus, while the skull displayed a relatively narrower neurocraniam medio-laterally but with larger optic regions.

Sexual size dimorphism was evident in the MANOVA but not PCA results in the skulls (but only in lateral view) and mandibles, while sexual shape dimorphism was present only in combination with age (in mandibles) and year of sampling (in the lateral skull), and in combination with both age and year (in the mandible alone). I had predicted that males would be larger than females as is common in rodents (Astùa *et al.* 2015) and this was in fact the case. Variation between years of sampling was present in size and shape in the skull (in ventral view), the mandibles, and the molars and was likely due to the inter-annual variation in the rainfall and temperature.

Allometry and age-related variation

Allometry, or the change in shape as a result of increasing size, can be highly influenced by age, since animals become larger as they age. Similar ontogenetic trajectories may result in similar shapes across different age groups because morphological units may simply be scaled-up forms of the same shape (Klingenberg 2010). I found similar ontogenetic trajectories between the sexes which may then explain why these factors did not separate in the PCA since similar growth would explain similarities in shape. Given the similar ontogenetic trajectories for the age classes but the significant differences in shape, variation in shape of the skull and mandible are likely not due to the effects of growth. Where skulls,

mandibles or dentition differ in size and/or shape, it may be a result of different ontogenetic trajectories by individuals experiencing different rates of growth at different points in their developmental history (Zelditch *et al.* 2004). Nonetheless, in the dentition, variation between age classes may largely be due to wear of the cusps due to mastication.

Growth rates may be affected by the availability of food, with rapid growth rates emerging in periods of food abundance following periods of limited food availability (Ortega *et al.* 2017; Owens, *et al.* 1993). In rats, growth rate slowed when the amount of food available decreased since more of the energy obtained from the available food went into maintaining metabolic activity and body function instead of growth (Gettys *et al.* 1988). In the large Japanese field mouse *Apodemus speciosus*, increased food availability resulted in larger cranial sizes (Yom-Tov & Yom-Tov 2004) and in the American marten *Martes americana* increased food abundance in winter resulted in larger cranial sizes (Yom-Tov *et al.* 2008). In the mosquito *Aedes aegypti,* individuals which experienced food shortages early in their development, experienced rapid growth with smaller overall sizes and lower reproductive success when food abundance was increased (Zeller & Koella 2016). Growth may also be influenced by low-protein diets early in postnatal development. In the cotton rat *Sigmodon hispidus*, protein deficient diets early in development resulted in slower growth rates and thus smaller cranial sizes (Lochmiller *et al.* 2000). In hibernating species, such as garden dormice *Eliomys quercinus*, generating larger body sizes and fat reserves are essential to surviving winter, such that individuals born later in the breeding season experience more rapid growth after weaning than individuals born earlier in the season (Stumpfel *et al.* 2017).

Mandibles become more robust as animals age in a range of mammals, including the yellow-bellied marmot *Marmota flaviventris* (Cardini & Tongiorgi 2003), the Japanese weasel *Mustela itatsi* (Suzuki *et al.* 2012), the southern sea otter *Enhydra lutris nereis* (Law *et al.* 2017), and the Andean fox *Lycalopex culpaeus* (Segura & Prevosti 2012). More robust jaws have greater bite force, which has been linked to intraspecific aggression and diet (Cardini & Tongiorgi 2003). For example, the dorso-ventral elongation and longitudinal shortening of the mandible through aging lead to increased bite forces in adult yellow-belied marmot *Marmota flaviventris* which aid adult males in competition for territories and access to females (Cardini & Tongiorgi 2003). In the Stripefoot Anole *Anolis lineatopus* larger adults had a greater bite force and ate harder prey items compared to juveniles (Herrel *et al.* 2006). A larger mandibular ascending ramus allows for larger insertion points for the masseter muscle (Cardini & Tongiorgi 2003), which increases as animals age (Pares-Casanova 2017).

Mandibular shape may vary due to age as a result of bone growth and epigenetic bone re-modelling due to stress. For example, older woodmice *Apodemus sylvaticus* have a higher articular condyle, a more curved alveolar region and a reduced coronoid process than the younger woodmice as a result of differences in the mechanical stresses due to variation in the food they eat, although the differences in the food eaten is not specified (Renaud 2005). Hard foods cause higher mechanical strain to the masticatory apparatus in mice under experimental laboratory conditions because these foods require greater force to break down and so animals that eat harder food experience greater mechanical strain and undergo greater bone remodelling (Anderson *et al.* 2014).

Molar shape and size are altered through wear on the occlusal surfaces. For this reason, as an individual ages, molar size and shape should change as the occlusal surface becomes worn (Renaud 2005). My results indicated that age class I was distinguishable from the other age classes in all three upper molars because the outer curves of the cusps were still distinguishable. In contrast, age class IV was distinguishable in shape from the other age classes due to the relatively rounded outlines. Size varied in the first two molars between age classes, with increased size with increased age in the first molar and, surprisingly, decreasing size with increasing age in the second molar. As in other studies of molar variation with age, variation in size and shape in my study is likely due to the increased wear of the occlusal surface. This relationship between age and molar abrasion has been shown in the wood mice *Apodemus sylvaticus* (Renaud 2005).

Sexual dimorphism

My results indicate that sexual size dimorphism, but not sexual shape dimorphism, was present in *Rhabdomys dilectus chakae* (lateral) skulls and mandibles, although not in any of the upper molars. The dimorphism was evident in the MANOVA results but not the PCA results. Male-biased sexual dimorphism in mammals has been linked to a polygynous mating system (Lindenfors *et al.* 2007) where males compete for access to females (Schulte-Hostedde *et al.* 2001). Larger male size functions in male-male competition and mate-defense since larger males are better able to defend a territory and/or females (Eisenberg 1981). Examples of mate defense can be seen in wolves *Canis lupis*, where larger male sizes lead to better mate-guarding of females (Morris & Brandt 2014), and in fallow deer *Dama dama*, where larger males have higher dominance ranks and greater mating success (McElligott *et al.* 2001). Females have been found to invest more heavily in reproduction instead of

growing larger (Andersson 1994), and so in mammals, females might be expected to be the smaller sex.

Increases in skeletal sizes are usually also accompanied by an increase in muscle mass (Ginot *et al.* 2018) and therefore a change in skeletal shape, because larger muscle mass requires robust skeletal support (Schulte-Hostedde *et al.* 2001). Larger points of muscle attachment by way of size and shape changes in the skulls and mandibles would, therefore, increase the strength of the jaws (Freeman & Lemen 2008). Victors of fights are likely to be those males that bite hardest and so the most reproductively successful males should have a predictably stronger bite force (Lailvaux & Irschick 2006). Reproductive success in males due to increased bite force related to larger sizes has been found in the Northern elephant seal *Mirounga angustirostris* and the South American sea lion *Otaria byronia* (Jones *et al.* 2013). In the stag beetle *Cyclommatus metallifer*, males have enlarged mandibles; males with larger mandibles, and therefore stronger bite forces, are more frequently the victors of male contests for mates (Goyens *et al.* 2014; Husak *et al.* 2009). Similar results have been found in the Tuatara *Sphenodon punctatus* in which successful males are those with larger heads and greater bite forces (Herrel *et al.* 2010).

No sexual shape dimorphism was evident in *Rhabdomys dilectus chakae*, which may be due to different selection pressures driving shape in the sexes in similar directions. Greater bite force for intrasexual competition for mates might explain why males are larger but does not explain why females are smaller. In many murid rodents, females hold intrasexual territories, excluding strange females from their nests with unweaned offspring (i.e. the pup defense hypothesis; Waterman *et al.* 2007). Little is known about social organization and mating systems of the *Rhabdomys dilectus chakae* population considered here. However, *Rhabdomys* in grassland localities (such as that studied here) maintain intra-sexually non-overlapping territories and a promiscuous mating system (i.e. females and males mate with multiple partners; Schradin and Pillay 2005). Females are intra-sexually aggressive (Schradin *et al.* 2010), and a greater bite force could be useful in territorial encounters. In this case, females may be expected to develop similar musculature and therefore cranial shapes to males. The lack of sexual shape dimorphism in my study may then make sense, because both sexes face similar selective pressures, i.e. intrasexual competition, and so males and females developed larger muscle attachment points, altering shape in the same way, allowing for increased bite force (Stockley & Bro- Jørgensen 2011).

Similar selective pressures due to competition would not explain the dimorphism in size, if both sexes were competing with same sex conspecifics. Even if the specifics of

competition differ, should they not display size monomorphism? As a result of the potential promiscuous mating system of *Rhabdomys dilectus chakae* in the grasslands, females raise their offspring alone, compared to the arid-living *R. pumilio* in which males display paternal care (Schradin and Pillay 2005). Maintaining a larger body size is more metabolically expensive particularly if environmental conditions deteriorate (Schulte-Hostedde 2001). Female *Rhabdomys dilectus chakae* are therefore more likely to invest less energy into their size and more energy into reproduction and caring for subsequent offspring. This, when combined with the competition between promiscuous males for access to receptive females, may explain the sexual size dimorphism in the skull found in my results. Sexual size dimorphism has also been linked to divergence in the diets between the sexes in the American mink *Mustela vison* (males, which were larger than females, consumed lagomorphs, while females consumed fish and crustaceans; Birks & Dunestone 1985), and in the royal python *Python regis* (where arboreal males as the smaller sex mainly ate birds, females were ground-dwelling and consumed mainly mammals; Luiselli & Angellici 1998). However, it is unlikely that dietary divergence is the cause of sexual dimorphism in *Rhabdomys dilectus chakae* because the diets of males and females are the same (Pillay unpublished data; Nel et al. 2015).

There was no sexual dimorphism of the molars, which is not surprising since molar size and shape are not usually sexually dimorphic in rodents (Renaud 2005). Monomorphic size and shape in molars has been found in wood mice *Apodemus sylvaticus* (Renaud 2005), Asian rat *Ratttus tanezumi* and the Polynesian rat *Rattus exulans* (Claude 2013). The similarities in molar shape and size is likely the consequence of similar diets of males and females (Lewis *et al.* 2002). Both sexes of *Rhabdomys dilectus chakae* experience the same local conditions and are likely exposed to the same (or at least, very similar) food resources (Schradin and Pillay 2005).

Year of sampling

The year of sampling was a significant predictor of shape variation in the skull, mandible, and first and third upper molars of *Rhabdomys dilectus chakae*. Size varied according to year of sampling for the skull, mandible, and second and third upper molars. The variation in size indicated that the skull (in lateral view) was smaller in 1994 when compared to 1995 and 1996, with the smallest specimens coming from 1997. The size of the mandible and first two upper molars was more variable in 1994 and 1997 than in 1995 and

1996 although the third upper molar displayed larger sizes in 1994 and 1997. Variation in morphology between years is usually due to differences in year-to-year prevailing weather conditions (Siepielski *et al.* 2009). Weather conditions in the temperature and rainfall can vary from year to year, which alter the quality and quantity of vegetation available in a habitat. As a result, changes to food abundance and the quality can have significant consequences on the morphology of individuals at a particular time (Skulason & Smith 1995). As resources change, individuals in the population may need to adapt to the changes in such a way as to cope with changes to food quality, type and competition among conspecifics for those resources (Renaud *et al.* 2015).

Rhabdomys pumilio is an annual species (i.e. lives for a year; Schradin et al. 2010). It is likely that the longevity of the grassland taxa (*R. dilectus*) is 1-2 years (Claire Dufour pers comm). This implies that striped mice experience the prevailing environments for their entire lives. Thus, the colder drier climate in 1994 and 1997 may have led to food-stress for *Rhabdomys dilectus chakae*. In the grasslands, *Rhabdomys dilectus chakae* consumes grass seeds, insects, berries and herbs (Schradin 2005). Grass seeds, insects, and the woodier herbs, in particular, would increase mechanical strain on the craniomandibular complex and likely lead to more robust skulls and mandibles as a result of strain (Renaud 2005). Hard foods cause higher mechanical strain to the masticatory apparatus because these foods require greater force to break down and so mice that eat harder food experience greater mechanical strain and undergo greater bone remodelling in laboratory mice (Anderson *et al.* 2014).

Molars, once fully erupted, do not experience any further growth and are only modified through the wear as a result of mastication (Renaud 2005). The differences in the allometric slopes for the molars between years suggest that part of the observed variation is likely a result of different growth patterns due to variation in resource abundance. It is thus feasible that the molar variation is related to food availability and type, ultimately related to rainfall and temperatures in each year. Piras *et al.* (2012) suggested that the size and shape of dentition may be influenced by the hardness of the foods that the animal eats. This has been shown in the molars of the bushy-tailed woodrat *Neotoma cinerea* where smaller molars were observed in populations in wetter conditions where vegetation was softer (Cordero & Eppes 2012). However, other studies have not been able to link weather/climate to morphology in rodents. For example, analysis of the first lower molar in populations of common vole *Microtus arvalis* found that molar shape varied more according to phylogeography than any climatic variations (Renvoise *et al.* 2012). In the wood mouse *Apodemus sylvaticus* molar

variation was suggested as being influenced by genetic exchange between populations (Renaud 2005).

Geographic patterns of size variation in crania due to rainfall, temperature, and food have been documented in rodents, such as in the kangaroo rat *Dipodomys merriami* and the plains pocket mouse *Perognathus flavescens* (Wolf *et al.* 2009), deer mice *Peromyscus maniculatus* (Holmes *et al.* 2016), Polish water shrews *Neomys anomalus* and *Neomys fodiens* (Rychlik *et al.* 2006), and in the common shrew *Sorex araneus* (Poroshin *et al.* 2010), that create population level differences in size and shape. However, I observed a within population phenomenon of rainfall and temperature that is not due to geographic differences in climatic factors, which suggests that the morphology in *Rhabdomys dilectus chakae* in my study is likely a plastic response to climatic variation across years.

Phenotypic plasticity in craniofacial skeletal components has been linked to a number of causal mechanisms including diet (Daegling 1992; He & Kiliaridis 2003; Renaud 2005; Segueri & Prevosti 2012; Yom-Tov *et al.* 2013; Anderson *et al.* 2014). Diet can induce plastic responses in morphology since the hardness of food can influence the size and shape of skeletal structures as well as the size of the masticatory muscles. Ferrets *Mustela putorius furo* which consumed hard foods early in their postnatal development were found to have more robust and enlarged zygomatic arches, as well as broader and longer coronoid processes (He & Kiliaridis 2003). In addition, the masticatory muscles were reduced in rats *Rattus rattus* fed a soft-diet (Kiliaridis *et al* 1985).

In short-lived species, individuals need to respond quickly to rapid changes in food availability to increase fitness. Phenotypic plasticity in behaviour and physiology is common in the genus *Rhabdomys* (Schradin *et al.* 2012; Schradin *et al.* 2010; Schradin & Pillay 2006). The sister species *Rhabdomys pumilio* responds rapidly behaviourally by increasing home range size based on resource availability (Schradin *et al.* 2010; Schradin & Pillay 2006), and physiologically by changing reproductive strategies (i.e. group vs solitary-living) based on environmental conditions (Schradin *et al.* 2012) to variation in food availability. There is also some indication of seasonal morphological plasticity in soft tissue (i.e. in the digestive tract, liver, and brain) in *Rhabdomys pumilio* (Schradin & Pillay unpublished). Phenotypic plasticity has not been tested in *Rhabdomys dilectus chakae*, but the potential for such plasticity exists (e.g. Rymer and Pillay 2012).

Comparisons with southern African rodents

My results in *Rhabdomys dilectus chakae* indicate that size increases with age in the skulls and first upper molar, with the first and fourth age classes significantly different from both each other and age classes II and III. Mandibular curves demonstrated significant differences between age classes I, II, III and IV (with age classes III and IV not significantly different from one another), while landmark points on the mandible indicated age class IV was significantly different from the first three age classes. It is likely then that age classes I and II indicate juveniles, age class III indicates an intermediate, sub-adult stage and age class IV indicates the adults.

These findings are similar to those of other studies of southern African rodents, although the number of tooth wear classes depends on the species studies. In the South African Cape dune mole-rat *Bathyergus suillus*, for example, variation is significantly different between juvenile age classes (II and III) and completely grown adults (age classes VI to IX; Hart *et al.* 2007). Similarly, in the Namaqua rock rat *Aethomys namaquensis* and the red rock rat *Aethomys chrysophilus*, little variation occurs between age classes I, II, and III, as well as between age classes IV to VI, although age classes IV to VI were significantly larger than age classes I to III (Chimimba & Dippenaar 1994). However, in the Bushveld gerbil *Tatera leucaster*, the first three age classes differed significantly from each other in size, while also differed significantly from the older age classes (IV to VI; Swanepoel *et al.* 1979). The Tete veld rat *Aethomys ineptus* showed significant differences in size between age classes V and VI (Abdel-Rahman *et al.* 2009) but in the Hottentot golden mole *Amblysomus hottentotus* age was a non-significant source of cranial variation (Bronner 1996).

In polygynous species such as the South African Cape dune mole-rat *Bathyergus suillus* (Hart *et al.* 2007), males are the larger sex. This has also been demonstrated in the Hottentot golden mole *Amblysomus hottentotus* (Bronner 1996), although, in this case, a polygynous mating strategy has only been inferred from the reproductive morphology of the sexes and not actually been documented (Retief *et al.* 2013). These findings support my own results with males of the promiscuous *Rhabdomys dilectus chakae* larger in size than the females.

Sexual dimorphism was absent in species such as the skull of the Tete veld rat *Aethomys ineptus* (Abdel-Rahmen *et al.* 2009), the Bushveld gerbil *Tatera leucaster* skull (Swanepoel *et al.* 1979), and the skull and mandible of the Namaqua rock rat *Aethomys namaquensis* and red rock rat *Aethomys chrysophilus* (Chimimba & Dippenaar 1994). However, in the latter two studies which used traditional morphometrics, the absence of

sexual dimorphism might have been due to the fact that traditional morphometrics are less sensitive to variation in rodents than to an actual lack of dimorphism in those species. While information is lacking on the breeding strategies employed by these species, it is believed that at least two of these species are likely monogamous (*Aethomys ineptus*, Chimimba & Linzey 2008; *Aethomys namaquensis*, Fleming & Nicolson 2004). However, a lack of sexual shape dimorphism in skulls and mandible (Bronner *et al.* 2007) has also been found in the Natal multimammate mouse *Mastomys natalensis* (which has both polygynous males and polyandrous females; Kennis *et al.* 2008) and the southern multimammate mouse *Mastomys coucha* (a polygamous species; Kennis *et al.* 2008).

Inter-annual variation was a significant contributor to size and shape variation in the skull and mandible in my study. However, comparisons to the literature are not possible because, to my knowledge, no other studies on southern African rodents has compared variation across years.

Conclusions

This study is the first attempt to investigate the non-geographic variation in the morphology of a taxon of the genus *Rhabdomys*. The identification of several putative taxa within the genus (Du Toit *et al.* 2012, Rambau *et al.* 2003), and the occurrence of these taxa in sympatry **(**Ganem *et al.* 2012; Meynard *et al.* 2012**)** makes studies like mine challenging since it is necessary to identify taxonomic groups to avoid taxon-specific variation in morphometric analyses and to ensure sufficient samples are available for analysis. I found such a population in the Willem Pretorius Nature Reserve in the Free State Province, which is located in a grassland biome.

Age, sex and year of sampling all had effects on the form of the skull, mandibles, and molars of *Rhabdomys dilectus chakae*. Age class IV had a skull that was not as robust or as gracile as the first three age classes, and a more robust mandible than the other age classes, while specimens from 1995 and 1996 had more gracile skulls and mandibles. No sexual dimorphism was found in the skulls or mandibles in the sample of *Rhabdomys dilectus chakae* with respect to shape. In terms of size age class IV had larger skulls, mandibles, and first molars than the other age classes. Size was sexually dimorphic in the skulls and mandibles, with males significantly larger than females. Specimens from 1994 and 1997 had smaller skulls and mandibles than in other years, and larger third upper molars.

Further studies should consider investigating the type of food and the variability of its abundance across the years and consequent influences on the shape and size of different skeletal structures to better understand the link between inter-annual diet and morphology. Given the age-related variation and sexual dimorphism clearly evident in *Rhabdomys dilectus chakae* in my study, future studies might investigate the intraspecific variation present in other populations of *Rhabdomys dilectus chakae* and compare the variation between populations to establish whether similar patterns are present across the geographic range of the subspecies. This may well be possible as my results differ from those found in a study on a population of *Rhabdomys dilectus chakae* from Midmar Dam (Neves 2015). Furthermore, due to the effects of age and sex on variation, any taxonomic studies on *Rhabdomys dilectus chakae* should consider age classes and sexes separately to ensure accurate interpretation of the results. Such studies should also be done in other species of *Rhabdomys* with the ultimate goal of describing the morphological variation across the genus and possibly providing support for the putative taxonomic distinctions through morphological divergence between the taxa.

References

Adams D.C., Rohlf F.J. & Slice D.E. 2004. Geometric morphometrics: ten years of progress following the 'revolution'. *Italian Journal of Zoology* 71:5-16

Adams D.C., Collyer M.L., Kaliontzopoulou A., & Sherratt E. 2017. Geomorph: Software for geometric morphometric analyses. R package version 3.0.5

Abdel-Rahman E.H., Taylor P.J., Contrafatto G., Lamb J.M., Bloomer P. & Chimimba C.T. 2009. Geometric craniometric analysis of sexual dimorphism and ontogenetic variation: a case study based on two geographically disparate species, *Aethomys ineptus* from southern Africa and *Arvicanthis niloticus* from Sudan (Rodentia: Muridae). *Mammalian Biology-Zeitschrift für Säugetierkunde* 74:361-373

Abiadh A., Colangelo P., Capanna E., Lamine-Cheniti T. & Chetoui M. 2010. Morphometric analysis of six *Gerbillus* species (Rodentia, Gerbillinae) from Tunisia. *Comptes Rendus Biologies* 333:680-687

Aeschbach M., Carrillo J.D. & Sanchez-Villagra M.R. On the growth of the largest living rodent: postnatal skull and dental shape changes in capybara species (*Hydrochoerus spp.*). *Mammalian Biology-Zeitschrift für Säugetierkunde* 81:268-280

Akbarirad S., Darvish J. & Aliabadian M. 2016. Increased species diversity of brush-tailed mice, genus *Calomyscus* (Calomyscidae, Rodentia), in the Zagros Mountains, western Iran. *Mammalia* 80:549-562

Alvarez A. & Perez S.I. 2013. Two- versus three-dimensional morphometric approaches in macroevolution: insight from the mandible of Caviomorph rodents. *Evolutionary Biology* 40:150-157

Alvarez A. & Arnal M. 2015. First approach to the paleobiology of extinct *Prospaniomys* (Rodentia, Hystricognathi, Octodontoidea) through head muscle reconstruction and the study of craniomandibular shape variation. *Journal of Mammalian Evolution* 22:519-533

Alvarez A., Perez S.I. & Verzi D.H. 2015. The role of evolutionary integration in the morphological evolution of the skull of Caviomorph rodents (Rodentia: Hystricomorpha). *Evolutionary Biology* 42:312-327

Anderson P.S.L., Renaud S. & Rayfield E.J. 2014. Adaptive plasticity in the mouse mandible. *BMC Evolutionary Biology* 14:1-9

Andersson M.1994. *Sexual selection*. Princeton University Press, Princeton NJ

Astúa D., Bandeira I. & Geise L. 2015. Cranial morphometric analyses of the cryptic rodent species *Akodon cursor* and *Akodon montensis* (Rodentia, Sigmodontinae). *Oecologia Australis* 19:143-157

Arbour J.H. & Brown C.M. 2014. Incomplete specimens in geometric morphometric analyses. *Methods in Ecology and Evolution* 5:16-26

Auffray J.C., Renaud S. & Claude J. 2009. Rodent biodiversity in changing environments. *Kasetsart Journal, Natural Sciences* 43:83-93

Bailey R.C. & Byrnes J. 1990. A new, old method for assessing measurement error in both univariate and multivariate morphometric studies. *Systematic Zoology* 39:124-130

Birks J.D.S. & Dunestone N. 1985. Sex-related differences in the diet of the mink *Mustela vison. Ecography* 8:245-252

Blanckenhorn W.U., Preziosi,R.F. & Fairbairn D. J. 1995. Time and energy constraints and the evolution of sexual size dimorphism—to eat or to mate? *Evolutionary Ecology* 9:369-381

Blois J.L., Feranec R.S. & Hadly E.A. 2008. Environmental influences on spatial and temporal patterns of body-size variation in California ground squirrels (*Spermophilus beecheyi*). *Journal of Biogeography* 35:602-613

Boelchini F. & Corti M. 2004. The taxonomy of the genus *Tachyoryctes*: a geometric morphometric approach. *Italian Journal of Zoology* 71:35-43

Bohoussou K.H., Cornette R., Akpatou B., Colyn M., Peterhans J.K., Kennis J., Sumbera R., Verheyen E., N'Goran E., Katuala P. & Nicolas V. 2015.The phylogeography of the rodent genus *Malacomys* suggests multiple Afrotropical Pleistocene lowland forest refugia. *Journal of Biogeography* 42:2049-2061

Bol'shakov V.N., Vasil'eva I.A., Gorodilova Y.V. & Chibiryak M.V. 2015. Coupled biotopic variation in populations of sympatric rodent species in the Southern Urals. *Russian Journal of Ecology* 46:339-344

Bonhomme V., Picq S., Gaucherel C. & Claude J. 2014. Momocs: Outline Analysis Using R. *Journal of Statistical Software* 56:1-24

Bonnet X., Lagarde F., Henen B.T., Corbin J., Nagy K.A., Naulleau G., Balhoul K., Chastel O., Legrand A. & Cambag R. 2001. Sexual dimorphism in steppe tortoises (*Testudo horsfieldii*): influence of the environment and sexual selection on body shape and mobility. *Biological Journal of the Linnean Society* 72:357-372

Bookstein F.L. 1989. Principal warps: Thin-plate splines and the decomposition of deformations. *IEEE Transactions on pattern analysis and machine intelligence* 11:567-585

Bookstein F.L. 1991. *Morphometric tools for landmark data: geometry and biology*. Cambridge University Press

Bookstein F.L., Streissguth A.P., Sampson P.D., Connor P.D. & Barr H.M. 2002. Corpus callosum shape and neuropsychological deficits in adult males with heavy fetal alcohol exposure. *Neuroimage* 15:233-251

Bover P., Alcover J.A., Michaux J. & Renaud S. 2010. The case of an insular molarless black rat: effects on lifestyle and mandible morphology. *Archives of Oral Biology* 55:576-582

Breno M., Leirs H. & Van Dongen S. 2011. Traditional and geometric morphometrics for studying skull morphology during growth in *Mastomys natalensis* (Rodentia: Muridae). *Journal of Mammalogy* 92:1395-1406

Bronner G.N. 1996. Non-geographic variation in morphological characteristics of the Hottentot golden mole, *Amblysomus hottentotus* (Insectivora: Chrysochloridae). *Mammalia* 60:707-727

Bronner G.N., van der Merwe M. & Njobe K. 2007. Nongeographic cranial variation in two medically important rodents from South Africa, *Mastomys natalensis* and *Mastomys coucha*. *Journal of Mammalogy* 88:1174-1194

Bryja J., Mikula O., Patzenhauerova H., Oguge N.O., Sumbera R. & Verheyen E. 2013. The role of dispersal and vicariance in the Pleistocene history of an East African mountain rodent, *Praomys delectorum*. *Journal of Biogeography* 41:196-208

Butler M.A. & Losos J.B. 2002. Multivariate sexual dimorphism, sexual selection, and adaptation in Greater Antillean *Anolis* lizards. *Ecological Monographs* 72:541-559

Cahill A.E., Aiello-Lammens M.E, Fisher-Reid M.C, Hua X., Karanewsky C.J., Ryu H.Y., Sbeglia G.C., Spagnolo F., Waldron J.B., Warsi O. & Wiens J.J. 2012. How does climate change cause extinction? *Proceedings of the Royal Society B* 280:20121890

Camilleri C. & Shine R. 1990. Sexual Dimorphism and dietary divergence: Differences in trophic morphology between male and female snakes. *Copeia* 1990:649-658

Cano A.R.G., Fernandez M.H. & Alvarez-Sierra M.A. 2013. Dietary ecology of murine (Muridae, Rodentia): a geometric morphometric approach. *PloS1* 8:e79080

Cardini A. 2003. The geometry of the marmot (Rodentia: Sciuridae) mandible: phylogeny and patterns of morphological evolution. *Systematic Biology* 52:186-205

Cardini A. & Tongiorgi P. 2003. Yellow-bellied marmots (*Marmota flaviventris*) 'in the shape space' (Rodentia, Sciuridae): sexual dimorphism, growth and allometry of the mandible. *Zoomorphology* 122:11-23

Cardini A. & Thorington Jr. 2006.Postnatal ontogeny of marmot (Rodentia, Scuridae) crania: allometric trajectories and species divergence. *Journal of Mammalogy* 87:201-215

Castiglia R., Solano E., Makundi R.H., Hulselmans J., Verheyen E. & Colangelo P. 2012. Rapid chromosomal evolution in the mesic four-striped grass rat *Rhabdomys dilectus* (Rodentia, Muridae) revealed by mtDNA phylogeographic analysis. *Journal of Zoological Systematics & Evolutionary Research* 50:165-172

Caumul R. & Polly P.D. 2005. Phylogenetic and environmental components of morphological variation: skull, mandible, and molar shape in marmots (Marmota, Rodentia). *Evolution* 59:2460-2472

Chimimba C.T. & Dippenaar N.J. 1994. Non-geographic variation in *Aethomys chrysophilus* (De Winton, 1897) and *A. namaquensis* (A. Smith, 1834) (Rodentia: Muridae) from southern Africa. *South African Journal of Zoology* 29:107-117

Chimimba C.T. & Linzey A.V. 2008. *Aethomys ineptus* (Rodentia: Muridae). *Mammalian Species* 809:1-7

Claude J. 2013. Log-shape ratios, Procrustes superimposition, elliptic Fourier analysis: three worked examples in R. *Hystrix, the Italian Journal of Mammalogy* 24:94-102

Colangelo P., Castiglia R., Franchini P. & Solano E. 2010. Pattern of shape variation in the eastern African gerbils of the genus *Gerbilliscus* (Rodentia, Muridae): Environmental correlations and implication for taxonomy and systematics. *Mammalian Biology-Zeitschrift für Säugetierkunde* 75:302-310

Cordeiro-Estrela P., Baylac M., Denys C. & Marinho-Filho J. 2006. Interspecific patterns of skull variation between sympatric Brazilian vesper mice: geometric morphometrics assessment. *Journal of Mammalogy* 87:1270-1279

Cordero G.A. & Eppes C.W. 2012. From desert to rainforest: phenotypic variation in functionally important traits of Bushy-tailed Woodrats (*Neotoma cinerea*) across two climatic extremes. *Journal of Mammalian Evolution* 19:135-153

Cornette R., Stoetzel E., Baylac M., Moulin S., Hutterer R., Nespoulet R., El Hajraoui M.A., Denys C. & Herrel A. 2015. Shrews of the genus *Crocidura* from El Harhoura 2 (Tmara, Morocco): The contribution of broken specimens to the understanding of Late Pleistocene-Holocene palaeoenvironments in North Africa. *Palaeogeography, Palaeoclimate, Palaeoecology* 436

Corti M. & Fadda C. 1996. Systematics of *Arvicanthis* (Rodentia, Muridae) from the Horn of Africa: a geometric morphometrics evaluation. *Italian Journal of Zoology* 63:185-192

Corti M., Aguilera M. & Capanna E. 1998. Phylogeny and size and shape changes in the skull of the South American rodent Proechimys. *Acta Zoologica Academiae Scientiarum Hungaricae* 44:139-150

Costa L.F., dos Reis S.F., Arantes R.A.T., Alves A.C.R. & Mutinari G. 2004. Biological shape analysis by digital curvature. *Pattern Recognition* 37:515-524

Cucchi T., Orth A., Auffray J-C., Renaud S., Fabre L., Catalan J., Hadjisterkotis E., Bonhomme F. & Vigne J-D. 2006. A new endemic species of the subgenus *Mus* (Rodentia, Mammalia) PN THE Island of Cyprus. *Zootaxa* 1241:1-36

Daegling D. 1992. Mandibular morphology and diet in the genus *Cebus*. *International Journal of Primatology* 13:545-570

De Freitas T.R.O., Fernandes F.A., Fornel R. & Roratto P.A. 2012. An endemic new species of tuco-tuco, genus *Ctenomys* (Rodentia: Ctenomyidae), with a restricted geographic distribution in southern Brazil. *Journal of Mammalogy* 93:1355-1367

D'Antro A & Lessa E.P. 2006. Geometric morphometric analysis of geographic variation in the Rio Negro tuco-tuco, *Ctenomys rionegrensis* (Rodentia: Ctenomyidae). *Mammalian Biology-Zeitschrift für Säugetierkunde* 71:288-298

Dos Reis S.F., Duarte L.C., Monteiro L.R. & von Zuben F.J. 2002a. Geographic variation in cranial morphology in *Thrichomys aspereoides* (Rodentia; Echimyidae). I. Geometric descriptors and patterns of variation in shape. *Journal of Mammalogy* 83:333-344

Dos Reis S.F., Duarte L.C., Monteiro L.R. & von Zuben F.J. 2002b. Geographic variation in cranial morphology in *Thrichomys aspereoides* (Rodentia: Echimyidae). II. Geographic units, morphological discontinuities, and sampling gaps. *Journal of Mammalogy* 83:345-353

Du Toit N., Jansen Van Vuuren B., Matthee S. & Matthee C.A. 2012. Biome specificity of distinct genetic lineages within the four-striped mouse *Rhabdomys pumilio* (Rodentia: Muridae) from southern Africa with implications for taxonomy. *Molecular Phylogenetics and Evolution* 65:75-86

Eisenberg J.F. 1981. *The mammalian radiations*. University of Chicago Press, Chicago

Ellis B.J., Jackson J.J. & Boyce T.W. 2006. The stress response systems: universality and adaptive individual differences. *Developmental Review* 26:175-212

Escude E., Montuire S., Desclaux E., Quere J-P., Renvoise E. & Jeannet M. 2008. Reappraisal of 'chronospecies' and the use of *Arvicola* (Rodentia, Mammalia) for biochronology. *Journal of Archaeological Sciences* 35:1867-1879

Escude E., Renvoise E., Lhomme V. & Montuire S. 2013. Why all vole molars (Arvicolinae, Rodentia) are informative to be considered as proxy for Quaternary paleoenvironmental reconstructions. *Journal of Archaeological Science* 40:11-23

Fadda C. & Corti M. 1998. Geographic variation of *Arvicanthis* (Rodentia, Muridae) in the Nile Valley. *Mammalian Biology-Zeitschrift für Säugetierkunde* 63:104-113

Fadda C. & Corti M. 2001. Three-dimensional geometric morphometrics of *Arvicanthis*: implications for systematics and taxonomy. *Journal of Zoological Systematics and Evolutionary Research* 39:235-245

Fairbairn D.J. 1997. Allometry for sexual size dimorphism: Pattern and Process in the Coevolution of Body Size in Males and Females. *Annual Review of Ecology and Systematics* 28:659-687

Fernandes F.A., Fornell R., Cordeiro-Estrela P. & Freitas T.R.O. 2009. Intra- and interspecific skull variation in two sister species of the subterranean rodent genus *Ctenomys* (Rodentia, Ctenomyidae): coupling geometric morphometrics and chromosomal polymorphism. *Zoological Journal of the Linnean Society* 220-237

Fleming P.A. & Nicolson S.W. 2004. Sex differences in space use, body condition and survivorship during the breeding season in the Namaqua rock mouse, *Aethomys namaquensis. African Zoology* 39:123-132

Freckleton R.P. & Jetz W. 2009. Space versus phylogeny: disentangling phylogenetic and spatial signals in comparative data. *Proceedings of the Royal Society of London B: Biological Sciences* 276:21-30

Freeman P. W. & Lemen C. A. 2008. A simple morphological predictor of bite force in rodents. *Journal of Zoology* 275:418–422

Ganem G., Meynard C.N., Perigault M., Lancaster J., Edwards S., Cominade P., Watson J. & Pillay N. 2012. Environmental correlates and co-occurrence of three mitochondrial lineages of striped mice (*Rhabdomys*) in the Free State Province (South Africa). *Acta Oecologica* 42:30-40

Gettys T.W., Mills S. & Henrickst, D.M. 1988. An evaluation of the relation between food consumption rate and equilibrium body-weight in male rats. *British Journal of Nutrition* 60:151-160

Ghalambor C.K. McKay J.K., Carroll S.P. & Reznick D.N. 2007. Adaptive versus non-adaptive phenotypic plasticity and the potential for contemporary adaptation in new environments. *Functional Ecology* 21:394-407

Greenberg R. & Olsen B. 2010. Bill size and dimorphism in tidal-marsh sparrows: Island-like processes in a continental habitat. *Ecology* 91:2428–2436

Ginot S., Claude J., Perez J. & Veyrunes F. 2017. Sex reversal induces size and performance differences among females of the African pygmy mouse, *Mus minutoides*. *Journal of Experimental Biology* 220:1947-1951

Ginot S., Herrel A., Claude J. & Hautier L. 2018. Skull size and biomechanics are good estimators of *in vivo* bite force in Murid rodents. *Anatomical Record* 301:256–266

Goyens J., Soons J., Aerts P. & Dirckx J. 2014. Finite-element modelling reveals force modulation of jaw adductors in stag beetles. *Journal of the Royal Society Interface* 11:20140908

Guerecheau A., Ledevin R., Henttonen H., Deffontaine., Michaux J.R., Chevret P. & Renaud S. 2010. Seasonal variation in molar outline of bank voles: An effect of wear? *Mammalian Biology-Zeitschrift für Säugetierkunde* 75:311-319

Gunduz I., Jaarola M., Tez C., Yeniyurt C., Polly D.P. & Searle J.B. 2007. Multigenic and morphometric differentiation of ground squirrels (*Spermophilus*, Scuridae, Rodentia) in Turkey, with a description of a new species. *Molecular Phylogenetics and Evolution* 43:916-935

Gunz P. & Mitteroecker P. 2013. Semilandmarks: a method for quantifying curves and surfaces. *Hystrix*, *the Italian Journal of Mammalogy* 24:103-109

Haines A.J. & Crampton J.S. 2000. Improvements to the method of Fourier shape analysis as applied in morphometric studies. *Palaeontology* 43:765-783

Hamilton W.D & Zuk M. 1982. Heritable true fitness and bright birds: a role for parasites? *Science* 218:384-387

Happold D.C.D. (ed). 2013. *Mammals of Africa. Volume III: Rodents, Hares and Rabbits*. Bloomsbury Publishing, London 545-547

Hart L., Chimimba C.T., Jarvis J.U.M., O'Riain J. & Bennet N.C. 2007. Craniometric sexual dimorphism and age variation in the South African Cape dune mole-rat (*Bathyergus suillus*). *Journal of Mammalogy* 88:657-666

Hautier L., Michaux J., Marivaux L. & Vianey-Liaud M. 2008. Evolution of the zygomasseteric construction in Rodentia, as revealed by a geometric morphometric

analysis of the mandible of *Graphiurus (Rodentia, Gliridae*). *Zoological Journal of the Linnaen Society* 154:807-821

Hautier L., Bover P., Alcover J.A. & Michaux J. 2009. Mandible morphometrics, dental microwear pattern, and palaeobiology of the extinct Balearic Dormouse *Hypnomys Morpheus*. *Acta Palaeontologica Polonica* 54:181-194

Hautier L., Lebrun R. & Cox P.G. 2012. Patterns of covariation in the masticatory apparatus of Hysticognathus rodents: implications for evolution and diversification. *Journal of Morphology* 273:1319-1337

He T. & Kiliaridis S. 2003. Effects of masticatory muscle function on craniofacial morphology on growing ferrets (*Mustela putorius furo*). *European Journal of Oral Sciences* 11:510-517

Helvaci Z., Renaud S., Ledevin R., Adriaens D., Michaux J., Çolak R., Kankiliç T., Kandemir İ., Yiğit N. & Çolak, E. 2012. Morphometric and genetic structure of the edible dormouse (*Glis glis*): a consequence of forest fragmentation in Turkey. *Biological Journal of the Linnean Society* 107:611-623

Henschel J.R., David J.H.M. & Jarvis J.U.M. 1982. Age determination and age structure of a striped fieldmouse, *Rhabdomys pumilio*, population from the Cape Flats. *South African Journal of Zoology* 17:136-142

Herrel A., Joachim R., Vanhooydonck B. & Irschick D.J. 2006. Ecological consequences of ontogenetic changes in head shape and bite performance in the Jamaican lizard *Anolis lineatopus*. *Biological Journal of the Linnean Society* 89:443-454

Herrel A., Moore J.A., Bredeweg E.M. & Nelson N.J. 2010. Sexual dimorphism, body size, bite force and male mating success in tuatara. *Biological Journal of the Linnean Society* 100:287-292

Hoffman A.A. & Sgrò C.M. 2011. Climate change and evolutionary adaptations. *Nature* 470:479-485

Holmes M.W., Boykins G.K., Bowie R.C. & Lacey E.A. 2016. Cranial morphological variation in *Peromyscus maniculatus* over nearly a century of environmental change in three areas of California. *Journal of morphology* 277:96-106

Holt R.D. & Gaines M.S. 1992. Analysis of adaptation in heterogeneous landscapes: implications for the evolution of fundamental niches. *Evolutionary Ecology* 6:433-447

Houston D. & Shine R. 1993. Sexual dimorphism and niche divergence: feeding habits of the Arafura filesnake. *Journal of Animal Ecology* 62:737-748

Husak J.F., Lappin A.K., & Van Den Bussche R.A. 2009. The fitness advantage of a high-performance weapon. *Biological Journal of the Linnean Society* 96:840-845

Jacquet F., Hutterer R., Nicolas V., Decher J., Colyn M., Couloux A. & Denys C. 2013. New status for two African giant forest shrews, *Crocidura goliath goliath* and *C. goliath nimbasilvanus* (Mammalia: Soricomorpha), based on molecular and geometric morphometric analyses. *African Zoology* 48:13-29

Jamniczky H.A. & Hallgrimsson B. 2009. A comparison of covariance structure in wild and laboratory muroid crania. *Evolutions* 63:1540-1556

Jojić V., Blagojević J. & Vujošević M. 2011. B chromosomes and cranial variability in yellow-necked field mice (*Apodemus flavicollis*). *Journal of Mammalogy* 92:396-406

Jojić V., Nenadović J., Blagojević J., Paunović M., Cvetkovic D. & Vujošević M. 2012. Phenetic relationships among four *Apodemus* species (Rodentia Muridae) inferred from skull variation. *Mammalian Biology-Zeitschrift für Säugetierkunde* 251:26-37

Jones K.E., Ruff C.B. & Goswami A. 2013. Morphology and biomechanics of the pinniped jaw: mandibular evolution without mastication. *The Anatomical Record* 296:1049-1063

Kaddour K.B., El Mouden E.H., Slimani T., Bonnet X. & Lagarde F. 2008. Sexual dimorphism in the Greek tortoise: A test of the body shape hypothesis. *Chelonian Conservation and Biology* 7:21-27

Kamilari M., Tryfonopoulos G., Fraguedakis-Tsolis S. & Chondropoulos B. 2013. Geometric morphometrics on Greek house mouse populations (*Mus musculus domesticus*) with Robertsonian and all-acrocentric chromosomal arrangements. *Mammalian Biology-Zeitschrift für Säugetierkunde* 78:241-250

Kennis J., Skuydts V., Leirs H. & van Hooft P.W. 2008. Polyandry and polygyny in an African rodent pest species *Mastomys natalensis*. *Special Issue: 10th International African Small Mammals Symposium (ASMS)*. *Mammalia* 72:150-160

Kiliaridis S., Engström C. & Thilande B. 1985. The relationship between masticatory function and craniofacial morphology: I. A cephalometric longitudinal analysis

Kimura Y., Jacobs L.L. & Flynn L.J. 2013. Lineage-specific responses of tooth shape in Murine Rodents (Murinae, Rodentia) to Late Miocene dietary change in the Siwaliks of Pakistan. *PloS 1* 8:e76070

Kingdon J. 1974. *East African Mammals*. London: Academic Press

Klingenberg C.P. 2010. Evolution and development of shape: integrating quantitative approaches. *Nature Reviews Genetics* 11:623-635

Klingenberg C.P. & McIntyre G.S. 1998. Geometric morphometrics of developmental instability: analyzing patterns of fluctuating asymmetry with Procrustes methods. *Evolution* 52:1363-1375

Klingenberg C.P., Barluenga M. & Meyer A. 2002. Shape analysis of symmetric structures: quantifying variation among individuals and asymmetry. *Evolution* 56:1909-1920

Kuhl F.P., & Giardina C.R. 1982. Elliptic Fourier features of a closed contour. *Computer graphics and image processing*, 18:236-258.

Kronfeld-Schor N. & Dayan T. 2008. Activity patterns of rodents: the physiological ecology of biological rhythms. *Biological Rhythms Research* 39:193-211

Krystufek B., Klenovsek T., Buzan E.V., Loy A. & Janzekovic F. 2012. Cranial divergence among evolutionary lineages of Martino's vole, *Dinaromys bogdanovi,* a rare Balkan paleoendemic rodent. *Journal of Mammalogy* 93:818-825

Lailvaux S.P. & Irschick D.J. 2006 A functional perspective on sexual selection: insights and future prospects. *Animal Behaviour* 72:263-273

Lalis A., Evin A. & Denys C. 2009. Morphological identification of sibling species: the case of West African *Mastomys* (Rodentia: Muridae) in sympatry. *Evolution* 332:480-488

Lalis A., Janier M., Koivogui L. & Denys C. 2015. Host evolution in *Mastomys natalensis* (Rodentia: Muridae): an integrative approach using geometric morphometrics and genetics. *Integrative Zoology* 10:505-514

Law C.J., Baliga V.B., Tinker T.M. & Mehta R.S. 2017. Asynchrony in craniomandibular development and growth in *Enhydra lutris nereis* (Carnivora: Mustelidae): are southern sea otters born to bite? *Biological Journal of the Linnean Society* 121:420–438

Lazzari V., Aguilar J-P., & Michaux J. 2010. Intraspecific variation and micro-macroevolution connection: illustration with the late Miocene genus *Prognomys* (Rodentia, Muridae). *Paleobiology* 36:641-657

Le Galliard J.F., Marquis O., & Massat M. 2010. Cohort variation, climate effects and population dynamics in a short-lived lizard. *Journal of Animal Ecology* 79:1296-1307

Le Grange A., Bastos A.D., Brettschneider H. & Chimimba C.T. 2015. Evidence of a contact zone between two Rhabdomys dilectus (Rodentia: Muridae) mitotypes in Gauteng province, South Africa. *African Zoology* 50:63-68

Leamy L.J., Meagher S., Taylor S., Carroll T. & Pottis W.K. 2001. Size and fluctuating asymmetry of morphometric characters in mice: their associations with inbreeding and t-haplotype. *Evolution* 55:2333-2341

Ledevin R., Michaux J.R., Deffontaine V., Henttonen H. & Renaud S. 2010a. Evolutionary history of the bank vole *Myodes glareolus*: a morphometric perspective. *Biological Journal of the Linnean Society* 100:681-694

Ledevin R., Quere J-P. & Renaud S. 2010b. Morphometrics as an insight into processes beyond tooth shape variation in a Bank Vole population. *PloS1* 5:e15470

Ledevin R., Chevret P., Ganem G., Britton-Davidian J., Hardouin E.A., Chapius J-L., Pisanu B., Mathias M.L., Schlager S., Auffray J-C. & Renaud S. 2016. Phylogeny and adaptation shape the teeth of insular mice. *Proceedings of the Royal Society of London Biology* 283:20152820

Leirs H., Verhagen R., & Verheyen W. 1994. The basis of reproductive seasonality in *Mastomys* rats (Rodentia: Muridae) in Tanzania. *Journal of Tropical Ecology* 10:55-66

Lewis P. J., Strauss R., Johnson E. & Conway W. C. 2002. Absence of sexual dimorphism in molar morphology of muskrats. *The Journal of Wildlife Management* 66:1189-1196

Lindenfors P., Gittleman J. L., & Jones K. E. 2007. Sexual size dimorphism in mammals. In D. J. Fairbairn, W. V. Blanckenhorn, & T. Szekely (Eds.). *Sex, size and gender roles: Evolutionary studies of sexual size dimorphism* (pp. 16–26). Oxford

Lochmiller R.L., Ditchkoff S.S. & Sinclair J.A. 2000. Developmental plasticity of postweaning Cotton rats (*Sigmodon hispidus*) as an adaptation to nutritionally stochastic environments. *Evolutionary Ecology* 14:127-142

Lohmann G.P. Eigenshape analysis of microfossils: A general morphometric procedure for describing changes in shape. *Mathematical Geology* 15:659-672

Lu X., Ge D., Xia L., Huang C. & Yang Q. 2014. Geometric morphometric study of the skull shape diversification in Sciuridae (Mammalia, Rodentia). *Integrative Zoology* 9:231-245

Luiselli L & Angellici F.M. 1998. Sexual size dimorphism and natural history traits are correlated with intersexual dietary divergence in royal pythons (*python regius*) from the rainforest of southeastern Nigeria. *Italian Journal of Zoology* 65:183-185

Macholan M., Mikula O. & Vohralik V. 2008. Geographic phonetic variation of two eastern-Mediterranean non-commensal mouse species, *Mus macedonicus* and *M. cypriacus* (Rodentia: Muridae) based on traditional and geometric approaches to morphometrics. *Zoologischer Anzeiger* 247:67-80

Maestri R., Monteiro L.R., Fornel R., Upham N.S., Patterson B.D. & de Freitas T.R.O. 2017. The ecology of a continental evolutionary radiation: Is the radiation of sigmodontine

rodents adaptive? *Evolution* 71:610-632

Malmgren J.C. & Thollesson M. 1999. Sexual size and shape dimorphism in two species of newts, *Triturus cristatus* and *T. vulgaris* (Caudata: Salamandridae). *Journal of Zoology* 249:127-136

Marcolini F., Piras P. & Martin R.A. 2009. Testing evolutionary dynamics on first lower molars of Pliocene *Ogmodontomys* (Arvicolidae, Rodentia) from the Meade Basin of Southwestern Kansas (USA): A landmark –based approach. *Palaios* 24:535-543

Martinez J.J. & Di Cola V. 2011. Geographic distribution and phonetic skull variation in two close species of *Graomys* (Rodentia, Cricetidae, Sigmodontinae). *Zoologischer Anzeiger* 250:175-194

Martinez J.J. & Gardenal C.N. 2016. Phylogenetic relationships among species of the Neotropical genus *Graomys* (Rodentia: Cricetidae): contrasting patterns of skull morphometric variation and genetic divergence. *Biological Journal of the Linnaean Society* 118:648-667

Matthews T. & Stynder D.D. 2011a. An analysis of two *Myosorex* species (Soricidae) from the Early Pliocene site of Langebaanweg (West Coast, South Africa) using geometric morphometrics, linear measurements, and non-metric characters. *Geobios* 44:87-99

Matthews T. & Stynder D.D. 2011b. An analysis of the *Aethomys* (Murinae) community from Langebaanweg (Early Pliocene, South Africa) using geometric morphometrics. *Palaeogeography, Palaeoclimatology, Palaeoecology* 302:230-242

McElligot A.G., Gammell M.P., Harty H.C., Paini D.R., Murphy D.T., Walsh J.T. & Hayden T.J. 2001. Sexual size dimorphism in fallow deer (*Damma dama*): do larger, heavier males gain greater mating success? *Behavioral Ecology and Sociobiology* 49:266-272

McGuire J.L. 2010. Geometric morphometrics of vole (*Microtus californicus*) dentition as a new paleoclimate proxy: shape change along geographic and climatic clines. *Quaternary International* 212:198-205

McGuire J.L. 2011. Identifying California *Microtus* species using geometric morphometrics documents Quaternary geographic range contractions. *Journal of Mammalogy* 92:1383-1394

McPhee E.M. 2004. Morphological change in wild and captive Oldfield mice *Peromyscus polionotus subgriseus*. *Journal of Mammalogy* 85:1130-1137

Meynard C.N., Pillay N., Perrigault M., Caminade P. & Ganem G. 2012. Evidence of environmental niche differentiation in the striped mouse (*Rhabdomys sp*.): inference from its current distribution in southern Africa. *Ecology and evolution* 2:1008-1023

Michaux J., Cucchi t., Renaud s., Garcia-Talavera F. & Hutterer R. 2007a. Evolution of an invasive rodent on an archipelago as revealed by molar shape analysis: the house mouse in the Canary Islands. *Journal of Biogeography* 34:1412-1425

Michaux J., Chevret P. & Renaud S. 2007b. Morphological diversity of Old World rats and mice (Rodentia, Muridae) mandible in relation with phylogeny and adaptation. *Journal of Zoological Systematics and Evolutionary Research* 45:263-279

Mitteroecker P. & Gunz P. 2009. Advances in geometric morphometrics. *Evolutionary Biology* 36:235-247

Monadjem A., Taylor P.J., Denys C. & Cotterill F.P.D. 2015. *Rodents of Sub-Saharan Africa: A biogeographic and taxonomic synthesis*. De Gruyter, Berlin Germany

Monteiro L.R., Bonato V. & Dos Reis S.F. 2005. Evolutionary integration and morphological diversification in complex morphological structures: mandible shape divergence in spiny rats (Rodentia, Echimyidae). *Evolution and Development* 7:429-439

Morris J.S. & Brandt E.K. 2014. Specialization for aggression in sexually dimorphic skeletal morphology in grey wolves (*Canis lupis*). *Journal of Anatomy* 225:1-11

Mullins S.K., Pillay N. & Taylor P.J. 2004. Cranial variation and geographic patterns within the *Dasymys rufulus*. *Journal of Mammalogy* 85:911-923

Nel K., Rimbach R. & Pillay N. 2015. Dietary protein influences the life- history characteristics across generations in the African striped mouse Rhabdomys. *Journal of Experimental Zoology*. 323A:97–108

Neves C.N. 2015. Cranio-morphometric analysis of nongeographic variation in three South African taxa of the Four-Striped Mouse. Honours research report, University of the Witwatersrand, Johannesburg, South Africa

Nengovhela A., Baxter R.M. & Taylor P.J. 2015. Temporal changes in cranial size in South African vlei rats (*Otomys*): evidence for the 'third universal response to warming'. *African Zoology* 50:1-7

Oleksyk T.K., Novak J.M., Purdue J.R., Gashchak S.P. & Smith M.H. 2004. High levels of fluctuating asymmetry in populations of *Apodemus flavicollis* from the most contaminated areas in Chernobyl. *Journal of Environmental Radioactivity* 73:1-20

Ortega J., López P. & Martín J. 2017. Environmental drivers of growth rates in Guadarrama wall lizards: a reciprocal transplant experiment. *Biological Journal of the Linnean Society* 122:340-350

Owens F.N., Dubeski P. & Hanson C.F. 1993. Factors that alter the growth and development of ruminants. *Journal of Animal Science* 71:3138-3150

Packer C. 1983. Sexual dimorphism: the horns of African antelopes. *Science* 221:1191-1193

Pares-Casanova P.M. 2017. Mandibular allometry in *Hydrochoerus hydrochaeris* (Linnaeus, 1766) (Hydrocherinae, Caviidae). *Papéis Avulsos de Zoologia* 57:451-457

Pillay N. 2000. Female mate preference and reproductive isolation in populations of the striped mouse *Rhabdomys pumilio. Behaviour* 137:1431-1441

Pillay N., Eborall J. & Ganem G. 2006. Divergence of mate recognition in the African striped mouse (*Rhabdomys*). *Behavioral Ecology* 17:757-64

Piras P., Marcolini F., Claude J., Ventura J., Kotsakis T. & Cubo J. 2012. Ecological and functional correlates of molar shape variation in European populations of *Arvicola* (Arvicolinae, Rodentia). *Zoologischer Anzeiger* 251:335-343

Polly D.P. 2001. On morphological clocks and paleophylogeography: towards a timescale for *Sorex* hybrid zone. *Genetica* 112:339-357

Polly D.P. 2003. Paleophylogeography: the tempo of geographic differentiation in marmots (*Marmota*). *Journal of Mammalogy* 84:369-384

Polly P.D., Killick L. & Ruddy M. 2011. Using left-right asymmetry to estimate non-genetic variation in vole teeth (Arvicollinae, Muridae, Rodentia). *Palaeontologia Electronica* 14:41A

Poroshin E.A., Polly D.P. & Wójcik J.M. 2010. Climate and morphological change on decadal scales: multiannual variation in the common shrew *Sorex araneus* in northeast Russia. *Acta Theriologica* 55:193-202

Preston B.T., Stevenson I.R., Pemberton J.M., Coltman D.W. & Wilson K. 2003. Overt and covert competition in a promiscuous mammal: the importance of weaponry and testes size to male reproductive success. *Proceedings of the Royal Society of London Biology* 27:633-640

Quintela F.M., Fornel R. & Freitas T.R.O. 2016. Geographic variation in skull shape of the water rat *Scapteromys tumidus* (Cricetidae, Sigmodontinae): isolation-by-distance plus environmental and geographic barrier effects? *Anais de Academia Brasileira de Ciencias* 88:451-466

R Core Team. 2014. R: A language and environment for statistical computing. R Foundation for Statistical Computing, Vienna, Austria. URL http://www.R-project.org/

Rambau R.V., Robinson T.J. & Stanyon R. 2003. Molecular genetics of *Rhabdomys pumilio* subspecies boundaries: mtDNA phylogeography and karyotypic analysis by inflorescence in situ hybridisation. *Molecular Phylogenetics and Evolution* 28:564-575

Renaud S. 2005. First upper molar and mandible shape of wood mice (*Apodemus sylvaticus*) from northern Germany: ageing, habitat and insularity. *Mammalian Biology-Zeitschrift für Säugetierkunde* 70:157-170

Renaud S., Michaux J., Jaeger J.J. & Auffray J.C. 1996. Fourier analysis applied to *Stephanomys* (Rodentia, Muridae) molars: nonprogressive evolutionary pattern in a gradual lineage. *Paleobiology* 22:255-265

Renaud S. & Millien V. 2001. Intra- and interspecific morphological variation in the field mouse species *Apodemus argenteus* and *A. speciosus* in the Japanese archipelago: the role of insular isolation and biogeographic gradients. *Biological Journal of the Linnean Society* 74:557-569

Renaud S. & Van Dam J. 2002. Influence of biotic and abiotic environment on dental size and shape evolution in a Late Miocene lineage of murine rodents (Teruel Basin, Spain). *Palaeogeography, Palaeoclimatology, Palaeoecology* 184:163-175

Renaud S. & Michaux J.R. 2003. Adaptive latitudinal trends in the mandible shape of *Apodemus* wood mice. *Journal of Biogeography* 30:1617-1628

Renaud S., Michaux J., Schmidt D.N., Aguilar J.P., Mein P. & Auffray J.C. 2005. Morphological evolution, ecological diversification and climate change in rodents. *Proceedings of the Royal Society of London B: Biological Sciences* 272:609-617

Renaud S., Auffray J-C. & Michaux J. 2006. Conserved phenotypic variation patterns, evolution along lines of least resistance, and departure due to selectin in fossil rodents. *Evolution* 60:1701-1717

Renaud S. & Michaux J.R. 2007. Mandibles and molars of the wood mouse, *Apodemus sylvaticus* (L.): integrated latitudinal pattern and mosaic insular evolution. *Journal of Biogeography* 34:339-355

Renaud S. & Auffray J-C. 2009. Adaptation and plasticity in insular evolution of the house mouse mandible. *Journal of Zoological Systematics and Evolutionary Research* 48:138-150

Renaud S., Rodrigues H.G., Ledevin R., Pisanu B., Chapius J-L & Hardouin E.A. 2015. Fast evolutionary response of house mice to anthropogenic disturbance on a Sub-Antarctic island. *Biological Journal of the Linnean Society* 114:513-526

Renvoisé E., Montuire S., Richard Y., Quéré J.P., Gerber S., Cucchi T., Chateau-Smith C. & Tougard, C. 2012. Microevolutionary relationships between phylogeographical

history, climate change and morphological variability in the common vole (Microtus arvalis) across France. *Journal of biogeography* 39:698-712

Retief T.A., Bennett N.C., Kinahan A.A. & Bateman P.W. 2013. Sexual selection and genital allometry in the Hottentot golden mole (*Amblysomus hottentotus*). *Mammalian Biology* 78:356-360

Richtsmeier J.T., Lele S.R. & Cole III T.M. 2005. Landmark morphometrics and the analysis of variation. *Variation: A central concept in biology*

Rohlf J.F. 2015a. tpsUtil program © v1.70, Ecology & Evolution, SUNY at Stony Brook

Rohlf J.F. 2015b. tpdDig2 program ©, v2.18, Ecology & Evolution, SUNY at Stony Brook

Rohlf F.J. & Archie J.W. 1984. A comparison of Fourier methods for the description of wing shape in mosquitos (Diptera: Culicidae). *Systematic Zoology* 33:302-317

Rohlf J.F. & Slice D. 1990. Extensions of the Procrustes method for the optimal superimposition of landmarks. *Systematic Biology* 39:40-59

Rychlik L., Ramalhinho G. & Polly P.D. 2006. Response to environmental factors and competition: skull, mandible and tooth shapes in Polish water shrews (*Neomys*, Soricidae, Mammalia). *Journal of Zoological Systematics and Evolutionary Research* 44:339-351

Rymer T. & Pillay N. 2012. The development of exploratory behaviour in the African striped mouse *Rhabdomys* reflects a gene x environment compromise. *Behavior Genetics* 42:845–856

Samuels J.X. 2009. Cranial morphology and dietary habits of rodents. *Zoological Journal of the Linnaen Society* 156:864-888

Samuels J.X. & Van Valkenburgh B. 2009. Craniodental adaptations for digging in extinct burrowing beavers. *Journal of Vertebrate Paleontology* 29:254-268

Sansalone G., Kotsakis T. & Piras P. 2016. New systematic insights about Plio-Pleistocene moles from Poland. *Acta Palaeontologica Polonica* 61:221-229

Santana S.E., Geipel I., Dumont E.R., Kalka M.B. & Kalko E.K. 2011. All you can eat: high performance capacity and plasticity in the common big-eared bat, *Micronycteris microtis* (Chiroptera: Phyllostomidae). *PloS1* 6:e28584

Saunders P.A., Perez J., Rohman M., Ronce O., Crotchet P-A & Veyrunes F. 2014. XY females do better than the XX in the African pygmy mouse, *Mus minutoides. Evolution* 68:2119-2127

Schradin C. 2005. When to live alone and when to live in groups: ecological determinants of sociality in the African striped mouse (*Rhabdomys pumilio* Sparrman, 1784). *Belgian Journal of Zoology* 135:77-82

Schradin C. & Pillay N. 2004. The Striped Mouse (*Rhabdomys pumilio*) from the Succulent Karoo, South Africa: a territorial group-living solitary forager with communal breeding and helpers at the nest. *Journal of Comparative Psychology* 118:37-47

Schradin C. & Pillay N. 2005a. Intraspecific variation in the spatial and social organization of the African striped mouse. *Journal of Mammalogy* 86:99-107

Schradin C. & Pillay N. 2005b. Demography of the striped mouse (*Rhabdomys pumilio*) in the succulent Karoo. *Mammalian Biology-Zeitschrift für Säugetierkunde* 70:84-92

Schradin C. & Pillay N. 2006. Female striped mice (*Rhabdomys pumilio*) change their home ranges in response to seasonal variation in food availability. *Behavioural Ecology* 17:452-458

Schradin C., König B. & Pillay N. 2010. Reproductive competition favours solitary living while ecological constraints impose group-living in African striped mice. *Journal of Animal Ecology* 79:515-521

Schradin C., Schmol G., Rödel H.G., Schoepf I., Treffler S.M., Brenner J., Bleeker M., Schubert M., König B. & Pillay N. 2010. Female home range size is regulated by resources distribution and intraspecific competition: a long-term field study. *Animal Behaviour* 79:195-203

Schradin C., Lindholm A.K., Johannesen J., Schoepf I., Yuen C., König B. & Pillay N. 2012. Social flexibility and social evolution in mammals: a case study of the African striped mouse (*Rhabdomys pumilio*). *Molecular Ecology* 21:541-553

Schulte-Hostedde A.I., Millar J.S. & Hickling G.J. 2001. Sexual dimorphism in body composition of small mammals. *Canadian Journal of Zoology* 79:1016-1020

Schluter D. 2001. Ecology and the origin of species. *Trends in Ecology and Evolution* 16:372-380

Seguri V. & Prevosti F. 2012. A quantitative approach to the cranial ontogeny of *Lycalopex culpaeus* (Carnivora: Canidae). *Zoomorphology* 131:79-92

Sheets H.D., Covino K.M., Panasiewicz J.M. & Morris S.R. 2006. Comparison of geometric morphometric outline methods in the discrimination of age-related differences in feather shape. *Frontiers in Zoology 3*:15

Sheets H.D., Kim K. & Mitchell C.E. 2004. A combined landmark and outline-based approach to ontogenetic shape change in the Ordovician trilobite *Triarthrus becki*. In *Morphometrics* p67-82. Springer Berlin Heidelberg

Shintaku Y. & Motokawa M. 2010. Geographic variation in skull morphology of the Large Japanese Field Mice, *Apodemus speciosus* (Rodentia: Muridae) revealed by geometric morphometric analysis. *Zoological Science* 33:132-145

Shintaku Y. & Motokawa M. 2016. Geographic variation in the skull morphology of the large Japanese field mice, *Apodemus speciosus* (Rodentia: Muridae) revealed by geometric morphometric analysis. *Zoological Science* 33:132-145

Siepielski A.M., DiBattista J.D. & Carlson S.M. 2009. It's about time: the temporal dynamics of phenotypic selection in the wild. *Ecology Letters* 12:1261-1276

Skinner J.D. & Chimimba C.T. 2005. *The mammals of the southern African sub-region*. Cambridge University Press

Skulason S., & Smith T.B. 1995. Resource polymorphisms in vertebrates. *Trends in ecology & evolution* 10:366-370

South African Weather Service. 22 January 2018. http://www.weathersa.co.za/compliments-complaints/climate-data-requests

Stillwell C.R. & Davidowits G. 2010. A developmental perspective on the evolution of sexual size dimorphism of a moth. *Proceedings of the Royal Society of Biology* 277:2069-2074

Stockley P. & Bro-Jørgensen J. 2010. Female competition and its evolutionary consequences in mammals. *Biological Reviews* 86:341-366

Stoetzel E., Denys C., Michaux J. & Renaud S. 2013. *Mus* in Morocco: a Quaternary sequence of intraspecific evolution. *Biological Journal of the Linnean Society* 109:599-621

Stumpfel S., Bieber C., Blanc S., Ruf T. & Giroud S. 2017. Differences in growth rates and pre-hibernation body mass gain between early and late-born juvenile garden dormice. *Journal of Comparative Physiology B*. 187:253-263

Stumpp R., Fuzessy L. & Palgia A.P. 2018. Environmental drivers acting on rodent rapid morphological change. *Journal of Mammalian Evolution* 25:131-140

Swanepoel P., Schlitter D.A. & Genoways H.H. 1979. A study of nongeographic variation in *Tatera leucogaster* (Mammalia: Rodentia) from Botswana. *Annals of the Carnegie Museum* 48:7-24

Swiderski D.L. 2003. Separating size from allometry: analysis of lower jaw morphology in the fox squirrel, *Sciurus niger*. *Journal of Mammalogy* 84:861-876

Suzuki S., Abe M. & Motokawa M. 2012. Integrative study on static skull variation in the Japanese weasel (Carnivora: Mustelidae). *Journal of Zoology* 288:57–65

Taylor P.J. 2000. Patterns of chromosomal variation in southern African Rodents. *Journal of Mammalogy* 81(2):317-331

Taylor P.J., Lavrenchenko L.A., Carleton M.D., Verheyen E., Bennet N.C., Oosthuizen C.J. & Maree S. 2011. Specific limits and emerging diversity patterns in East African populations of laminate-toothed rats, genus *Otomys* (Muridae: Murinae: Otomyini): revision of the *Otomys typus* complex. *Zootaxa* 3024:1-66

Taylor P.J., Kumirai A. & Contrafatto G. 2005. Species with fuzzy borders: the taxonomic status and species limits of Saunders' vlei rat, *Otomys saundersiae* Roberts, anee? (Rodentia, Muridae, Otomyini). *Mammalia* 69:297-322

Trivers R. 1972. *Parental investment and sexual selection*. Biological Laboratories, Harvard University

Van Dam J.A. 1997. *The small mammals from the upper Miocene of the Teruel-Alfambra region (Spain): paleobiology and paleoclimatic reconstructions* 156:1-204 Utrecht University

Vessey S.H. & Vessey K.B. 2007. Linking behavior, life history and food supply with the population dynamics of white-footed mice (*Peromyscus leucopus*). *Integrative Zoology* 2:123-130

Vincent S.E., Herrel A. & Irschick D.J. 2004. Sexual dimorphism in head shape and diet in the cottonmouth snake (*Agkistrodon piscivorus*). *Journal of Zoology* 264:53-59

Vucetich M.G., Deschamps C.M., Vieytes E.C. & Montalvo C.I. 2014. Late Miocene capybaras from Argentina: skull anatomy, taxonomy, evolution, and biochronology. *Acta Palaeontologica Polonica* 59:517-535

Wallace S.C. 2006. Differentiating *Microtus xanthognathus* and *Microtus pennsylvanicus* lower first molars using discriminant analysis of landmark data. *Journal of Mammalogy* 87:1261-1269

Waterman J., Wolff J.O. & Sherman P.W. 2007. Male mating strategies in rodents. *Rodent societies: an ecological and evolutionary perspective* 27-41

Webster M. & Sheets A.D. 2010. A Practical Introduction to Landmark-Based Geometric Morphometrics. *Quantitative Methods in Paleobioogy* 16:163-188

Wilson L.A.B. 2013. Geographic variation in the greater Japanese shrew-mole, *Urotrichus talpoides*: combining morphological and chromosomal patterns. *Mammalian Biology-Zeitschrift für Säugetierkunde* 78:267-275

Wolf M., Friggens M., & Salazar-Bravo J. 2009. Does weather shape rodents? Climate related changes in morphology of two heteromyid species. *Naturwissenschaften* 96:93-101

Yazdi F.T. & Adriaens D. 2013. Cranial variation in *Meriones tristrami* (Rodentia: Muridae: Gerbillinae) and its morphological comparison with *Meriones persicus, Meriones vinogradovi* and *Meriones libycus*: a geometric morphometric study. *Journal of Zoological Systematics and Evolutionary Research* 51:239-251

Yazdi F.T., Adriaens D. & Darvish J. 2015. Cranial phenotypic variation in *Meroines crassus* and *M. libycus* (Rodentia, Gerbillinae), and a morphological divergence in *M. crassus* from the Iranian Plateau and Mesopotamia (Western Zagros Mountains). *European Journal of Taxonomy* 88:1-28

Yom-Tov Y. & Yom-Tov S. 2004. Climatic change and body size in two species of Japanese rodents. *Biological Journal of the Linnean Society* 82:263–267

Yom-Tov Y., Yom-Tov S. & Jarrel G. 2008. Recent increase in body size of the American marten *Martes americana* in Alaska. *Biological Journal of the Linnean Society* 93:701–707

Yom-Tov Y., Yom-Tov S. & Zachos F.E. 2013. Temporal and geographical variation in skull size of the red fox (*Vulpes vulpes*) and the Eurasian badger (*Meles meles*) in Austria. *Biological Journal of the Linnean Society* 108:579-585

Zahn C.T. & Roskies R.Z.1972. Fourier descriptors for plane closed curves. *IEEE Transactions on Computers* 21:269-281

Zelditch M.L., Bookstein F.L. & Lundrigan B.L. 1992. Ontogeny of integrated skull growth in the cotton rat *Sigmodon fulviventer*. *Evolution* 46:1164-1180

Zelditch M.L., Swiderski D.L. & Sheets H.D. 2004. *Geometric morphometrics for biologists: a primer*. Academic Press

Zeller M. & Koella J.C. 2016. Effects of food variability on growth and reproduction of *Aedes aegypti*. *Ecology and Evolution* 6:552-559

Appendices

Appendix 1a. Landmark definitions adapted from Maestri *et al.* (2017) & Jojić *et al.* (2011), for the 31 landmarks used on the ventral skull. The first five landmarks occur along the midline of the skull and so are shared between both left and right sides of the ventral surface. Landmarks 6 to 18 occur on the right side of the skull while landmarks 19 to 31 occur on the left

Landmark	Definition of landmark
1	Antero-medial position of intersection of left and right incisors
2	Posterior-most point of the palatine
3	Central point on the suture joining the basisphenoid bone to the basioccipital bone
4	Central positon between left and right occipital condyle on the basioccipital edge of the foramen magnum
5	Posterior-most position of the foramen magnum on the midline of the occipital
6 & 19	Anterior-most point of the incisive foramen
7 & 20	Point of intersection along the incisive foramen edge, on the suture between the premaxilla and maxilla bones
8 & 21	Posterior-most point of the incisive foramen
9 & 22	Posterior-most point of the anterior canalis nervi pterygoidei in the alisphenoid
10 & 23	Point of intersection of the outer edge of the foramen magnum and the medial border of the occipital condyle
11 & 24	Lateral-most point of the occipital condyle
12 & 25	Rostral tip of the post-tympanic hook
13 &26	Caudal point of initial contact between the squamosal bone and the lateral border of the jugal bone
14 & 27	Rostral point of initial contact between the squamosal bone and the medial border of the jugal
15 & 28	Posterior-most point of the third molar
16 & 29	Most anterior point of the first molar
17 & 30	Rostral point of initial contact between the jugal and maxilla junction
18 & 31	Most rostral point on the lateral edge of the upper maxillary process at the infraorbital foramen

Appendix 1b. Definitions for the 15 landmarks used on the lateral view of the skull definitions adapted from Maestri *et al.* (2017) & dos Reis *et al.* (2002a). Landmarks are the same for both the left and right side of the skull

Landmark	Definition of lateral skull landmark
1	Anterior-most intersection between the premaxilla and nasal bones
2	Outer angle of the upper incisor alveolus, where it meets the premaxilla
3	Tip of the incisor blade
4	Point of contact between the inferior border of the incisor and the premaxilla
5	Intersection of the most anterior point of the first molar and the maxilla
6	Intersection of the most posterior point of the third molar and the maxilla
7	Ventral point of the occipital condyle
8	Dorsal point of the occipital condyle
9	Posterior-most point of the parietal bone at the sagittal and nuchal crest intersection
10	Intersection on the lateral border of the parietal and interparietal bones
11	Initial point of contact on the suture between the frontal and parietal bones on the dorsal surface of the brain case
12	Caudal point of initial contact between the squamosal bone and the lateral border of the jugal
13	Rostral point of initial contact between the squamosal bone and the medial border of the jugal
14	Rostral point of initial contact between the lacrimal bone and the medial border of the maxillary process.
15	Most rostral point of the lateral edge of the maxillary process at the infraorbital foramen

Appendix 1c. Landmark definitions for the 13 landmarks used for the mandible adapted from Shintaku *et al.* 2016), Samuels (2009), and Cardini & Tongiorgi (2003). Landmarks are the same for both left and right hemi-mandible

Landmark	Definition of landmark
1	Tip of coronoid process
2	Maximum curvature of the mandibular notch
3	Anterior-most point of the articular surface of the mandibular condyle
4	Posterior-most point of the articular surface of the mandibular condyle
5	Anterior-most point of the curve between the mandibular condyle and angular process
6	Tip of the angular process
7	Ventral-most point on the ventral border of the angular process
8	Point of maximum inward curvature on the ventral edge of the dentary
9	Point of maximum outward curvature on the ventral edge of the dentary
10	Antero-ventral point of the incisive alveolus
11	Antero-dorsal point of the incisive alveolus
12	Point of maximum curvature of the incisive alveolar
13	Intersection between first molar and dentary

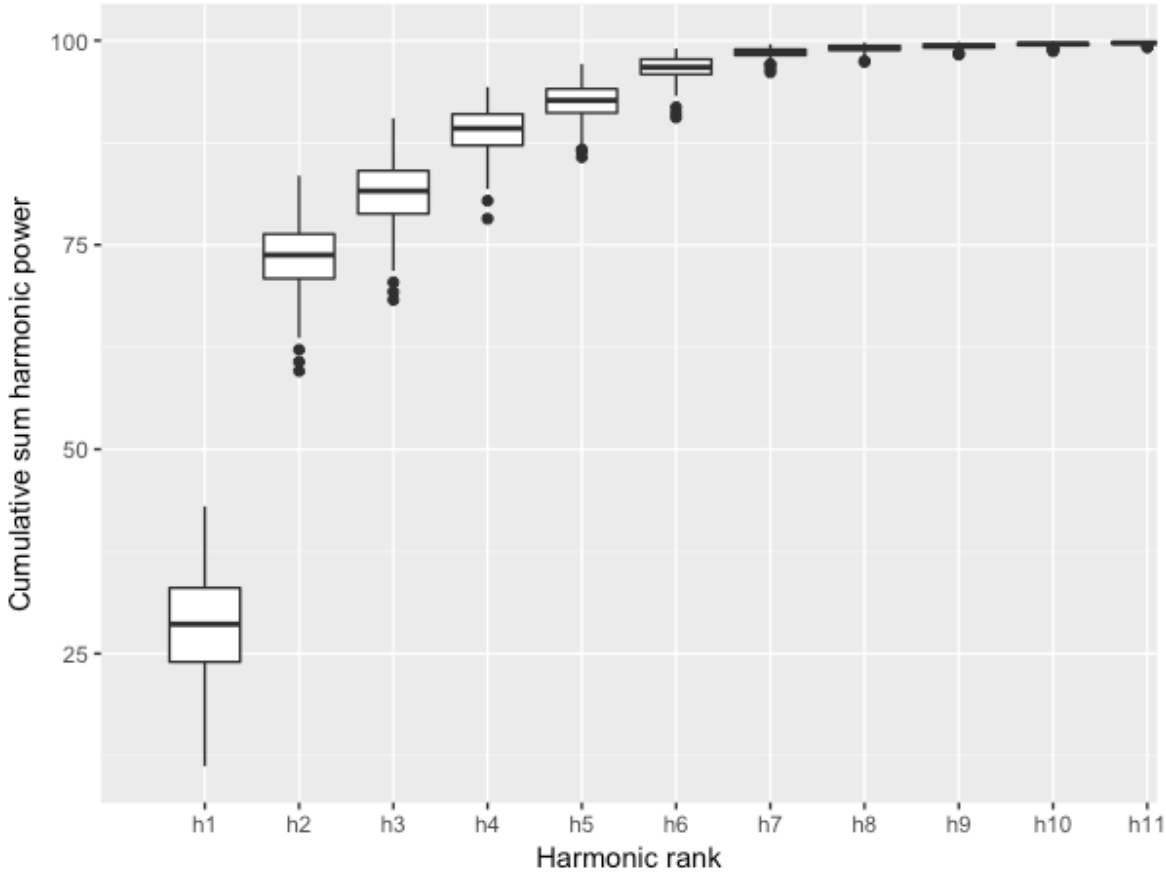
Appendix 2. Table of ANOVA results of measurement error for 30 specimens, with two sets of images digitized twice for the ventral skull, lateral skull, and mandible each. NA indicates values were not available

Structure	Effect	SS	MS ($x10^{-5}$)	d.f.	F	P-value
Ventral	Individual	0.06939189	8.25112	841	7.71	<0.0001
skull	Imaging	0.00113843	3.92564	29	3.67	<0.0001
	Digitization	0.00547855	0.31486	1740	0.59	NA
Lateral	Individual	0.00310699	0.35712	870	4.80	<0.0001
skull	Imaging	0.00005072	0.16907	30	2.27	0.0001
	Digitization	0.00014199	0.00789	1800	NA	NA
Mandible	Individual	0.2254846	35.34241	638	16.98	<0.0001
	Imaging	0.00087541	3.97914	22	1.91	0.0075
	Digitization	0.02891625	2.19062	1320	NA	NA

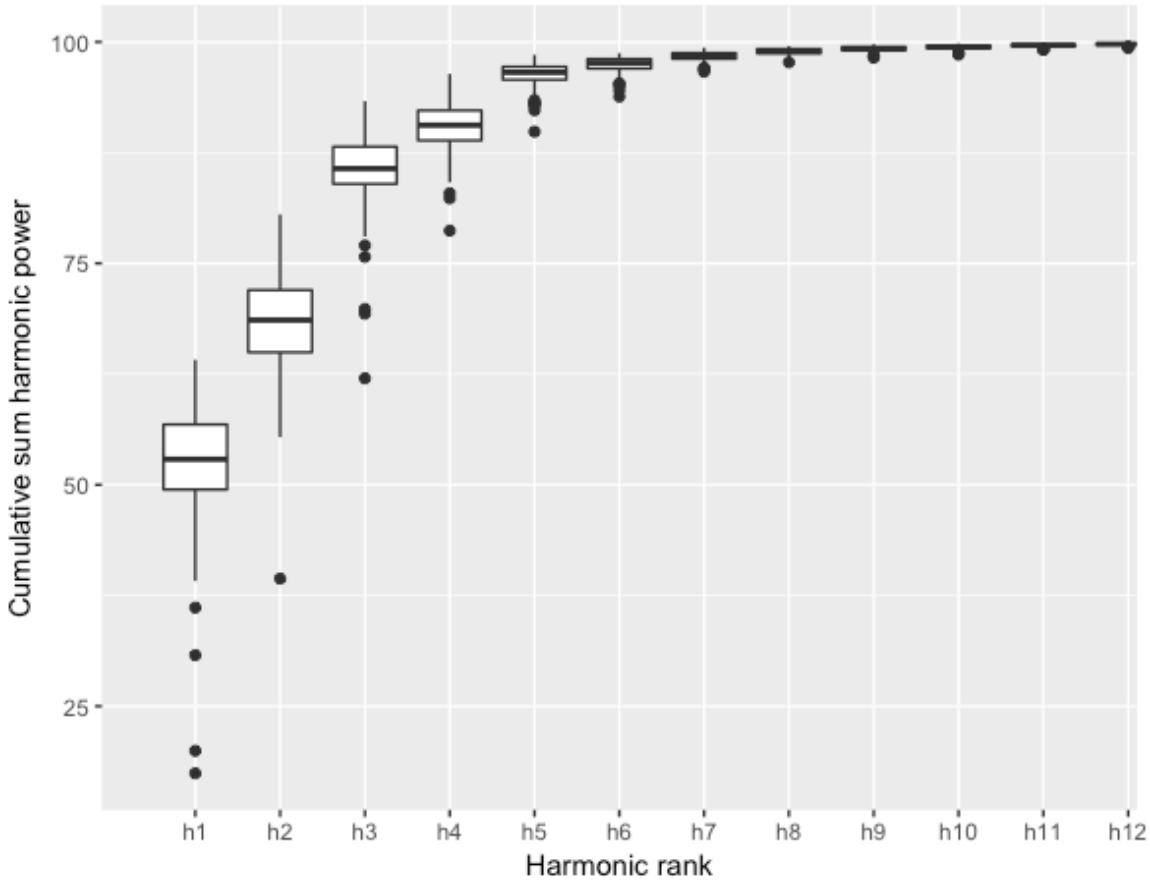
Appendix 3. ANOVA results of the variation in asymmetry in the ventral skull, lateral skull, and mandible (using landmark analysis, and landmarks combined with semi-landmarks). Values in bold are statistically significant

Morpho-structure	Component	Effect	d.f.	MS	F	p-value
Ventral skull	Shape	**Individual**	**158**	**1.39410**	**7.91**	**<0.0001**
		Side	**1**	**1.89749**	**10.77**	**<0.0001**
		Individual:Side	**158**	**1.7626**	**1.64**	**<0.0001**
	Size	**Individual**	**158**	**1.49246 x10^{-3}**	**5.40**	**<0.002**
		Side	**1**	**1.96163 x 10^{-3}**	**7.09**	**<0.002**
		Individual:Side	158	2.7654 x10^{-4}	1.60	0.996
Lateral skull	Shape	**Individual**	**158**	**3.2854**	**5.77**	**<0.001**
		Side	**1**	**7.9191**	**13.90**	**<0.001**
		Individual:Side	158	0.5698	1.92	0.682
	Size	Individual	158	3.7846x10^{-4}	1.44	0.791
		Side	1	2.1180ex10^{-5}	0.08	0.815
		Individual:Side	158	2.6243x10^{-4}	1.29	0.981
Mandible (landmark Analysis)	Shape	Individual	115	0.0069371	5.60	0.412
		Side	**1**	**0.0240385**	**19.41**	**<0.001**
		Individual:Side	**115**	**0.0012382**	**7.55**	**<0.001**
	Size	**Individual**	**115**	**3.2994**	**70.85**	**<0.001**
		Side	1	0.0192	0.41	0.493
		Individual:Side	115	0.0466	0.17	1.000
Mandible (landmark & Semi-Landmark)	Shape	**Individual**	**115**	**0.0055357**	**7.45**	**<0.05**
		Side	**1**	**0.0274523**	**36.94**	**<0.001**
		Individual:Side	**115**	**0.0007432**	**5.53**	**<0.001**
	Size	**Individual**	**115**	**8.5394**	**82.43**	**<0.001**
		Side	1	0.0316	0.30	0.559
		Individual:Side	115	0.1036	0.14	1.000

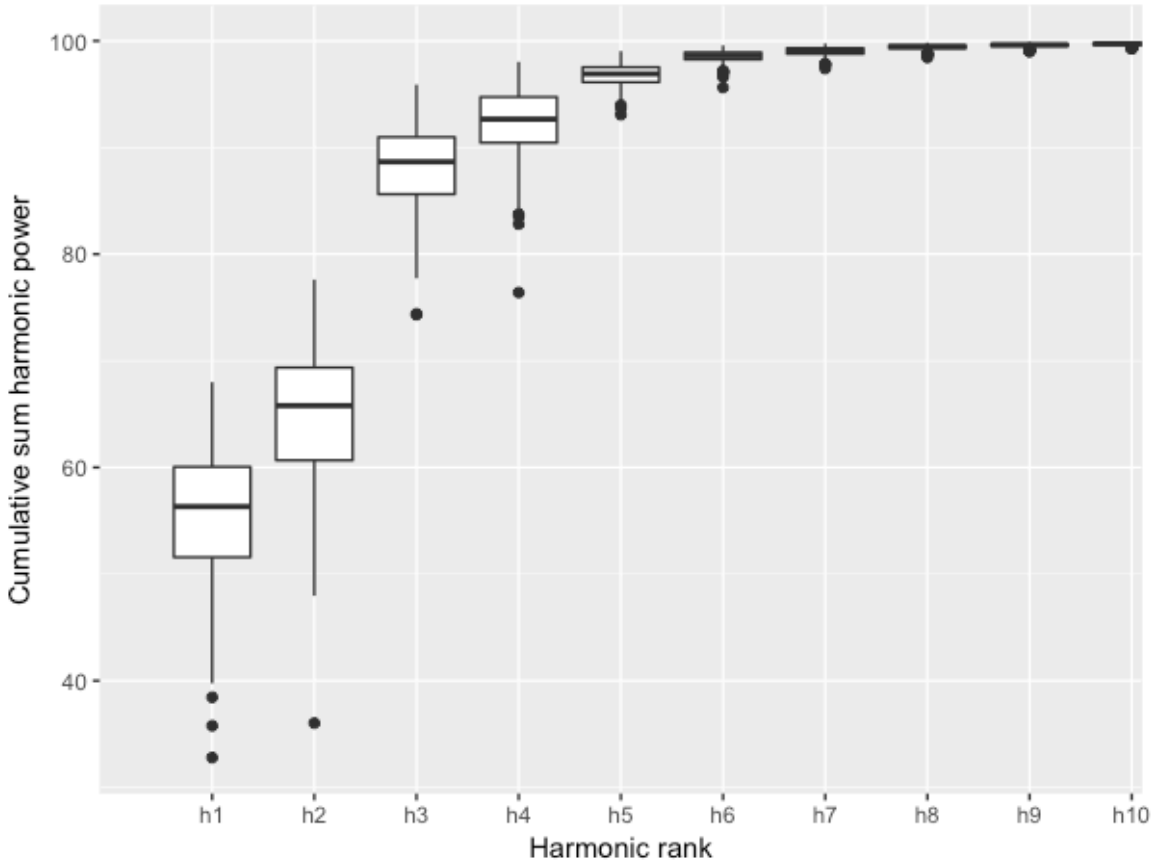
Appendix 4. Figures indicating the cumulative harmonic Fourier power of the upper molars and the information each harmonic cumulatively explained.



Appendix 4a. Cumulative harmonic Fourier power spectrum for the Fourier coefficients of the first upper molar indicating the shape information explained in cumulative harmonic ranks. At the sixth harmonic rank 95% of variation is accounted for and so the first six harmonics were retained.



Appendix 4b. Cumulative harmonic Fourier power spectrum for the Fourier coefficients of the second upper molar indicating the shape information explained in cumulative harmonic ranks. At the fifth harmonic rank 95% of variation is accounted for and so the first five harmonics were retained.



Appendix 4c. Cumulative harmonic Fourier power spectrum for the Fourier coefficients of the third upper molar indicating the shape information explained in cumulative harmonic ranks. At the fifth harmonic rank 95% of variation is accounted for and so the first five harmonics were retained.

Appendix 5. Accumulative proportion of variance explained by PC Axes

Structure	Cumulative Percentage of Principal Component Axes (%)								
Ventral Skull	PC 1	PC 2	PC 3	PC 4	PC 5	PC 6	PC 7	PC 8	PC 9
	17.51	28.80	39.47	48.09	54.35	60.22	65.47	69.77	73.62
	PC 10	PC 11	PC 12	PC 13	PC 14	PC 15	PC 16	PC 17	PC 18
	77.03	79.57	81.97	84.08	86.09	87.86	89.49	91.00	92.36
	PC 19	PC 20	PC 21						
	93.54	94.70	95.65						
Lateral Skull	PC 1	PC 2	PC 3	PC 4	PC 5	PC 6	PC 7	PC 8	PC 9
	16.99	31.75	40.85	48.93	56.53	63.86	69.86	74.16	78.19
	PC 10	PC 11	PC 12	PC 13	PC 14	PC 15	PC 16	PC 17	PC 18
	81.56	84.39	86.71	88.69	90.31	91.85	93.25	94.44	95.50
Mandible (landmarks)	PC 1	PC 2	PC 3	PC 4	PC 5	PC 6	PC 7	PC 8	PC 9
	26.67	40.69	52.92	60.67	67.38	73.50	78.24	81.98	85.72
	PC 10	PC 11	PC 12	PC 13	PC 14	PC 15			
	87.29	89.89	91.82	93.43	94.94	96.08			
Mandible (semi-landmarks)	PC 1	PC 2	PC 3	PC 4	PC 5	PC 6	PC 7	PC 8	PC 9
	24.94	36.97	46.51	54.40	61.11	66.80	71.21	74.94	78.39
	PC 10	PC 11	PC 12	PC 13	PC 14	PC 15	PC 16	PC 17	PC 18
	81.28	84.17	86.29	88.17	89.72	90.96	92.01	93.00	93.80
	PC 19	PC 20							
	94.51	95.12							
First upper molar	PC 1	PC 2	PC 3	PC 4	PC 5	PC 6	PC 7	PC 8	PC 9
	32.12	51.80	62.35	68.95	73.40	77.45	81.17	84.16	86.69
	PC 10	PC 11	PC 12	PC 13	PC 14	PC 15			
	88.89	90.73	92.17	93.36	94.31	95.05			
Second upper molar	PC 1	PC 2	PC 3	PC 4	PC 5	PC 6	PC 7	PC 8	PC 9
	43.73	60.78	70.60	77.22	81.24	84.90	87.82	90.06	91.72
	PC 10	PC 11	PC 12	PC 13					
	94.97	94.12	94.97	95.66					
Third upper molar	PC 1	PC 2	PC 3	PC 4	PC 5	PC 6	PC 7	PC 8	PC 9
	46.81	60.82	69.99	75.49	75.49	83.68	86.78	89.16	91.11
	PC 10	PC 11	PC 12	PC 13					
	92.68	93.76	94.70	95.45					